

**Targeting and Anchoring of Munc13-1 and ubMunc13-2
to Active Zones by RIM1 α**

PhD Thesis

**in partial fulfilment of the requirements
for the degree “Doctor of Philosophy (PhD)/Dr. rer. nat.”
in the Neuroscience Program
at the Georg August University Göttingen,
Faculty of Biology**

submitted by

Yaisa Seretha Andrews-Zwilling

born in

Port of Spain, Trinidad and Tobago

2005

Declaration

This thesis has been written independently and with no other sources and aids than required.

Yaisa Seretha Andrews-Zwilling

September 23rd, 2005.

Table of Contents

	Title	Page
	Abbreviations	8
1	Introduction	11
1.1	The Presynaptic Terminal and the Synaptic Vesicle Cycle	13
1.2	The Unc-13 Protein Family	15
1.3	The Role of Munc13 in the Synaptic Vesicle Cycle	17
1.4	Molecular Mechanisms of Munc13 Mediated Vesicle Priming	21
1.5	The RIM Family of Proteins	23
1.6	The Role of α RIMs	24
1.7	Introduction to the Initial Analysis of the Munc13- α RIM Interaction	26
1.7.1	Minimum α RIM Binding Site in the Munc13 Amino Termini	26
1.7.2	Physiological Role of the Munc13- α RIM Interaction	28
1.8	Aims of the Present Study	31
2	Materials and Methods	32
2.1	Materials	32
2.1.1	Apparatus	32
2.1.2	Chemicals	33
2.1.3	Kits	35
2.1.4	Materials Used	35
2.1.5	Material for Cell Culture	36
2.1.6	Bacterial and Yeast Strains and Cell Lines	37
2.1.7	Vectors	37
2.1.8	Primary Antibodies	38
2.1.9	Secondary Antibodies	38
2.1.10	Media and Solutions	39
2.1.11	cDNA Clones	42
2.1.12	Conditional Munc13-1 Knock Out Vector	45
2.2	Methods	46
2.2.1	Production of Competent Bacteria	46

2.2.2	Electroporation of Plasmid DNA into Bacteria	47
2.2.3	DNA Plasmid Preparation	47
2.2.3.1	DNA Mini Preparation	47
2.2.3.2	Plasmid Preparation from the QIAGEN Protocol	48
2.2.4	Determination of DNA Concentration	48
2.2.5	Restriction Digests	48
2.2.6	Dephosphorylation of the 5' end with Alkaline Phosphatase	48
2.2.7	Agarose Gel Electrophoresis	49
2.2.8	Isolation of DNA Fragments from Agarose Gels	49
2.2.9	Ligation	49
2.2.10	DNA Sequencing	50
2.2.11	Polymerase Chain Reaction (PCR)	50
2.2.12	Random Mutagenesis PCR	51
2.2.13	Site Directed Mutagenesis	51
2.2.14	Yeast Two-Hybrid Screens and Related Methods	52
2.2.14.1	Overview	52
2.2.14.2	Media and Solutions for the Yeast Two-Hybrid System	53
2.2.14.3	Procedure for the Yeast Two-Hybrid System	55
2.2.14.3.1	Transformation of DNA into Yeast	55
2.2.14.3.2	β -Galactosidase Test	55
2.2.14.3.3	Preparation of Plasmid DNA from Yeast	56
2.2.15	Biochemical Experiments	57
2.2.15.1	Sodium Dodecyl Sulphate Polyacrylamide Gel Electrophoresis (SDS-PAGE)	57
2.2.15.2	Coomassie Blue Staining	58
2.2.15.3	Transfer of Proteins from Acrylamide Gel to Membrane, Western Blotting	59
2.2.15.4	Immunostaining of Blots with HRP-Labelled Secondary Antibody and Visualisation with Enhanced Chemilluminescence (ECL)	59
2.2.15.5	Immunostaining of Blots with Infra-Red Labelled Secondary Antibody and Visualisation with the Odyssey System	61
2.2.15.6	Expression of GST-Fusion Proteins	61
2.2.15.7	Production of Crude Synaptosomal Extract from Rat Brain	63

2.2.15.8	Subcellular Fractionation	63
2.2.15.9	Determination of Protein Concentration	64
2.2.15.10	Cosedimentation Experiments to Investigate Protein-Protein Interactions	64
2.2.16	Cell Culture and Immunocytochemistry	65
2.2.16.1	Treatment of Coverslips for Culturing HEK293 and Primary Neuronal Cultures to be used for Microscopy	65
2.2.16.2	HEK293 Cell Culture	65
2.2.16.3	Primary Mouse and Rat Neuron Culture	66
2.2.16.4	Transfection of Primary Rat Neuron Culture and HEK293 Cells by Calcium Phosphate Precipitation	68
2.2.16.5	Phorbol Ester Binding-Translocation Assays	69
2.2.17	Immunohistochemistry	70
3	Results	71
3.1	Identification of α RIM-Binding Deficient Munc13-1 and ubMunc13-2 Mutants in Reverse Yeast Two-Hybrid Assays	71
3.2	Confirmation of α RIM1-Binding Deficient Mutants	76
3.2.1	Analysis of α RIM-Binding Deficient Mutants of Munc13-1 and ubMunc13-2 in <i>in vitro</i> Binding Assays	76
3.2.2	Immunocytochemical Analysis	80
3.2.2.1	Analysis of α RIM-Binding Deficient Mutants of Munc13-1 and ubMunc13-2 in Living Cells	80
3.2.2.2	Phorbol Ester Induced Translocation of Munc13-1	82
3.2.3	Analysis of Intracellular Trafficking of Munc13-1 and Munc13-1 ^{1121N} in Primary Cultures of Hippocampal Neurons	85
3.2.4	Potential Role of RIM1 α in Synaptic Localisation of Munc13	88
3.3	Analysis of the Subcellular Distribution of Munc13-1 and ubMunc13-2 in RIM1 α Knock Out Mice	91
3.3.1	Whole Brain Protein Level Analysis	91
3.3.2	Subcellular Distribution of Munc13-1 and ubMunc13-2	94
3.3.3	Analysis of Membrane-Bound and Soluble Protein Levels of Munc13-1 and ubMunc13-2	96

3.3.4	Distribution of Munc13-1 in Hippocampus of Wild Type and RIM1 α Knock Out Littermates	99
3.4	Generation of Munc13-1 Conditional Knock Out Vector	103
4	Discussion	106
4.1	Differential Evolution of RIM Binding and Priming Modules in Munc13 Proteins	106
4.2	Identification of Structural Changes in the Munc13-1 and ubMunc13-2 Amino Termini which Abolish α RIM Binding	108
4.3	Identified Munc13-1 and ubMunc13-2 Mutants do not Bind to RIM1 α in <i>in vitro</i> Binding Assays and in Living Cells	109
4.4	Potential Role of α RIMs in the Targeting/Anchoring of Munc13-1 and ubMunc13-2	111
4.5	Munc13-1 and ubMunc13-2 Show Altered Protein Concentration Levels and Distribution in RIM1 α Knock Out Animals	113
4.6	Munc13-1 and ubMunc13-2 are the Main “Output” Molecules of RIM1 α Function	114
5	Outlook	117
6	References	119
7	Curriculum Vitae	132
8	Publications	134
9	Acknowledgements	135

Abbreviations

AMBA	Acrylamide / N, N'-methylene-bis-Acrylamide
aa	amino acid
APS	Ammonium persulfate
ATP	Adenosine triphosphate
ATPase	ATP hydrolysing enzyme
bp	base pairs
BSA	Bovine serum albumin
dH ₂ O/ddH ₂ O	distilled /double distilled water
CA	<i>Cornu ammonis</i> (Ammons Horn), neuroanatomically defined region of the Hippocampus
C1-Domain	Phorbol ester/Diacylglycerol Binding Domain
C2-Domain	Structural part of a protein where Ca ²⁺ binding properties are often found
<i>C. elegans</i>	<i>Caenorhabditis elegans</i>
CNS	Central Nervous System
DAG	Diacylglycerol
DMEM	Dulbecco's Modified Eagle Medium
DMSO	Dimethylsulfoxide
DNA	Deoxyribonucleic Acid
DOC2	Double C2 domain
DKO	Double knockout
dNTPs	Deoxynucleoside Triphosphate
DTT	Dithiothreitol
<i>E. coli</i>	<i>Escherichia coli</i>
EDTA	Di-Sodium-Ethylenediamine-Tetra-Acetate
EGFP	Enhanced Green Fluorescent Protein
EPSC	Evoked Post Synaptic Current
EYFP	Enhanced Yellow Fluorescent Protein
et al.	et alteres
EtOH	Ethanol
ES	Embryonal Stem (Cells)
F1 Generation	First generation

F2 Generation	Second generation
Fig.	Figure
g	Gram
GDP	Guanosine Diphosphate
GFP	Green Fluorescent Protein
GST	Glutathione-S-Transferase
GTP	Guanosine Triphosphate
g_{\max}	gravitational acceleration (980665 m/s ²)
His	Histidine
hr	Hour
I121N	Amino acid Substitution Isoleucine to Asparagine in Position 121
IPSP	Inhibitory Post Synaptic Potential
IPTG	Isopropyl- β -thiogalactopyranoside
kDa	Kilo Dalton
KO	Knock out, Synonym for the Removal of a Gene in the Mouse
L	Litre
LB	Luria Bertani medium
LTD	Long-term depression
LTP	Long-term potentiation
M	Molar
mA	Milliampere
mfLTP	Mossy Fibre LTP (NMDA-Receptor Independent form of LTP)
mg	Milligram
min	Minute
ml	Millilitre
mM	Millimolar
$M_r \times 10^{-3}$	Relative Molecular Weight in kDa
mRNA	"messenger" RNA
n-	nano- (1 x10 ⁻⁹)
NMDA	N-Methyl-D-Aspartate
NSF	N-ethyl-maleinimide Sensitive Factor
OD	Optical density
PAGE	Poly Acrylamide Gel Electrophoresis
PBS	Phosphate Buffered Salt Solution

PDBU	Phorbol-12,13-dibutyrate
pH	negative logarithm of H ⁺ concentration
PDZ	Protein Interaction Domain, Acronym for PSD-95, Dlg, ZO-1
PKA	Protein Kinase A (cAMP-dependent Kinase)
PKC	Protein Kinase C
PLC	Phospholipase C
PMSF	Phenyl Methyl Sulphonyl Fluoride
PSD	Post Synaptic density, electron Dense Specialisation of the Post Synapse
PSD-95	Postsynaptic density - 95 kDa protein
RNA	Ribonucleic Acid
RNase	Ribonuclease
Rpm	Revolutions per minute
RT	Room temperature
s	Seconds
s.d.	Standard Deviation
s.e.m.	Standard Error of the mean
SDS	Sodium dodecyl sulphate
SNAP	Soluble NSF attachment factor
SNAP-25	Synaptosome associated protein of 25 kDa
SNARE	SNAP-receptor
TB	terrific broth
TEMED	N,N,N',N'-Tetramethylethylene diamine
TPA	Tetradecanoyl-Phorbol-Acetate
Tris	Tris (hydroxymethyl)-amino methane
μ	micro- (1 x 10 ⁻⁶)
UV	Ultra Violet
V	Volt
V/v	Volume/volume
WT	Wild Type
W/v	Weight/volume
YTH	Yeast Two-Hybrid
X-Gal	5-Bromo-4-Chloro-3-Indoyl-β-D-Galactoside

1. Introduction

The brain of higher vertebrates is an extremely complex organ. Billions of neurons each form thousands of synapses, which generate precise anatomical circuits. Neurons encode information using electrical activity. Signal transmission between neurons occurs at specialised contact structures called synapses, where the electrical activity is either transmitted directly as an electrical signal, or converted into a chemical signal in the form of neurotransmitter release from the presynapse. The synaptic junctions of chemical synapses are asymmetric structures composed of three compartments: the presynaptic bouton, the synaptic cleft and the postsynaptic signal reception apparatus (Garner et al., 2000; Figure 1).

In contrast to most other secretory processes, the release of neurotransmitter at chemical synapses is spatially restricted to the active zone, which is located precisely opposite the postsynaptic signal reception apparatus (Garner et al., 2000; Dresbach et al., 2001). The active zone is composed of an electron-dense, insoluble proteinaceous material and is localised at the presynaptic plasma membrane, where exocytosis takes place in a temporally highly coordinated manner. The postsynaptic reception apparatus, found juxtaposed to the active zone in the postsynaptic plasma membrane, is also identifiable ultrastructurally by the presence of an electron-dense thickening, called the postsynaptic density, in which postsynaptic receptors, ion channels and other signalling proteins are clustered (Scannevin and Huganir, 2000). Molecular, biochemical and morphological studies have shown that the presynaptic active zone and the postsynaptic density can be biochemically purified. They contain a diverse collection of structural proteins that serve to organise these two membrane specialisations (Garner et al., 2000; Dresbach et al., 2001; Scannevin and Huganir, 2000; Figure 1).

Usually, only a fraction of synaptic vesicles in close proximity of the active zone mature to a fusion-competent primed state before their fusion with the plasma membrane can be triggered by the elevation of the intracellular Ca^{2+} concentration. This fraction of synaptic vesicles is referred to as the readily releasable pool and is constituted of those vesicles that are immediately available for release. The presence of multiple vesicles in the readily releasable pool provides a reservoir for triggering

release and allows the synapse to repetitively release neurotransmitters during bursts of action potentials. During an action potential, Ca^{2+} influx normally triggers neurotransmitter release from a presynaptic terminal only unreliably, with one release event per five to ten Ca^{2+} signals (Dobrunz and Stevens, 1997), resulting in a low overall synaptic release probability. Whenever release is triggered, usually only a single synaptic vesicle undergoes exocytosis, although all of the vesicles in the readily releasable pool appear to be ready for fusion.

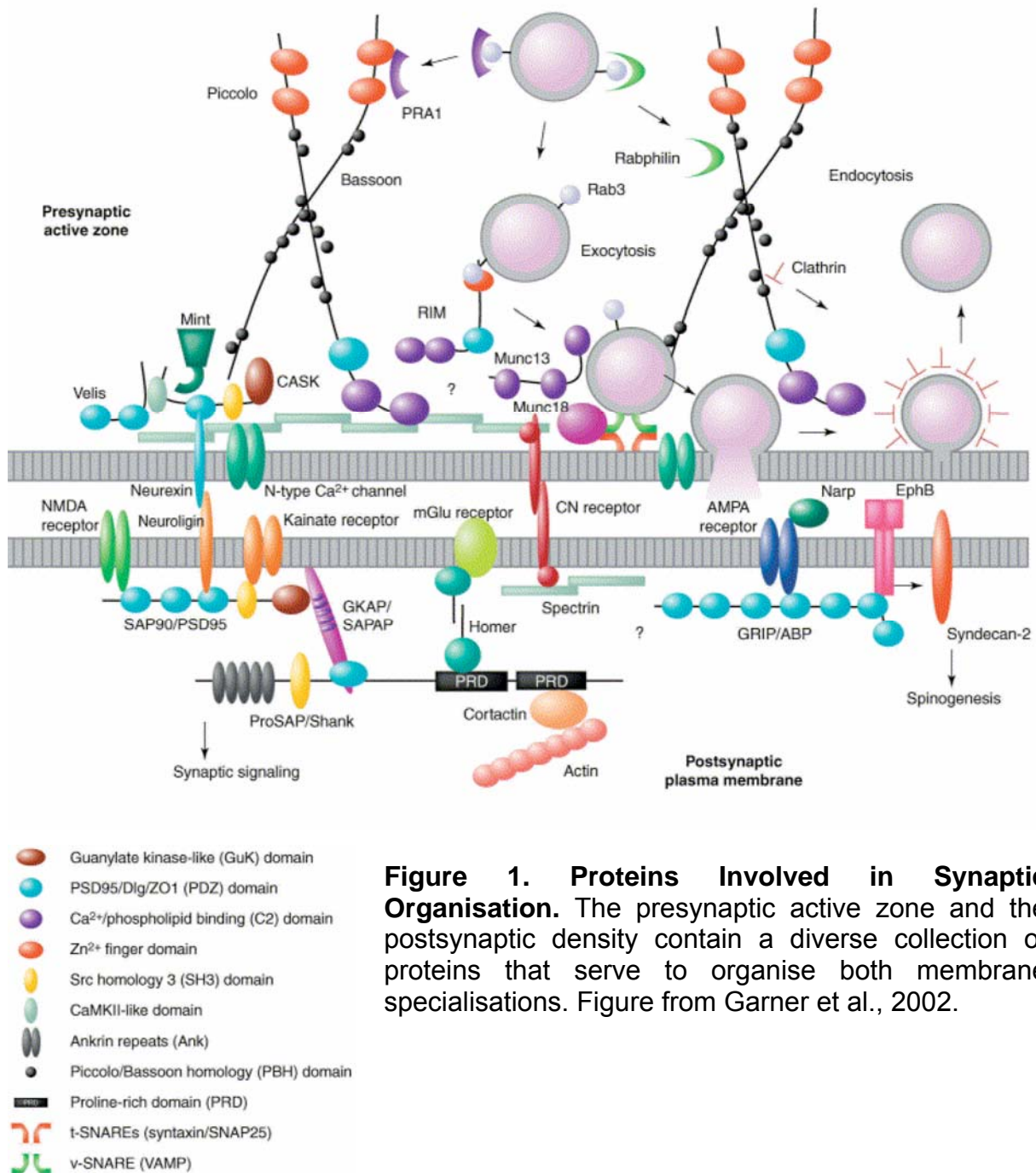


Figure 1. Proteins Involved in Synaptic Organisation. The presynaptic active zone and the postsynaptic density contain a diverse collection of proteins that serve to organise both membrane specialisations. Figure from Garner et al., 2002.

The restriction of exocytosis to a single vesicle is probably not an active process, but

simply caused by the low release probability of each individual vesicle. This suggests that the overall synaptic release probability is the sum of the individual vesicular release probabilities. Consistent with this idea, the number of vesicles in the readily releasable pool appears to be a major determinant of the synaptic release probability (Dobrunz and Stevens, 1997). The size of the readily releasable pool of primed vesicles, which determines the efficacy and capacity of a synapse, is tightly regulated by active zone-specific processes. Furthermore, dynamic changes in the size of the readily releasable pool of vesicles form the basis for adaptive and plastic properties of synapses. Short-term changes (milliseconds to seconds) can increase or decrease the effectiveness of the synapse and are involved in sensory adaptation or rhythm generation. Long-term changes (lasting hours to days) are essential for many complex brain processes such as learning and memory (Südhof et al., 1995; Brünger et al., 2000; Abbott et al., 2000; Rettig et al., 2002).

1.1 The Presynaptic Terminal and the Synaptic Vesicle Cycle

The presynaptic bouton is a specialised compartment of the axon where the presynaptic plasma membrane comes in close contact with the postsynaptic plasma membrane. This specialisation is characterised by an active zone with an associated cluster of vesicles at the internal face of the presynaptic membrane (Figure 2). Electron microscopy revealed that active zones of central synapses are disk-like structures containing a hexagonal grid and synaptic vesicles embedded in the depressions of the grid (Akert et al., 1971). In contrast, active zones of neuromuscular synapses are composed of an elongated ridge containing vesicles lined up like beads on a string (Harlow et al., 2001). Seven large non-membrane proteins bind to each other, and probably form a large single complex at the active zone (Dresbach et al., 2001; Lonart, 2002; Figure 1). Mammalian unc-13s, **Munc13s** (Munc13-1, -2, and -3; Brose et al., 1995) and Rab3-interacting molecules, **RIMs** (RIM1 α , 2 $\alpha/\beta/\gamma$, 3 γ , and 4 γ ; Wang et al., 1997a, 2000; Wang and Südhof, 2003) are multidomain proteins that interact with many synaptic components through their various domains and also interact with each other through their amino termini. **Piccolo** and **Bassoon** are very large homologous proteins (Cases-Langhoff et al., 1996; tom Dieck et al., 1998), and are part of the presynaptic cytomatrix. ELKS/Rab3-interacting molecule/CAST, **ERCs** (ERC1b and ERC2; Wang et al.,

2002; Ohtsuka et al., 2002) are coiled-coil proteins whose carboxy-terminus binds to RIMs, and RIM binding proteins, **RIM-BPs** (RIM-BP 1, 2, and 3; Wang et al., 2000) are SH3- domain proteins that also bind to RIMs. Finally, **α -liprins** (Liprin α 1– α 4) bind to RIMs (Schoch et al., 2002), ERCs (Ko et al., 2003), and receptor protein tyrosine phosphatases (Serra-Pages et al., 1998).

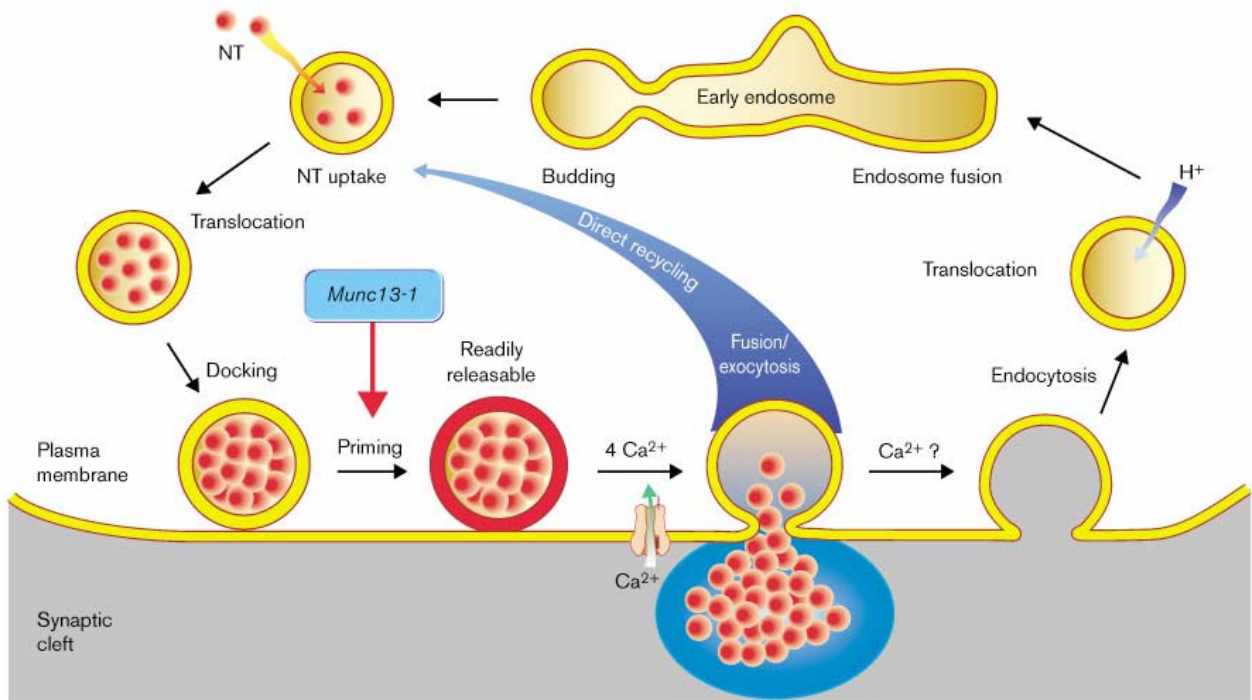


Figure 2. The Synaptic Vesicle in the Presynaptic Nerve Terminal. Synaptic vesicles packed with neurotransmitter by active transport are targeted to the active zone where they dock. After docking, the vesicles undergo a priming reaction that makes them competent for Ca^{2+} triggered fusion. After pore opening, synaptic vesicles undergo endocytosis and recycle via several routes: fast recycling without an endosomal intermediate or clathrin-mediated endocytosis with recycling via endosomes. Analyses of deletion mutations in the *unc-13/Munc13* genes indicate that Unc-13/Munc13 prime synaptic vesicles. Figure from Brose et al., 2000.

The synaptic vesicle cycle, where two of the above mentioned proteins, Munc13s and RIMs, play important roles, can be divided into a number of sequential steps (Südhof, 1995; Figure 2). Neurotransmitters are first actively transported into synaptic vesicles (*neurotransmitter uptake*) and the synaptic vesicles are targeted to and clustered at the active zone (*translocation*). The vesicles then dock at the active zone (*docking*), and acquisition of fusion competence follows docking with some delay. Priming may require multiple steps and may involve both lipid and protein changes upon which the vesicles achieve a state of fusion competence for the Ca^{2+} -triggered fusion-pore

opening (*priming and exocytosis*). After exocytosis, synaptic vesicles endocytose and recycle probably by three alternative pathways: (a) “kiss-and-stay” recycling, where vesicles are reacidified and refilled with neurotransmitters without undocking, thus maturing directly into new synaptic vesicles and remaining in the readily releasable pool; (b) “kiss-and-run” recycling, where vesicles undock and recycle locally and are reacidified and refilled with neurotransmitters (*direct recycling*); (c) vesicles endocytose via clathrin-coated pits and reacidify and refill with neurotransmitters either directly or after passing through an intermediate endosomal compartment where sorting of components occurs (*endocytosis and translocation*) (Figure 2). While vesicle exocytosis occurs only at the active zone, endocytic retrieval of vesicular components may occur both at the active zone and in a peri-active zone area (Roos & Kelly, 1999).

The priming step in the synaptic vesicle cycle was originally inferred from the observation that, during repetitive stimulation, exocytosis slows down before the number of docked vesicles declines (Südhof, 1995; Zucker, 1996). In addition, the speed of Ca^{2+} -triggered exocytosis indicates that vesicles do not undergo complex multistep reactions before fusion. Studies on members of the Unc-13 protein family have provided direct evidence for their involvement in the priming step of the synaptic vesicle cycle. Priming is an essential and rate-limiting step in regulated exocytosis.

1.2 The Unc-13 Protein Family

Caenorhabditis elegans (*C. elegans*) *unc-13* mutants were originally discovered as members of a large group of mutants with an uncoordinated (*unc*) phenotype (Brenner, 1974). The *unc-13* mutants were paralysed and had irregular pharyngeal movements. *Unc-13* belongs to a subgroup of *unc* mutants that are characterised by the presence of abnormal accumulations of acetylcholine, resistance to inhibitors of acetylcholinesterase, and normal activities of acetylcholine esterase, choline acetyltransferase and postsynaptic acetylcholine receptors (Brenner, 1974; Hosono and Kamiya, 1991).

Members of the Unc-13-/Munc13-protein family have a complex domain structure containing a C1-domain, and two or three C2-domains (Figure 3). These domains

were first characterised in protein kinase C (PKC) as conserved domain 1 and 2, and are present in a large number of other proteins (Brose et al., 1995). In *C. elegans*, at least two Unc-13 splice variants are expressed. They are identical in the carboxy-terminal two-thirds of their primary sequence starting with the C1-domain (the R region), but differ in their non-homologous amino termini. One of these variants, called MR, carries a short amino terminus (M region), whereas the other one, LR, has a long amino terminus with an amino-terminal C2-domain (L region) (Maruyama et al., 1991; Richmond et al., 1999). There are three splice variants of Unc-13 expressed in *Drosophila melanogaster*, all of which have the same evolutionary highly conserved R region but divergent amino termini that are not homologous to any of the *C. elegans* Unc-13 variants (Xu et al., 1998; Aravamudan et al., 1999).

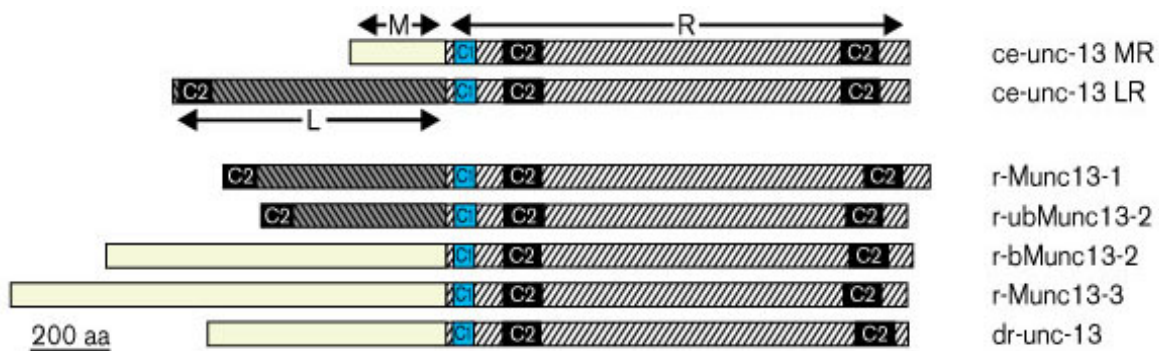


Figure 3. The Domain Structure of the Unc-13 Homologs. Amino termini are on the left and carboxy termini are on the right. *C. elegans* Unc-13 (ce-unc-13) is expressed in two variants (MR and LR). The L region is conserved in the rat homologs r-Munc13-1 and r-ubMunc13-2 whereas all other Unc-13 homologs have unrelated amino termini. aa, amino acid; C1, C₁-domain; C2, C₂-domain; ce, *Caenorhabditis elegans*; dr, *Drosophila melanogaster*; r, *Rattus norvegicus*; L, left; M, middle; R, right. Figure from Brose et al., 2000.

Mammals, in contrast to invertebrates, have at least three different *Munc13* genes (*Munc13-1*, *Munc13-2*, and *Munc13-3*) (Brose et al., 1995; Augustin et al., 1999). *Munc13-1* and *Munc13-3* are neuron and neuroendocrine cell specific, whereas *Munc13-2* is expressed as a brain-specific (bMunc13-2) and a ubiquitously expressed (ubMunc13-2) amino-terminal splice variant (Song et al., 1998; Betz et al., 2001). The R region of *C. elegans* and the Unc-13 carboxy-terminal two-thirds of all mammalian Munc13 isoforms are very similar to each other and are highly conserved across all isoforms and species. However, only Munc13-1 and ubMunc13-2 contain

an amino terminus with homology to the Unc-13 L region of *C. elegans*. The amino termini of bMunc13-2 and Munc13-3 are not homologous to each other or to other known proteins. This striking mosaic of sequence similarities indicates that *unc-13/Munc13* genes consist of two modules that have evolved differentially and may have independent functional roles. The carboxy-terminal sequences starting with the C1-domain (corresponding to the R region of *C. elegans* Unc-13) are highly conserved throughout evolution. In contrast, the C2-domain-containing amino terminus corresponding to the L region of *C. elegans* Unc-13 is only conserved in Munc13-1 and ubMunc13-2, whereas other isoforms have completely divergent amino termini that represent later evolutionary acquisitions (Figure 3).

Among the conserved regions in the Unc-13 family, the C1 and C2 domains have been characterised in more detail. The Munc13 C1-domain, binds to the lipid second messenger, diacylglycerol and to phorbol esters with high affinity. Like PKCs, Unc-13s translocate to the plasma membrane in response to phorbol-ester binding (Betz et al., 1998; Ashery et al., 2000). The C2 domains serve as Ca^{2+} /phospholipid-binding or protein interaction domains in a large number of different proteins (Brose et al., 1995). However, although the central C2 domain of all Unc-13 homologs (C2B) meets the structural requirements to form a Ca^{2+} -binding site, Ca^{2+} binding to this domain has not yet been demonstrated for Munc13-1, Munc13-2 or Munc13-3. An alternative Ca^{2+} -dependent regulation of Unc-13 proteins occurs via Calmodulin where Munc13-1 and ubMunc13-2 bind Calmodulin in a Ca^{2+} dependent manner via an evolutionarily conserved Calmodulin recognition motif. Calmodulin binding causes increased priming activity and readily releasable pool sizes and activation of the Calmodulin-Munc13 complex by residual Ca^{2+} represents a molecular correlate for the phenomenon of Ca^{2+} -dependent vesicle pool refilling. This mechanism controls short term plasticity characteristics and is likely to be evolutionarily conserved (Junge et al., 2004).

1.3 Role of Munc13 in the Synaptic Vesicle Cycle

Munc13-1 is expressed throughout the brain, with highest levels in the olfactory bulb, striatum, cerebral cortex, hippocampus and cerebellum. Expression of Munc13-2 can be detected mainly in the olfactory bulb, cerebral cortex and hippocampus and

Munc13-3 is mainly expressed in the brain stem and cerebellum (Augustin et al., 1999). All Munc13 isoforms are expressed in the nervous system and are specifically enriched at the presynaptic active zone (Brose et al., 1995; Betz et al., 1998; Augustin et al., 1999; Figure 4).

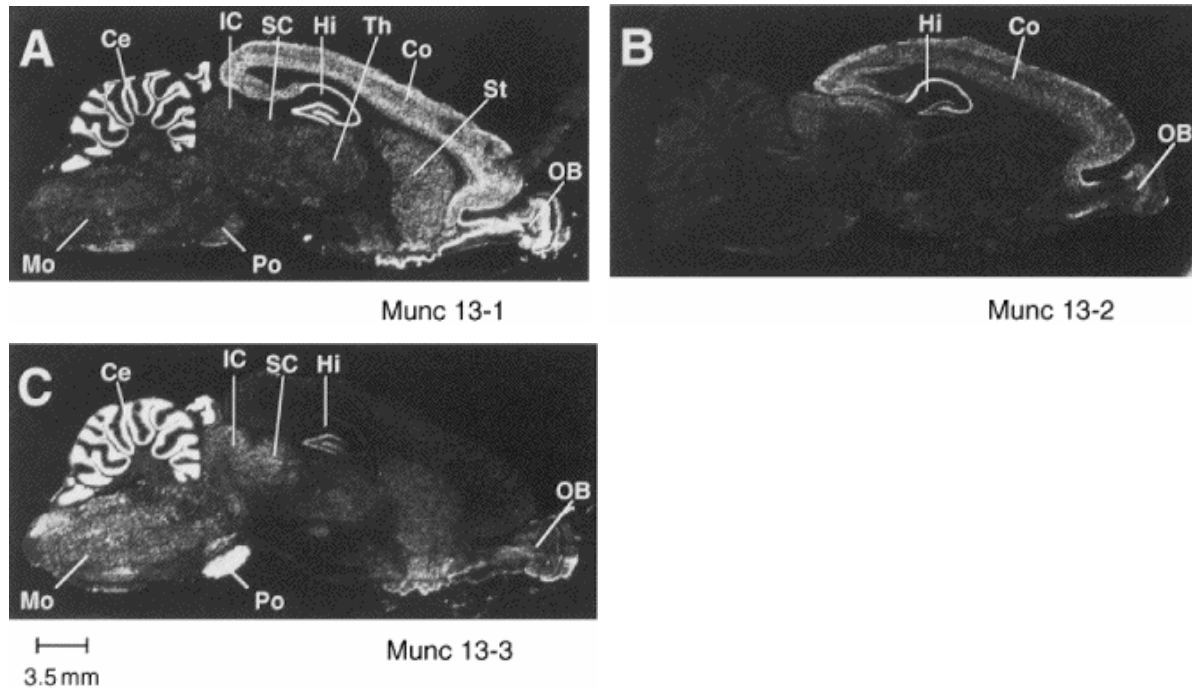


Figure 4. Distribution of Munc13 mRNA in Adult Rat Brain (A) Munc13-1, (B) Munc13-2 and (C) Munc13-3. Munc13-1 and Munc13-2 as well as Munc13-1 and Munc13-3 exhibit some level of redundancy in the rostral and caudal regions of the brain, respectively, while there exists a complementary expression pattern of Munc13-2 (rostral brain regions; CA regions of hippocampus) compared with Munc13-3 (caudal brain regions; dentate gyrus). Abbreviations: Ce, cerebellum; Co, cerebral cortex; Hi, hippocampus; IC, inferior colliculus; Mo, medulla oblongata; OB, olfactory bulb; Po, pons; SC, superior colliculus; St, striatum; Th, thalamus. Scale bar 3.5 mm. Figure from Augustin et al., 1999.

Mice lacking the brain-specific Munc13-1 isoform die immediately after birth and, while the brain and other organs of newborn Munc13-1 knock out mice show no obvious alterations in cytoarchitecture and connectivity, a striking 90% reduction in neurotransmitter release from Munc13-1-deficient cells was observed by electrophysiological analysis of individual glutamatergic hippocampal primary neurons (Augustin et al., 1999). Similar observations were made in *C. elegans* and *Drosophila melanogaster* lacking Unc-13 or Dr-Unc-13, respectively (Aravamudan et al., 1999; Richmond et al., 1999). The mutant phenotype of Munc13-1 knock out

synapses in mouse hippocampus is restricted to glutamatergic neurons. Gamma-aminobutyrate (GABAergic) neurons are not affected by the loss of Munc13-1 (Augustin et al., 1999b; Rosenmund et al., 2002; Figure 5). The entire readily releasable pool can be exocytosed upon application of hypertonic sucrose as a mechanical stimulus (Rosenmund & Stevens, 1996) and utilising this method, it was observed that the reduction in evoked glutamate release from Munc13-1-deficient neurons was due to a 90% reduction in the size of the readily releasable vesicle pool (Augustin et al., 1999). The few remaining fusion competent vesicles which are available in the Munc13-1 knock out are due to the presence of the second isoform of Munc13 expressed in the hippocampus, Munc13-2, which is responsible for vesicle priming in Munc13-1 independent hippocampal synapses (Rosenmund et al., 2002). Neurons lacking both Munc13-1 and Munc13-2 show neither evoked nor spontaneous release events, yet form normal numbers of synapses with typical ultrastructural features (Rosenmund et al., 2002).

Munc13-1 and Munc13-2 exhibit a complex pattern of functional redundancy. In GABAergic hippocampal neurons, the loss of Munc13-1 or Munc13-2 can be compensated for by the presence of the respective other, whereas in glutamatergic hippocampal neurons, Munc13-1 can compensate for Munc13-2 loss but not vice versa (Figure 5). In both cell types, the complete absence of Munc13 priming factors leads to the elimination of readily releasable vesicles and total arrest of synaptic vesicle priming, demonstrating that Munc13-mediated vesicle priming is not a transmitter specific phenomenon, but is a general and essential feature of two different fast neurotransmitter systems (Varoqueaux et al., 2002). Unlike the mammals, *C. elegans* and *Drosophila melanogaster* contain only one *unc-13/dr-unc-13* gene each and show no transmitter or synaptic specific functions. Synaptic transmission is completely shut down in these knock out mutants (Aravamudan et al., 1999; Richmond et al., 1999).

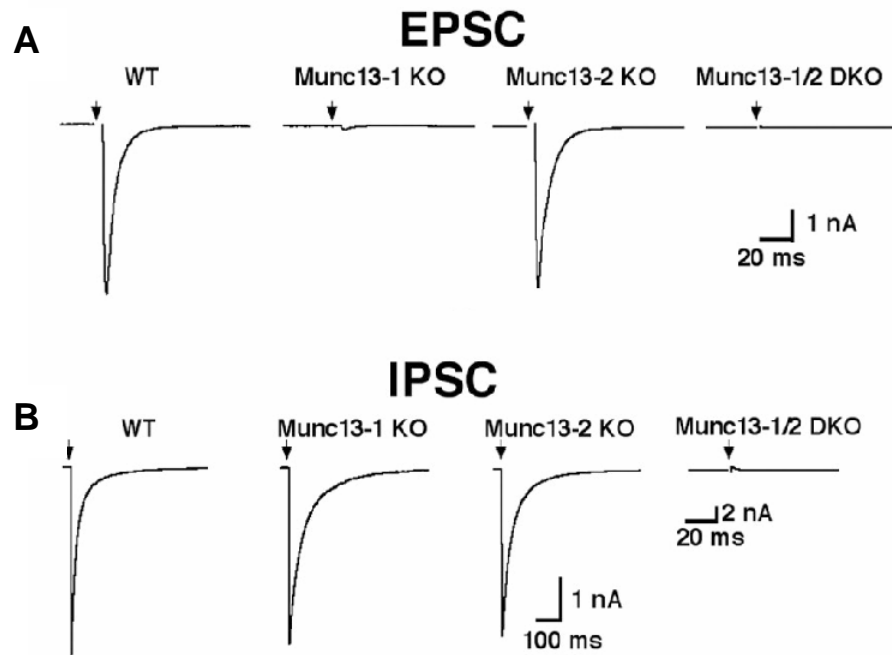


Figure 5. Excitatory and Inhibitory Post Synaptic Potentials of Munc13-Gene Modified Mice. (A) Excitatory postsynaptic currents (EPSCs) from wild type and Munc13-2 knock out neurons were not significantly different, however Munc13-1 deletion led to a 90% reduction of readily releasable vesicles and evoked transmitter release and neurons lacking both Munc13-1 and Munc13-2 show neither evoked nor spontaneous release events. **(B)** Elimination of Munc13-1 and Munc13-2 had no apparent effect on inhibitory synaptic transmission, however neurons lacking both Munc13-1 and Munc13-2 show neither evoked nor spontaneous release events, indicating that the two Munc13 isoforms are completely redundant in GABAergic cells. Figure from Varoqueaux et al., 2002.

The third Munc13 homologue, Munc13-3, is coexpressed with Munc13-1 in the cerebellum (Augustin et al., 1999a; Figure 4). Munc13-3 deletion mutants, like Munc13-2 knock out animals, are viable and fertile, exhibit no obvious physical or behavioural abnormalities and have a normal life expectancy (Augustin et al., 2001). Munc13-3 is, like Munc13-1 and Munc13-2, a presynaptic protein and is localised to the synaptic neuropil of the cerebellar molecular layer but is not found in Purkinje cell dendrites. Munc13-3 deletion mutants exhibit increased paired-pulse facilitation at parallel fibre-Purkinje cell synapses, which indicates a reduction in release probability. In addition, mutant mice display normal spontaneous motor activity but have an impaired ability to learn complex motor tasks. Munc13-3 loss leads to a reduced release probability at parallel fibre-Purkinje cell synapses by interfering with

vesicle priming but it is not essential for GABAergic neurotransmitter-vesicle priming in the cerebellum (Augustin et al., 2001).

1.4 Molecular Mechanisms of Munc13 Mediated Vesicle Priming

The first insights into the molecular basis of Unc-13 function have been obtained by the identification of interaction partners. So far, the Unc-13- or Munc13-interacting proteins, which bind to the highly conserved R region of Unc-13/Munc13 include Syntaxin 1, a core complex component with an essential role in exocytosis (Betz et al., 1997), msec7-1, a GDP/GTP exchange factor for the Arf family of small G-proteins (Neeb et al., 1999) and Unc-18, a regulator of core complex formation and essential component of the secretory apparatus (Sassa et al., 1999). The initial search for Unc-13/Munc13 interaction partners concentrated on the conserved carboxy terminal regions of the proteins. The divergent amino termini were largely neglected because of the apparent lack of conservation. However, the presence of the evolutionary conserved amino terminal module in ubMunc13-2, Munc13-1, and *C. elegans* Unc-13LR indicated a common functional role for the amino termini of these proteins (Figure 3). Calcium-calmodulin (Xu et al., 1998) binds to a 21-residue conserved binding site just amino-terminal to the C1-domain of *Drosophila melanogaster* Unc-13, Munc13-1 and ubMunc13-2 with a 1:1 stoichiometry and causes increased priming activity and readily releasable pool sizes (Junge et al., 2004). RIM1 (Rab3a Interaction Molecule) was identified in a yeast two-hybrid study (Betz et al., 2001) as a Munc13-1/ubMunc13-2 amino terminal interacting partner.

One of the best understood steps of the synaptic vesicle cycle is the Ca^{2+} triggered fusion reaction. It is now well established that efficient membrane fusion *in vivo* requires the interaction of small cytoplasmically exposed membrane proteins called Soluble N-ethylmaleimide-sensitive factor attachment protein receptors, SNAREs (Söllner et al., 1996). For synaptic vesicle exocytosis, the relevant SNAREs are synaptobrevin/vesicle-associated membrane protein 1 and 2 (VAMP 1 and 2), Syntaxin 1, and synaptosomal-associated protein of 25 kilo-Daltons (SNAP25) (Trimble et al., 1988; Oyler et al., 1989; Bennett et al., 1992; Söllner et al., 1993). Synaptobrevins/VAMPs are localised primarily on synaptic vesicles, syntaxin and SNAP25 primarily on the plasma membrane (Sutton et al., 1998). Initially, SNARE

complex formation is driven by the progressive zippering of vesicle and plasma membrane SNAREs, which may lead to stalk-like hemifusion of the synaptic vesicle with the plasma membrane (Söllner et al., 1993; Jahn et al., 2003). Full zippering of this four-helix bundle in the SNARE complex (and thus full fusion) may then be blocked until a Ca^{2+} signal is sensed by the exocytotic Ca^{2+} sensor. Although zippering of SNARE proteins may be the final trigger for membrane fusion, a variety of other factors play critical roles in exocytosis by controlling SNARE function, as emphasised by the growing list of SNARE-interacting proteins. Many of these regulatory factors occur as specialised isoforms at synapses. Two such factors, Unc-13/Munc13 and Unc-18/Munc18-1 (a member of the Sec1/Munc18 (SM) protein family), are particularly important given the dramatic effect produced by their absence, i.e. a complete block of synaptic vesicle exocytosis (Richmond et al., 1999, Verhage et al., 2000, Varoqueaux et al., 2002).

SNARE complex formation is believed to be regulated in part by the conformation of Syntaxin 1. Munc18-1 directly promotes the stability of Syntaxin 1 but is not required for its targeting or function as such (Toonen et al., 2005). However, Munc18/Sec1 may act by regulating Syntaxin 1 function as initially shown by the property of yeast Syntaxins to suppress mutations in Sec1 (Aalto et al., 1993). The amino terminal region of Syntaxin 1 contains a three-helix domain that folds back onto the SNARE motif forming a closed conformation. This 'closed' Syntaxin is unable to bind other SNARE proteins and therefore is incompatible with formation of the SNARE complex (Dulubova et al., 1999). Munc18-1 interacts strongly with the closed conformation of Syntaxin 1, suggesting an inhibitory role on fusion (Misura et al., 2000). Additionally, the Munc18/Sec1 protein family is needed for fusion. Indeed, there is a complete absence of synaptic vesicle exocytosis in Munc18-1 knockout mice (Verhage et al., 2000; Toonen et al., 2005). Munc18-1 may therefore have a second role downstream to Syntaxin inhibition, as supported by the property of yeast Sec1 to bind the assembled yeast SNARE complex (Carr et al., 1999). The displacement of Munc18-1 is postulated to be achieved by other proteins known to be important for priming, e.g. Munc13 and RIM (Richmond et al., 2001; Rizo & Südhof, 2002). Evidence in support of this idea comes from *C. elegans*, where loss of exocytosis due to mutant Unc-13 or RIM and the lethal Unc-13 deletion mutant phenotype are rescued by overexpression of the Syntaxin 1 mutant that is unable to form the 'closed'

conformation (Koushika et al., 2001; Richmond et al., 2001).

1.5 The RIM Family of Proteins

RIMs are multidomain adaptor proteins. They were initially discovered as putative effectors for Rab3 and are encoded by four genes in mammals (*RIM1*, *RIM2*, *RIM3 γ* and *RIM4 γ* , Wang et al., 1997; Wang and Südhof, 2003). Like Munc13s, RIMs are one of only seven proteins known to be specifically localised to the presynaptic active zone (Garner et al., 2000). Mammalian RIM1 and RIM2 specify full-length transcripts encoding two closely related isoforms RIM1 α and RIM2 α (referred to as the α RIMs) that are composed of an amino terminal zinc finger domain, a central PDZ and two carboxy terminal C2 domains (C2A domain and C2B domain; Wang et al., 1997; Figure 6).

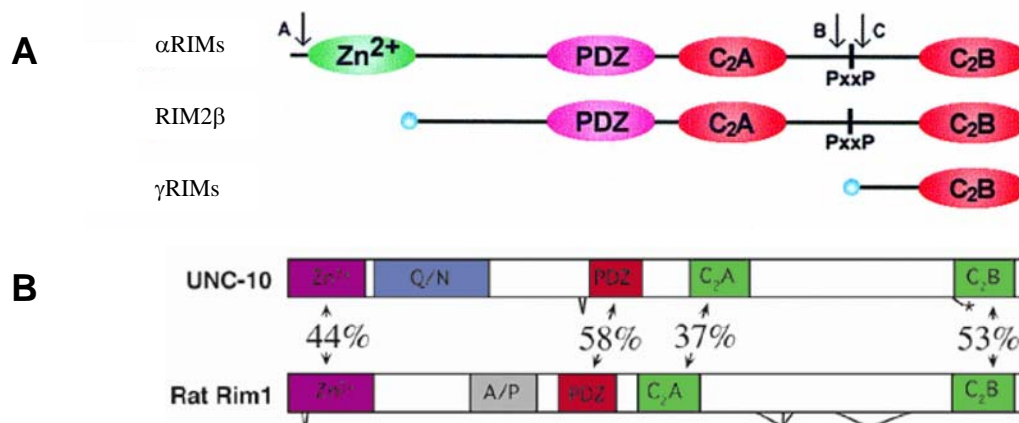


Figure 6. Structure of the RIM Protein Family. (A) Diagram of the domain composition of RIMs and the location of the splice sites. The four domains of α RIMs are the amino terminal zinc finger (Zn²⁺), the central PDZ domain and the carboxy terminal C2A and C2B domains. In the linker between the C2A and the C2B domains lies a proline-rich sequence that binds to the SH3 domains of RIM-BP1 and BP2. **(B)** Comparison of the domain organisation of the *C. elegans* Unc-10 and mammalian RIM1 α proteins (Koushika et al., 2001). The percentage of sequence identity between shared domains is depicted. The alanine and proline rich domain (A/P) and alternative splice forms were identified by Wang et al., 1997. Figures from Koushika et al., 2001; Wang and Südhof, 2002.

The RIM2 gene specifies not only the full-length transcript encoding RIM2 α (originally RIM2), but also a shorter transcript lacking the amino terminal zinc finger (RIM2 β), as well as an even shorter transcript encoding a protein that is composed of only the carboxy terminal C2B domain with flanking sequences, RIM2 γ (originally NIM2; Wang et al., 2000; Wang and Südhof, 2003). RIM3 γ (originally named NIM3) and RIM4 γ are the remaining gene products that are composed of only a C2B domain with flanking sequences (Wang et al., 2000, Wang and Südhof, 2003; Figure 6). The RIM1 α and RIM2 α transcripts, but not the RIM2 γ and RIM3 γ transcripts, are subject to extensive alternative splicing at multiple positions, creating a large number of potential isoforms. RIM1 α is the most abundant isoform in the mammalian brain (Wang et al., 1997; Wang et al., 2000). In invertebrates, only a single RIM form was described in *Caenorhabditis elegans* as the product of the *unc-10* gene (Koushika et al., 2001; Figure 6).

1.6 The Role of α RIMs

RIM1 α and RIM2 α (the α RIMs) are thought to function in neurotransmitter release by interacting directly or indirectly with most other known active zone proteins and they are regulated by phosphorylation (Calakos et al., 2004). They interact with Rab proteins, which are Ras-like GTPases that play important roles in mediating vesicular membrane trafficking in eukaryotic cells and include Rab3, which is bound to synaptic vesicles in a GTP dependent manner and has been implicated in the transport and docking of synaptic vesicles at the presynaptic active zone (Fischer von Mollard et al., 1990; Geppert et al., 1994; Nonet et al., 1997). In addition to Rab3, several other α RIM interaction partners have been described. The amino terminal Zn²⁺-finger domain of RIM1 α and RIM2 α binds to both Rab3 and the amino terminus of Munc13-1/ubMunc13-2, allowing the formation of a tripartite complex (Betz et al., 2001; Wang et al., 2001, Schoch et al., 2002; Dulubova et al., 2005). The central PDZ domains of RIMs interact with ERCs, a family of proteins that are largely composed of coiled coils. The ERCs are alternatively spliced proteins that are found at the active zone, but they are also present in other neuronal subcompartments and even expressed in non-neuronal cells. They may be important for the genesis of active zones (Nakata et al., 1999; Ohtsuka, 2000; Monier et al., 2002; Wang et al., 2002). A proline-rich sequence in the linker between the C2A and the C2B domain of

RIMs interact with the SH3 domain of another family of brain-specific adaptor proteins called RIM-BPs (Wang et al., 2000). The carboxy terminal C2B domain of RIMs, finally, binds to liprins (Schoch et al., 2002), which are also adaptor proteins and in invertebrates are essential for regulating the active zone size (Zhen et al., 1999; Kaufmann et al., 2002). In addition, the C2B domain binds to the Ca^{2+} sensor Synaptotagmin 1, which in turn regulates neurotransmitter release (Coppola et al., 2001; Schoch et al., 2002). These multiple interactions with proteins from the active zone and with components of the neurotransmitter release machinery indicate that RIMs form a protein scaffold that organises the active zone and regulates transmitter release.

Since RIM1 α and RIM2 α are highly homologous proteins with redundant functions, many experiments were carried out with either one or the other isoform to learn about their function. Genetic experiments in *C. elegans* and mice have confirmed that RIM1 α is essential for normal neurotransmitter release (Koushika et al., 2001; Schoch et al., 2002; Castillo et al., 2002). RIM1 α has been implicated in both short- and long-term synaptic plasticity. Deletion of RIM1 α in mice and the *unc-10* gene in *C. elegans* impairs neurotransmitter release without altering the structure of the synapse and without causing any structural abnormalities or changes in brain architecture (Koushika et al., 2001). Analysis of autapses from RIM1 α knock out mice have shown RIM1 α to function as a modulator of release that operates during priming, as evidenced by a decrease in the readily releasable pool of vesicles, i.e. RIM1 α normally enhances release probability by increasing the size of the readily releasable pool (Calakos et al., 2004). Deletion of RIM1 α also provides evidence that RIM1 α plays an important role in the regulation of vesicular release probability during repetitive stimulation and the kinetics of asynchronous release (Calakos et al., 2004).

Interestingly, in mice, the physiological consequences of RIM1 α mutations differed depending on the type of synapse studied (Schoch et al., 2002; Castillo et al., 2002). In excitatory synapses that are capable of N-methyl-D-aspartate (NMDA)-dependent long-term potentiation, e.g., Schaffer collateral/commissural fibre synapses in the CA1 region of the hippocampus, and in inhibitory synapses in the hippocampus, deletion of RIM1 α caused a large increase in paired-pulse facilitation, which indicated lowered neurotransmitter release probability in response to Ca^{2+} influx, a decline in

synaptic transmission and changes in short-term synaptic plasticity (Schoch et al., 2002). RIM1 α knock out mice additionally showed increased posttetanic potentiation but normal long-term potentiation at the Schaffer collateral to CA1 pyramidal neuron synapses (Schoch et al., 2002). Mossy fibre long-term potentiation, as opposed to NMDA-receptor dependent long-term potentiation, has a principal presynaptic component and requires activation of protein kinase A. In synapses that exhibit this type of long-term potentiation, e.g. mossy fibre synapses in the CA3 region of the hippocampus and at the parallel fibre/Purkinje cell synapse in the cerebellum, deletion of RIM1 α had no detectable effect on acute neurotransmitter release, but prevented long-term potentiation (Castillo et al., 2002). Consistent with a physiological importance of the RIM1 α -Rab3A interaction, Rab3A deletions in mice exhibit a similar, synapse-specific phenotype as RIM1 α deletions, i.e. they are deficient in mossy fibre long-term potentiation and exhibit increased paired pulse facilitation (Geppert et al., 1994; Geppert et al., 1997; Castillo et al., 1997). The phenotype exhibited by RIM1 α knock out mice, though not as extreme as that of Munc13-1 mice, includes dramatic deficits in associative learning and locomotor responses (Powell et al., 2004).

1.7 Introduction to the Initial Analysis of the Munc13- α RIM Interaction

In order to identify Munc13-amino terminal interaction partners, the first 181 residues of ubMunc13-2, which are homologous to the amino-terminus of Munc13-1, were fused to the DNA binding domain of the bacterial repressor LexA and used as a bait construct, pLexN-ubMunc13-2(1-181), in a yeast two-hybrid screen of a rat brain cDNA prey library. The amino terminal Rab3-binding zinc finger region of the active zone protein RIM1 α , was identified as an interaction partner. Apart from RIM1 α , no proteins with a putative or likely synaptic or active zone function were identified in the yeast two-hybrid screen (Betz et al., 2001).

1.7.1 Minimum α RIM Binding Site in the Munc13 Amino Termini

The use of semiquantitative galactosidase assays with the first 344 amino acid residues of RIM1 α and pLexN-ubMunc13-2(1-181) demonstrated that the interaction

was highly specific for the ubMunc13-2 amino terminus, as pPrey-RIM1(1-344) interacted strongly with pLexN-ubMunc13-2(1-181) but not with the ubMunc13-2 control bait vector, pLexN-ubMunc13-2(273-408). A similar bait construct containing residues 1–150 of Munc13-1, pLexN-Munc13-1(1-150) interacted strongly with pPrey-RIM1(1-344), while a control construct, pLexN-Munc13-1(710-1181), showed no interaction. Moreover, a bait construct containing the C2B domain of Munc13-1 (pLexN-Munc13-1(444-1181)) did not interact with pPrey-RIM1(1-344). These data demonstrated that RIM1 α binding is a common feature of the conserved amino termini of Munc13-1 and ubMunc13-2 and is not caused by a C2 domain-specific structural motif (Betz et al., 2001). The amino terminal regions of Munc13-1 and ubMunc13-2 also contain a highly degenerate core C2 domain at their very amino termini (Figure 3). This domain was not sufficient for the RIM1 α interaction since none of the bait vectors representing parts of the RIM1 α binding regions of Munc13-1 and ubMunc13-2 [pLexN-Munc13-1(1-71), pLexN-Munc13-1(65-150), pLexN-ubMunc13-2(1-71), pLexN-ubMunc13-2(66-181)] were found to interact with RIM1 α . This indicated that the first 150 residues of Munc13-1 and the first 181 residues of ubMunc13-2 form a functional RIM1 α binding site, while the respective individual C2 domains alone do not. Hence, RIM1 α binding is not a general feature of C2 domains but rather a characteristic of the whole conserved Munc13-1/ubMunc13-2 amino terminal region (Betz et al., 2001). Recent experiments with RIM2 α have now shown that while residues 1-150 of Munc13-1 are sufficient for RIM α binding, inclusion of the C2 domain as well as a long carboxy terminal extension (residues 3-317) is necessary for strong binding (Dulubova et al., 2005).

The amino terminal region of RIM1 α (residues 1–344) that was found to interact with Munc13-1 and ubMunc13-2 contains a zinc finger structure and the same region was previously shown to bind to Rab3a in a GTP-dependent manner (Wang et al., 1997). It was initially thought that Munc13-1 and Rab3a cannot bind to RIM1 α simultaneously and the respective binding sites of both Munc13-1 and Rab3a were mapped to residues 131–214 of RIM1 α (Betz et al., 2001). Recent data obtained using RIM2 α indicated that the amino terminus of the α RIM proteins is comprised of the zinc finger, two helices (a1 and a2) and a SGAWFY motif (Figure 7). The minimal Munc13-1 binding region was the zinc finger domain, helix a2 and the SGAWFY motif (residues 82-155) of RIM2 α , whereas helix a1 of RIM2 α was sufficient for Rab3a

binding (Dulubova et al., 2005; Figure 7). The SGAWFY motif participates in Rab3a binding, and this interaction is released upon Munc13-1 binding while the interaction of Rab3a with helix a1 persists (Dulubova et al., 2005). This observation explained why Munc13-1 competed with Rab3a binding to RIM1 α in previous GST-pulldown experiments, which were performed with a RIM1 α fragment lacking helix a1 (pGex RIM1aa131-214) and also demonstrated that Munc13-1, RIM α and Rab3a form a tripartite complex (Dulubova et al., 2005).

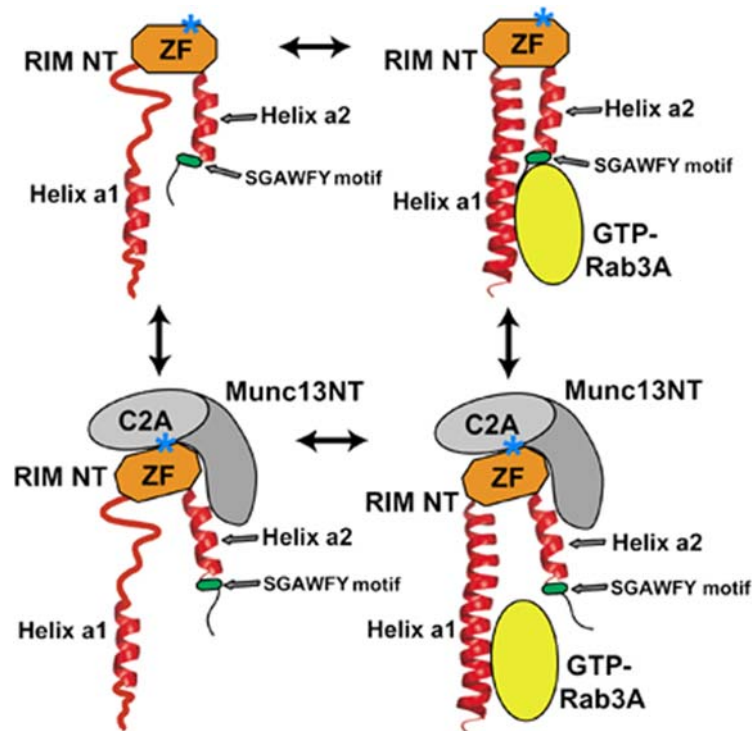


Figure 7. Models of the Interactions of RIM2 α with Munc13-1 and Rab3a. RIM NT, α RIM amino terminal sequence; Munc13 NT, Munc13-1 amino terminal sequence; ZF, α RIM zinc finger domain. The positions of the two α -helices (a1 and a2) and the SGAWFY motif are modelled according to the crystal structure of the rabphilin/Rab3a complex (Ostermeier and Brunger, 1999). Note that the helices may not be completely structured in the absence of Rab3a. A star indicates the approximate location of the mutation on RIM2 α that disrupts Munc13-1 binding. Figure from Dulubova et al., 2005.

1.7.2 Physiological Role of the Munc13- α RIM Interaction

The effects of overexpression of the RIM1 α binding region of Munc13-1, Munc13-1(1-451)EGFP, full-length Munc13-1, Munc13-1(1-1736)EGFP and a RIM1 α binding-deficient, priming-competent Munc13-1 construct, Munc13-1(520-1736)EGFP, were studied in wild type, glutamatergic neurons. Overexpression of

Munc13-1(1-451)EGFP led to a dramatic reduction of excitatory postsynaptic responses upon action potential-evoked release from mouse wild type neurons 8–10 hours post-infection. In contrast, overexpression of the full-length Munc13-1(1-1736)EGFP, for 8–26 hours post-infection and the amino terminally truncated, RIM1 α binding-deficient form, Munc13-1(520-1736)EGFP, for 8–10 hours post-infection, had no effect. This showed that Munc13-1(1-451)EGFP acts in a dominant-negative manner and causes a decrease in neurotransmitter release upon overexpression in wild type neurons (Betz et al., 2001). Experiments using hypertonic sucrose solution showed that vesicular release probability was not altered by the Munc13-1(1-451)EGFP overexpression and that the observed reduction in excitatory postsynaptic current (EPSC) amplitude was due to an underlying reduction in the size of the readily releasable vesicle pool. Munc13-1-deficient neurons are characterised by a drastically reduced pool of readily releasable vesicles (Augustin et al., 1999), and overexpression of Munc13-1(1-451)EGFP in wild type neurons created a phenocopy of Munc13-1-deficient nerve cells (Betz et al., 2001).

Overexpression of full-length Munc13-1(1-1736)EGFP in Munc13-1-deficient cells led to a significant increase of EPSCs as compared to uninfected Munc13-1 knockout cells, demonstrating that the Munc13-1 deletion mutant phenotype can be rescued by overexpression of full-length Munc13-1. In contrast, overexpression of the RIM1 α binding region of Munc13-1 alone or of the RIM1 α binding-deficient but priming-competent form of Munc13-1 had no effect on EPSC amplitudes in Munc13-1-deficient neurons. These findings confirmed that the changes observed in wild type mouse neurons overexpressing the dominant-negative Munc13-1(1-451)EGFP were due to an interference with a Munc13-1-specific reaction (Betz et al., 2001). In contrast to full-length Munc13-1, the priming-deficient Munc13-1(1-451)EGFP or RIM1 α binding-deficient form of Munc13-1, Munc13-1(520-1736)EGFP, could not rescue the Munc13-1 knockout phenotype 8–10 hours post-infection. However, the RIM1 α binding-deficient form of Munc13-1 (520-1736) but not the priming-deficient Munc13-1(1-451), led to a 50% rescue of the Munc13-1 knockout phenotype when cells were analysed at 22–26 hours post-infection. Overexpression of full-length Munc13-1(1-1736)EGFP completely reconstituted a wild type phenotype in knock out cells (Betz et al., 2001).

From biochemical data on Semliki Forest virus-mediated overexpression of proteins in various cell types, estimated post-infection levels of overexpressed Munc13-1 protein at 22–26 hours are increased 40- to 100-fold in comparison to wild type levels (Ashery et al., 2000) which can essentially flood the cells including the processes and presynaptic terminals. Therefore, it can be concluded from the post-infection time course of effects caused by overexpression of Munc13-1(520-1736)EGFP in Munc13-1 knockout neurons (no effect at 8–10 hours; partial rescue at 22–26 hours post-infection) that the RIM1 α binding-deficient Munc13-1(520-1736)EGFP is dysfunctional in neurons. However, once expression levels of Munc13-1(520-1736)EGFP in neurons reach extremely high levels, flooding neuronal processes and presynaptic terminals, it can function as a priming protein in presynaptic terminals, albeit with a significantly lower efficiency than full-length Munc13-1. Thus, both the RIM1 α binding amino terminus as well as the R region of Munc13-1 that carries the priming activity are necessary for proper function in neurons (Betz et al., 2001).

Recent electrophysiological experiments in the calyx of Held synapse have shown that application of a short RIM2 α fragment spanning the zinc finger domain (which is responsible for Munc13-1 binding), severely decreases the readily releasable pool of vesicles, while the mutant non-Munc13-1 binding, RIM2 α zinc finger domain (RIM2 α aa22-155^{K97E/K99E}) does not. However, the recovery of vesicles into the readily releasable pool was unchanged (Dulubova et al., 2005). These results imply that the α RIM-Munc13-1 interaction determines the total amount of primed and readily releasable vesicles, possibly by providing a site for vesicle priming, but does not affect the rate of replenishment of new readily releasable vesicles after depletion. The α RIM-Munc13-1 interaction was also shown to be important for both a fast-releasing and a more slowly releasable subpool of readily releasable vesicles, which can be distinguished at the calyx of Held synapse (Sakaba and Neher, 2001; Dulubova et al., 2005). The notion that the α RIM-Munc13-1 interaction plays a role in vesicle priming has all together been supported by the correlation between the decrease in priming and the reduction in Munc13-1 levels observed in RIM1 α deficient mice (Schoch et al., 2002; Calakos et al., 2004). This view is additionally supported by the fact that there exists a decrease in the readily releasable pool caused both by overexpression of a 451-residue amino terminal fragment of Munc13-1 in hippocampal cultures (Betz et al., 2001) and by expression of a short

RIM2 α fragment spanning the zinc finger domain RIM2 α (22-155) in the calyx of Held (Dulubova et al., 2005).

1.8 Aims of the Present Study

All of the above information shows the importance of the α RIMs and Munc13s. The accumulated data indicate that the interaction between these two active zone proteins may be a key regulator of presynaptic activity, with a link between Rab and SNARE function via Munc13. The interaction between Munc13s and α RIMs may couple synaptic vesicle priming with presynaptic plasticity. At the moment there exists a large body of both electrophysiological and genetic data on both proteins, and though some structural data have recently been obtained on the α RIMs (Dulubova et al., 2005) not much is known about the structural aspect of the Munc13s. It has been shown that the double point mutation K97E/K99E in the RIM2 α zinc finger domain disrupts the Munc13-1- α RIM interaction. Further electrophysiological experiments indicated that while the wild type RIM2 α had an effect on the readily releasable pool, the double mutant had no effect, proving the significance of the α RIM-Munc13-1 interaction (Dulubova et al., 2005).

The main aim of this study is to gain new insight into the molecular mechanism by which the vesicle priming proteins, Munc13-1/ubMunc13-2 and the α RIMs are functionally integrated into the protein machinery of the active zone. This was achieved via the identification of single point mutations in the Munc13 amino terminus, which destroy the Munc13- α RIM interaction. Using this tool, I identified the functional role of the α RIMs to be one of either synaptic targeting or anchoring of Munc13-1 and ubMunc13-2. The mutant Munc13 studies were complimented by analysis of the RIM1 α knock out mice, where the loss of RIM1 α results in a significant decrease in the protein levels and perturbed distribution of both Munc13-1 and ubMunc13-2.

Finally, the first step toward establishing a Munc13-1 conditional knock out was made by the cloning of a knock out vector, which will allow elimination of Munc13-1 in a cell-type restricted and temporally controlled manner.

2. Materials and Methods

2.1 Materials

2.1.1 Apparatus

Centrifuges	Beckmann Instruments GmbH, München Eppendorf GmbH, Hamburg Heraeus GmbH, Hanau
DNA Sequencer	Applied Biosystems
Developer	Agfa-Gevaert GmbH, Martsel, Belgium
Electroporation Apparatus	BioRad Laboratories GmbH, München
Freezer	Liebherr, Ochsenhausen
Electroporation system for Agarose Gels	Life-Technologies Gibco-BRL GmbH, Eggenstein-Leopoldshagen
Electroporation system for SDS-PAGE	BioRad Laboratories GmbH, München
Gel Dryer	Biometra GmbH, Göttingen
Gel Photography Apparatus	Intas GmbH, Göttingen
Heating block	Eppendorf GmbH, Hamburg
Incubators	Adolf Kühne AH, Heraeus GmbH, Hanau New Brunswick Scientific GmbH, Nürtingen
Refrigerator	Liebherr, Ochsenhausen
PCR Machine	Biometra GmbH, Göttingen
pH Meter	Knick, Schütt GmbH Göttingen
Pipettes, Pipetteboy	Gilson, Villiers-le-Bel, France Brandt GmbH, Wertheim
Shaking Incubator	New Brunswick Scientific GmbH, Nürtingen
1.5mL Eppendorf Shaker	Eppendorf GmbH, Hamburg
Sonicator	B. Braun Biotech International GmbH, Melsungen
Sterile Bank	Heraeus GmbH, Hanau
Water Bath	B. Braun Biotech International GmbH, Melsungen
UV-Cross Linker	Biometra GmbH, Göttingen

2.1.2

Chemicals

Agarose	Life-Technologies Gibco-BRL GmbH, Eggenstein-Leopoldshafen
Alkaline Phosphatase	Roche Diagnostics GmbH
Amino Acids	Sigma-Aldrich GmbH, Deisenhofen
Ammonium Persulfate (APS)	Sigma-Aldrich GmbH, Deisenhofen
Aprotinin	Roche Diagnostics GmbH
Bacto-Tryptone	DIFCO Laboratories GmbH, Augsburg
Bacto-Peptone	DIFCO Laboratories GmbH, Augsburg
Bacto-Agar	DIFCO Laboratories GmbH, Augsburg
Bacto-Yeast Extract	DIFCO Laboratories GmbH, Augsburg
Bacto-Yeast Nitrogen Base w/o Amino Acids	DIFCO Laboratories GmbH, Augsburg
Bradford Reagent	Bio-Rad Laboratories GmbH, München
Coomassie Brilliant Blue R250	BioMol Feinchemikalien GmbH, Hamburg
[α - ³² P]dCTP	Amersham-Buchler GmbH & Co, Braunschweig
DMSO Hybri-Max	Sigma-Aldrich GmbH, Deisenhofen
DNA-Standard <i>Bst</i> E II	New England Biolabs, Schwalbach
dNTPs	Pharmacia Biotech GmbH, Freiburg
Dry Milk	Glücksklee Magermilchpulver, Nestle Deutschland AG, Frankfurt/Main
ECL-Reagent	Amersham-Buchler GmbH & Co., Braunschweig
Ethidium Bromide	Sigma-Aldrich GmbH, Deisenhofen
Ficoll 400	Pharmacia Biotech GmbH, Freiburg
Fluoromount-G	Southern Biotechnology Associates, Birmingham, Al, USA
Glutathione	Sigma-Aldrich GmbH, Deisenhofen
Glutathione-Agarose	Sigma-Aldrich GmbH, Deisenhofen
Glycine	Bio-Rad Laboratories GmbH, München
Goat Serum	Life Technologies Gibco BRL GmbH Eggenstein

Igepal	Sigma-Aldrich GmbH, Deisenhofen
IPTG	BioMol Feinchemikalien GmbH, Hamburg
Leupeptin	Roche Diagnostics GmbH
Lysozyme	Sigma-Aldrich GmbH, Deisenhofen
N,N,N',N' Tetramethylethylendiamine (TEMED),	Bio-Rad Laboratories, GmbH München
Protein Molecular Weight Standards for SDS-Page	<i>Prestained SDS-PAGE Standards</i> , Bio-Rad Laboratories GmbH, München <i>Low Molecular Weight Range</i> , Sigma-Aldrich GmbH, Deisenhofen
PBS	Sigma-Aldrich GmbH, Deisenhofen
PEG 8000	Sigma-Aldrich GmbH, Deisenhofen
<i>Pfu</i> -Polymerase	Stratagene GmbH, Heidelberg
Phosphatidyl Choline	Avanti Polar Lipids, Alabaster/Alabama, USA
Phosphatidyl Serine	Avanti Polar Lipids, Alabaster/Alabama, USA
PMSF (Pentylmethylsulfonylfluoride)	Roche Diagnostics GmbH
Ponceau S	Sigma-Aldrich GmbH, Deisenhofen
Proteinase K	Roche Diagnostics GmbH
Protein Assay	Bio-Rad Laboratories GmbH, München
Protein G-Sepharose (4 Fast Flow)	Pharmacia Biotech GmbH, Freiburg
Restrictions Endonucleases	Roche Diagnostics GmbH or New England Biolabs, Schwalbach
RNase A	Sigma-Aldrich GmbH, Deisenhofen
Salmon Sperm - DNA	Sigma-Aldrich GmbH, Deisenhofen
SDS	Roche Diagnostics GmbH
Secondary Antibodies	Bio-Rad Laboratories GmbH, München
Sodium Cholate	Wako Chemicals GmbH, Neuss
T4 DNA-Ligase	Roche Diagnostics GmbH
<i>Taq</i> -Polymerase	ABI, Weiterstadt or Qiagen GmbH, Hilden
□-TPA	BioMol Feinchemikalien GmbH, Hamburg
□-TPA	Sigma-Aldrich GmbH, Deisenhofen
Tris Base	Sigma-Aldrich GmbH, Deisenhofen
Triton X-100	Roche Diagnostics GmbH

Tween 20 (Polyoxyethylensorbitanmonolaurat)	Polyoxyethylensorbitan Monolaurat, Sigma-Aldrich GmbH, Deisenhofen
X-Gal	BIOMOL Feinchemikalien GmbH, Hamburg

2.1.3 Kits

Plasmid Mini-, Midi- and Maxi Kits	Qiagen GmbH, Hilden
QIAquick PCR Purification Kit	Qiagen GmbH, Hilden
QIAquick Gel extraction Kit Protocol	Qiagen GmbH, Hilden
GeneMorph PCR Mutagenesis Kit	Stratagene GmbH, Heidelberg

2.1.4 Materials Used

Centricon 10	Amicon GmbH, Witten
Dialysis Tubes	Spectrum Medical, Los Angeles, USA
ECL- Film	Amersham-Buchler GmbH & Co., Braunschweig
Electroporation Cuvettes	Bio-Rad Laboratories GmbH, München
Hybond-N ⁺ Nylon-Membranes	Amersham-Buchler GmbH & Co., Braunschweig
Millipore GmbH, Eschborn	International Ltd., Maidstone, England
Nitrocellulose-Filter (Ø 137 mm) Type HA, 0,45 µm	Millipore GmbH, Eschborn
Plastic Tubes	Greiner, Falcon und Brandt
Reactions Eppendorf Tubes	Eppendorf, Hamburg
Film	Kodak
Whattman-Cellulose Filter Nr. 1 (Ø 150 mm)	Biometra GmbH, Göttingen
Whattman 3MM Chr	Whattman International Ltd, Maidstone, England

2.1.5 Material for Cell Culture

D-PBS	Life-Technologies Gibco-BRL GmbH, Eggenstein-Leopoldshafen
L-Glutamine	100x, Life-Technologies Gibco-BRL GmbH, Eggenstein-Leopoldshafen
Penicillin/Streptomycin	500x, Roche Diagnostics GmbH

For HEK 293-Cell Culture:

DMEM	with L-Glutamine, 4500 mg/l D-Glucose, without Sodium Pyruvate, Life-Technologies Gibco-BRL GmbH, Eggenstein-Leopoldshafen
Foetal Calf Serum	Heat inactivated, tested for Viruses and Mycoplasma, Life-Technologies Gibco-BRL GmbH, Eggenstein-Leopoldshafen
Trypsin-EDTA	1x, Life-Technologies Gibco-BRL GmbH, Eggenstein-Leopoldshafen
Cell Culture Flasks	Firms Greiner, Costar, Falcon and Nunc

For Primary Rat and Mouse Neuron-Cell Culture:

Albumin, Bovine	Sigma-Aldrich GmbH, Deisenhofen
B-27-Supplement	Life-Technologies Gibco-BRL GmbH
Cell Culture Flasks	Firms Greiner, Costar, Falcon and Nunc
Cysteine	Sigma-Aldrich GmbH, Deisenhofen
Dubelcco's MEM (DMEM)	with L-Glutamine, 4500 mg/l D-Glucose, without Sodium Pyruvate, Life-Technologies Gibco-BRL GmbH, Eggenstein-Leopoldshafen
Foetal Calf Serum	Heat inactivated, tested for Viruses and Mycoplasma, Life-Technologies Gibco-BRL GmbH, Eggenstein-Leopoldshafen
GlutaMAX™ I - Stock	Life-Technologies Gibco-BRL GmbH
Hank's Balanced Salt Solution (HBSS)	Life-Technologies Gibco-BRL GmbH

Neurobasal Medium	with L-Glutamine, 4500 mg/l D-Glucose, without Sodium Pyruvate, Life-Technologies Gibco-BRL GmbH, Eggenstein-Leopoldshafen
OptiMEM1 w/GlutaMAX™ I	Life-Technologies Gibco-BRL GmbH
Papain	Worthington Biomedical Corporation/Cell Systems
Poly-D-Lysine	Sigma-Aldrich GmbH, Deisenhofen
Trypsin Inhibitor	Sigma-Aldrich GmbH, Deisenhofen
Trypsin-EDTA	Life-Technologies Gibco-BRL GmbH

2.1.6 Bacterial and Yeast Strains and Cell Lines

<i>Escherichia coli</i> XL1-Blue	Stratagene GmbH, Heidelberg
<i>Escherichia coli</i> XL10-Gold	Stratagene GmbH, Heidelberg
<i>Escherichia coli</i> BL21/DE3	Stratagene GmbH, Heidelberg
HEK293	Human Embryonal Kidney fibroblast, transformed with Adenovirus Typ 5 DNA; Eurobio Laboratories eurobio GmbH, Raunheim
<i>Saccharomyces cerevisia</i> L40	Vojtek et al., 1993

2.1.7 Vectors

pBluescript II SK +/-	Stratagene, Heidelberg
pcDNA-3	Invitrogen, NV Leek, Nederland
pCMV5	Andersson et al., 1989
pCR2.1-TOPO	Invitrogen, NV Leek, Nederland
pCR-XL-TOPO	Invitrogen, NV Leek, Nederland
pEGFP-N1	Clontech, Heidelberg
pET 28a, pET 32c	Novagen, Merck Biosciences, GmbH
pFIEx-HR	Provided by Norbert B. Ghyselinck, PhD, France
pGex-KG	Guan and Dixon, 1991
pLexN	Vojtek et al., 1993
pQE-32	Qiagen GmbH, Hilden

pSFV1	Life-Technologies Gibco-BRL GmbH
pVP16	Vojtek et al., 1993

2.1.8 Primary Antibodies

Bassoon	Monoclonal, Stressgen Biotechnologies
bMunc13-2 (44)	Polyclonal provided by Dr. F. Varoqueaux, Göttingen
GDP Dissociation Inhibitor (GDI)	Polyclonal, provided by Prof. Dr. Reinhard Jahn, Göttingen
Green Fluorescence Protein (GFP) 3E6	Monoclonal, Molecular Probes
Green Fluorescence Protein (GFP)	Polyclonal, AbCam
(HIS) ₆	Monoclonal, Qiagen GmbH
Microtubule Associated Protein 2 (MAP2)	Monoclonal, Chemicon
Munc13-1 (40)	Polyclonal provided by Dr. F. Varoqueaux, Göttingen
Neurofilament	Polyclonal, Chemicon
NMDAR	Monoclonal, Brose et al., 1994.
RIM1/2	Monoclonal, Transduction Laboratories
Synaptophysin 7.2	Sigma-Aldrich GmbH, Deisenhofen
Synapsin	Monoclonal and polyclonal, Synaptic Systems
ubMunc13-2 (52)	Polyclonal provided by Dr. F. Varoqueaux, Göttingen
VGLUT1 and VGLUT2	Polyclonal (Guinea Pig), Chemicon

2.1.9 Secondary Antibodies

Anti Mouse (from Goat)	Horse Radish Peroxidase Conjugate, Bio-Rad
Anti Mouse (from Goat)	Alexa Fluor 488, 555, 633, 680 Molecular Probes
Anti Mouse (from Goat)	LI-COR IRDye 800 infrared dye, Rockland Immunochemicals
Anti Guinea Pig (from Goat)	Alexa Fluor 488, 555, 633 Molecular Probes

Anti Rabbit (from Goat)	Alexa Fluor 488, 555, 633, 680 Molecular Probes
Anti Rabbit (from Goat)	Horse Radish Peroxidase Conjugate, Bio-Rad
Anti Rabbit (from Goat)	LI-COR IRDye 800 infrared dye, Rockland Immunochemicals

2.1.10 Media and Solutions

1000x Ampicillin Stock Solution: 100mg/ml

300x Kanamycin-Stock: 10mg/ml

10x TBE (Agarose gel and Running Buffer Stock Solution) (per Litre):

108g Tris Base, 55g Boric Acid, 40ml 0.5M EDTA pH 8

Agarose gel-Probe Buffer (6x):

0.15% Bromophenol blue, 60% (v/v) Glycerine in H₂O.

Coomassie Brilliant Blue Solution :

0.15% Coomassie Brilliant Blue R250, 10% Acetic Acid, 25% Isopropanol, in H₂O, filtered.

Coomassie Decolouriser:

30% Methanol, 10% Acetic Acid in H₂O, filtered.

LB-Medium (per Litre):

10g NaCl, 10g Bacto-Tryptone, 5g Bacto-Yeast extract. Autoclave for 15 minutes at 121°C.

LB Plates:

As above for LB Medium, then add 15g Bacto-Agar added to 1L LB Medium. Autoclave for 15 minutes at 121°C. Depending on the type of selection, the required antibiotic was added after autoclaving when the solution was approximately 50°C).

NZY+ Broth (per Litre):

10g NZ amine (casein hydrolysate), 5g yeast extract, 5g NaCl, Adjust pH to 7.5 with NaOH. Autoclave for 15 minutes at 120°C. Add the following before use: 12.5ml 1M MgCl₂, 12.5ml 1M MgSO₄, 20ml of filter sterilized 20% (w/v) glucose.

PBS (per Litre):

8g NaCl , 0.2g KCl, 1.44g Na₂HPO₄·7 H₂O, 0.24g KH₂PO₄·H₂O. Adjust pH to 7.4.

Ponceau S Solution:

0.1% (w/v); 5% Acetic Acid; filtered

STET-Buffer (100ml):

8% Sucrose, 13.3ml 60% Sucrose, 0.5% Triton X-100, 5.0ml 10% Triton X-100, 50mM Tris-HCl, pH 8, 5.0ml 1M Tris-HCl, pH 8, 50mM EDTA, 10ml 0.5M EDTA. Sterilize by filtration.

TBS (10x):

0.2M Tris/HCl pH 7.4, 1.4M NaCl

1x TE-Buffer:

10mM Tris-HCl pH 7.4, 1mM EDTA. Autoclave for 15 minutes at 121°C.

Western Blot-Buffer A:

5% Goat serum, 5% Dried Milk, 1x TBS, 0.1% Tween 20

Western Blot-Buffer B:

1x TBS, 0.1% Tween 20

Western Blot-Buffer C:

1x TBS

Western Blot-Transfer Buffer:

3g Tris Base, 14.4g Glycine, 800ml H₂O, 200ml Methanol.

Media and Solutions for Homology-Screenings and Southern Blots

Top-Agar (0,7%):

100ml LB-Medium, 0.7g Agarose

SM-Buffer (per Litre):

5.8g NaCl, 2.0g MgSO₄ * 7H₂ O, 50ml 1M Tris/HCl; pH 7.5. Autoclave.

20x SSC:

3M NaCl , 0.3M Na₃ -Citrate

50x Denhardt´s:

1% Calf Serum Albumin, 1% Ficoll 400, 1% Polyvinylpyrrolidon in H₂O

20x SSPE (per Litre):

175.3g NaCl, 27.6g KH₂ PO₄ * H₂ O, 7.4g EDTA. Adjust pH to 7.4

Denaturing Solution:

1.5M NaCl, 0.5M NaOH

Neutralising Solution:

1.5M NaCl, 1M Tris/HCl; pH 7.4, mM EDTA

Prehybridisation Solution (100 ml):

50ml Formamide, 10ml 50x Denhardt´s solution, 15ml 10% SDS, 25ml 20x SSPE, 5ml d-H₂O, 1ml denatured Salmon Sperm - DNA (10mg/ml) (denatured by heating directly before use).

Hybridisation Solution:

Prehybridisation solution with radioactively marked DNA-Probes.

Media and Solutions for the Yeast-Two-Hybrid System

YPAD-Medium:

10g Bacto-Yeast-Extract, 20g Bacto-Peptone, 0.1g Adenine, dissolve in 900ml d-H₂O, autoclave then add 100ml 20% Glucose-Solution.

YEPD-Plates:

10g Bacto-Yeast-Extract, 20g Bacto-Peptone, 20g Bacto-Agar, dissolve in 900ml d-H₂O, autoclave for 15 minutes at 120°C then add 100ml 20% Glucose-Solution.

Selection Plates (per Litre):

1.2g Bacto-Yeast Nitrogen Base w/o Amino Acids, 5g Ammonium Sulphate, 10g Succinate, 6g NaOH, add required amino acids:

0.1g of Adenine, Arginine, Cysteine, Leucine, Lysine, Tryptophane and Uracile

0.05g Histidine, Isoleucine, Methionine, Phenylalanine, Proline, Serine and Tyrosine

0.051g Valine, 20g Bacto-Agar dissolve in 900ml d-H₂O. Autoclave for 15 minutes at 121°C. After cooling to 50°C add 0.1g/l Threonine, 0.05g/l Aspartic Acid and 100ml 20% Glucose solution.

- UT: Selection medium without Uracile and Tryptophane

- UTL: Selection medium without Uracile, Tryptophane and Leucine

- L + UT: Selection medium without Leucine

Lysis Buffer for Yeast:

2.5M LiCl, 50mM Tris/HCl pH 8.0, 4% Triton X-100, 62.5mM EDTA

Z-Puffer (per Litre):

16.1g Na₂HPO₄*7H₂O, 5.5g NaH₂PO₄*H₂O, 0.75g KCl, 0.246g MgSO₄*7H₂O, 2.7ml β-Mercaptoethanol. Adjust pH to 7.0.

X-Gal Solution:

50mg/ml in Dimethyl Formamide

2.1.11 cDNA Clones

Annotation: Expression constructs will be described by the vectors, the cloned cDNA fragments and the expressed amino acids are shown in brackets. Full-length expression constructs are shown only by the vector and the cDNA.

NCBI Gen-Bank Numbers:

Rattus norvegicus Munc13-1: U24070

Rattus norvegicus ubMunc13-2: AF159706

Rattus norvegicus RIM1: NM052829

Rattus norvegicus RIM2: AF199322

pCMV-5-RIM1 α (Wang et al., 1997) kindly provided by Dr. T.C. Südhof. The amino acid numbering for RIM1 α obtained from Wang et al., 1997.

All Munc13-1 clones used were based on the Munc13-1-cDNA, which due to alternative splicing, aa 1414-1437, as well as aa 1533-1551 are eliminated.

The following plasmid vectors, whose construction have already been described, (Augustin 1998; Betz 1998), were kindly provided by Dr. I. Augustin, Dr. A. Betz, Dr. H. Junge and Prof. Dr. N. Brose:

pCDNA-Munc13-1

pCDNA-ubMunc13-2

pEGFP-N1-Munc13-1

pEGFP-N1-ubMunc13-2

pGex-Munc13-1

pGex-Munc13-1(3-317)

pGex-ubMunc13-2(3-320)

pGex-RIM1(131-214)

pGex-RIM1(131-344)

pLexN-Munc13-1 (1-150)

pPrey85-RIM1 (1-344)

pSFV1-Munc13-1

pSFV1-ubMunc13-2

The following information gives the cloning strategy used for production of the constructs utilised in this thesis for the first time. High fidelity Pfu-polymerase, was used for the PCR cloning, and the oligo-nucleotides (house numbered) are given in 5' and 3' directions. The oligo-nucleotides were made by I. Thanhäuser, D. Schwerdfeger and F. Benseler with the department owned Oligo synthesizer (ABI

5000 DNA/RNA Synthesizer). All constructs were verified by both restriction digests and sequencing.

pEGFP-N1-Munc13-1^{I121N}

EcoRI and SacII were used to excise an 820bp fragment from pEGFP-N1-Munc13-1 full-length and this was directly subcloned into pBluescript II KS+. Oligos 3535/3531 were used for site directed mutagenesis on the pBluescript Munc13-1 (bp 1040-1860) and with the use of a silent point mutation, the restriction site TaqI was engineered. After the point mutations were introduced, the fragment was again excised and returned to the full-length pEGFP-N1-Munc13-1.

3535: CAAGGACCCACCTTCCACCGCAACCTCCTCGACGCACATTTTGAG

3531: CTCAAAATGTGCGTTCGAGGAGGTTGCGGTGGAAGGTGGGGTCCTTG

pEGFP-N1-ubMunc13-2^{I121N}

SpeI and ApaI were used to excise an 898bp fragment from pEGFP-N1-ubMunc13-2 full-length and this was directly subcloned into pBluescript II KS+. Oligos 3187/3185 were used for site directed mutagenesis on the pBluescript ubMunc13-2 (bp 1-1898) and with the use of a silent point mutation, the restriction site SacI was engineered. After the point mutations were introduced, the fragment was again excised and returned to the full-length pEGFP-N1-ubMunc13-2.

3187:CCCAACTCCTCATAAAAAGTTGCTTGGTACACGATTTGAGCTCCCTTTTGA
CATC

3185:GGGATGTCAAAGGGAGCTCAAATCGTGTACCAAGCAAGTTTTTATGAGG
AGTTG

pET32c-RIM1(131-214)

RIM1(131-214) was excised from pGex-RIM1(131-214) with EcoRI and SacI and subcloned directly into pET32c.

pGex-Munc13-1 (3-317)^{I121N}

Oligos 3535/3531 were used for site directed mutagenesis on the pGex-Munc13-1 (3-317) clone. With use of a silent point mutation, the restriction site TaqI was engineered.

3535: CAAGGACCCACCTTCCACCGCAACCTCCTCGACGCACATTTTGAG

3531: CTCAAAATGTGCGTTCGAGGAGGTTGCGGTGGAAGGTGGGGTCCTTG

pGex-ubMunc13-2(3-320)^{I121N}

Oligos 3187/3185 were used for site directed mutagenesis on the pGex-ubMunc13-2 (3-320) clone. With use of a silent point mutation, the restriction site *SacI* was engineered.

3187:CCCAACTCCTCATAAAAACTTGCTTGGTACACGATTTGAGCTCCCTTTTGA
CATC

3185:GGGATGTCAAAGGGAGCTCAAATCGTGTACCAAGCAAGTTTTTATGAGG
AGTTG

pLexN ubMunc13-2 (1-181)

Oligos 1280/2869 were used to PCR amplify the needed cDNA fragment from pCDNA-ubMunc13-2 and the restriction sites *EcoRI*- and *BamHI* were engineered. The fragment was digested with *EcoRI/BamHI* and subcloned into pLexN.

1280: GCGGAATTCATGTCGCTGCTCTGCGTGCGT

2869: GCGGGATCCCAAATAGGTCCAGTGACGACA

pLexN-Munc13-1(1-150)^{I121N}

Oligos 3535/3531 were used for site directed mutagenesis on the pGex-Munc13-1 (3-317) clone. With use of a silent point mutation, the restriction site *TaqI* was engineered.

3535: CAAGGACCCACCTTCCACCGCAACCTCCTCGACGCACATTTTGAG

3531: CTCAAAATGTGCGTTCGAGGAGGTTGCGGTGGAAGGTGGGGTCCTTG

pQE32-RIM1(1-344)

RIM1(1-344) was excised from pPrey85-RIM1 (1-344) with *BamHI* and *PstI* and subcloned directly into pQE32.

2.1.12 Conditional Munc13-1 Knock Out Vector

A previously published mouse genomic clone (pM13-27.1; Augustin et al., 1999b; Figure 31A) was used to construct the targeting vector for the generation of the Munc13-1 conditional knock out in the pFlEx-HR plasmid (provided by Dr. N. Ghyselinck). Exons 5 and 6, which encode the Munc13-1 C1 domain were targeted for knock out. The following oligos were used for the creation of the *5' arm*, *Short arm exon 5* and *floxed exons 5 and 6*, which were initially cloned into the pCR2.1 TOPO

plasmid and the 3' arm which was initially cloned into the pCR-XL-TOPO plasmid, before being subcloned into the pFIEEx-HR vector:

3' arm with MfeI and SmaI sites included for subcloning:

6811: GCGCATTTAAATCCCCAAACATATCAGATATCC

6009: GCGCAATTGCCCACTGCACCATTTTCTGG

5' arm with NotI and XhoI sites included for subcloning and BglII site added for Southern Blot analysis:

6010: GCGCTCGAGAGATCTCAGCTGGGTCGTGGTGAATAAAGG

6014: GCGGCGGCCGCGACAGGTGAAGTTGGACGTCAC

Floxed exons 5 and 6 with NruI and EcoRV sites included for subcloning:

6011: GCGTCGCGACCTACAAGTTGAGAAC

6015: GCGATATCGAGTTTTGCTCAGTGGGTGTC

Short arm exon 5 with PmeI and EcoRV sites included for subcloning:

6011: GCGTCGCGACCTACAAGTTGAGAAC

6012: GCGGTTTAAACGACTGCACCAATGACTGTGGTG

The Thymidine Kinase boxes were in the pBluescript plasmid and could be subcloned via the NotI site. pBluescript TK boxes plasmid was kindly provided by Dr. Andrea Betz.

2.2 Methods

2.2.1 Production of Competent Bacteria

100 ml LB-Medium is transfected with a single colony of the desired bacterial strain and incubated while shaking over night at 37°C. The cells are diluted 1:100 in one litre of LB-medium and shaken at 37°C until an OD₆₀₀ of 0.5 to 0.7 is reached. The cells are centrifuged for 15 minutes at 4000 x g_{max}, 4°C, then resuspend in one litre of ice cold 10% Glycerine in sterile H₂O. This washing step is repeated with 0.5 and 0.25 litre of 10% Glycerine in water. After the last washing step, the cells are

resuspend in 4ml 10% Glycerine, aliquoted and flash frozen in liquid Nitrogen and stored at -80°C .

2.2.2 Electroporation of Plasmid DNA into Bacteria

40 μl of competent bacteria, thawed gently on ice and 1 μl DNA (1 volume of the Ligation diluted 1/1 with dest. H_2O or 1/1000 dilution of a plasmid preparation) are mixed, incubated for one minute on ice in an electroporation cuvette (0.1cm, BioRad) and an electric pulse (*E. coli* Pulser, BioRad) of 1.80kV is administered. The cells are then immediately removed from the cuvette with 1ml LB-Medium and allowed to recover for 1 hour, at 37°C in a shaking incubator. After recovery, the cells are carefully centrifuged and the pellet resuspended in 100 μl of LB-Medium and plated out on selection plates.

2.2.3 DNA Plasmid Preparation

2.2.3.1 DNA Mini Preparation

This method from Holmes et al., 1981, is used for the quick analysis of clones after transformation to determine the success of transfer of the plasmid DNA into the bacterial cells, e.g. after a ligation. Single colonies are chosen and incubated overnight at 37°C in 2ml selection medium. 1.5ml of this culture are decanted into eppendorf tubes and centrifuged for 60 seconds at full tilt. Remove the supernatant resuspend the pellet in 300 μl STET (0.8% Sucrose, 0.5 % Triton X-100, 50mM Tris/HCl pH 8, 50mM EDTA). Add 25 μl of fresh lysozyme (10mg/ml) heat to 100°C on a heating block for 1 minute sharp then centrifuged at full tilt for 10 minutes. Removed the pellet and add 100 μl 7.5M NH_4Ac and 400 μl isopropanol to the supernatant. Centrifuge immediately for 30 minutes at full speed. Decant supernatant and dry pellet dried at room temperature for 1 minute. Resuspended in 50 μl TE (10mM Tris-HCl pH 7.4, 1mM EDTA pH 8.0).

2.2.3.2 Plasmid Preparation from the QIAGEN Protocol

DNA preparation by the “large-scale preparation of plasmid DNA: lysis by alkali” from Sambrook et al., 1989 or the he QIAGEN plasmid purification kits which allow for the isolation of supercoiled plasmid DNA with high yields can be used. This option is used when DNA is needed for sequencing or subcloning. The procedures were carried out as outlined in the QIAGEN plasmid purification handbook.

2.2.4 Determination of DNA Concentration

Due to their physical and chemical properties, DNA molecules in solution can absorb UV-light and this absorption can be measured by a spectrophotometer (GeneQuant RNA/DNA Calculator from Pharmacia, Uppsala). The higher the concentration, the greater the optical density at 260nm. The following relationship exists between the optical density (OD) and the DNA concentration:

Single stranded DNA: 1 OD₂₆₀ = 36mg/ml

Double stranded DNA: 1 OD₂₆₀ = 50mg/ml

2.2.5 Restriction Digests

Restriction digestion is the process of cleaving double stranded DNA molecules into discrete fragments with restriction endonucleases, which recognise specific sequences in the DNA molecule. Companies also deliver 10x concentrated buffer along with the enzymes for optimal reaction conditions. For digestion, plasmid DNA is incubated with the restriction mixture for 1.5 to 2 hours and the enzyme specific temperature, whereas genomic DNA is digested over night.

2.2.6 Dephosphorylation of the 5' end with Alkaline Phosphatase

Alkaline phosphatase catalyses the hydrolysis of 5'-phosphate residue from DNA, RNA and ribo- and deoxyribonucleoside triphosphates. The digested vector is treated

with alkaline phosphatase before ligation with the desired insert to prevent autoligation of the vector. The dephosphorylation protocol is provided by the producer.

2.2.7 Agarose Gel Electrophoresis

Agarose gel electrophoresis is used to separate, identify and purify negatively charged DNA based on their size. In agarose gel electrophoresis, the DNA is forced to move through a sieve of molecular proportions that is made of agarose. The positions of the bands are made visible and can be photographed in UV-light with ethidium bromide (254 or 314nm). Usually 0.7 to 2% gels are used. The Agarose is dissolved by heating in 100ml of the required 1x buffer, and 0.5µg/ml Ethidium Bromide is added after cooling to approx. 50°C, then poured into the gel chamber. DNA is then separated at constant voltage (80-120V) in the required 1x buffer. TBE-buffer for plasmid DNA and TAE for genomic DNA.

Gel and running buffer:

10x TBE

50x TAE (per Litre): 242g Tris Base, 57.1ml Acetic Acid, 100ml 0.5M EDTA pH 8.0.

6x Probe buffer: 0.25% Bromo phenol blue, 40% (w/v) Sucrose in H₂O.

2.2.8 Isolation of DNA-Fragments from Agarose Gels

The product QIAquick PCR purification Kit from the Qiagen firm was used. The protocol, outlined in the QIAquick Spin Handbook for purifying PCR fragments is provided by the producers.

2.2.9 Ligation

DNA ligases catalyse the formation of phosphodiester bonds between juxtaposed 5' phosphate and a 3'-hydroxyl terminus in duplex DNA. T4 ligase, which uses ATP as a source of energy, can ligate both sticky and blunt ends.

Reaction mixture: 20-100ng digested vector DNA and approximately double the amount of “insert” DNA. To a final volume of 20µl, 2µl of 10x T4 ligation buffer 1µl T4 ligase was added. Incubate at 16°C for 4-16 hours.

2.2.10 DNA-Sequencing

All DNA synthesis and sequencing was carried out by D. Schwerdfeger, I. Thanhäuser and F. Benseler from Department 5000 MPI for Experimental Medicine, using the department owned Oligo synthesizer, ABI 5000 DNA/RNA Synthesizer, and the *Applied Biosystems 373 DNA Sequencer* (modified from Sanger et al., 1977).

2.2.11 Polymerase Chain Reaction (PCR) (*Saiki et al., 1998*)

PCR is a rapid procedure for in vitro enzymatic amplification of a specific segment of DNA. The required materials include: the segment of double-stranded DNA to be amplified, two single stranded oligonucleotide primers flanking it (added in vast excess compared to the DNA to be amplified), high fidelity Pfu-polymerase, deoxyribonucleosides (dNTPs), buffer and salt. *Taq*-Polymerase is used for DNA synthesis for Genotyping mice.

The reaction mixture is as follows:

PCR with <i>Pfu</i> -Polymerase:	PCR for Genotyping:
5µl 1:100 diluted Template DNA	1µl Tail Prep DNA
0.2µl 5´ Oligo-nucleotide (5pmol)	0.1µl 5´ Oligo-nucleotide (5pmol)
0.2µl 3´-Oligo-nucleotide (5pmol)	0.1µl 3´-Oligo-nucleotide (5pmol)
2µl dNTP-Mix (2.5mM each)	.□µl dNTP-Mix (2.5mM each)
5µl 10x Polymerase-Puffer	2.5µl 10 x Polymerase-Puffer
1µl <i>Pfu</i> -Polymerase	0.25µl <i>Taq</i> -Polymerase
Final volume to 50µl with H ₂ O	Final volume to 25µl with H ₂ O

The PCR product to be used for cloning reactions, were purified with the *QIAquick PCR Purification Kit* from Qiagen.

2.2.12 Random Mutagenesis PCR

Random mutagenesis is powerful tool for elucidating protein structure-function relationships and for modifying proteins to improve or alter their characteristics. Error prone PCR is a random mutagenesis technique for generating amino acid substitutions in proteins by introducing mutations into the gene during PCR. Mutations are deliberately introduced using the error prone DNA polymerase, Mutazyme™, from the GeneMorph PCR mutagenesis kit.

The reaction mixture is as follows:

PCR with <i>Mutazyme</i> -Polymerase:
1µl 1:200 diluted Template DNA (ca. 10ng)
0.2µl 5' Oligo-nucleotide (5pmol)
0.2µl 3'-Oligo-nucleotide (5pmol)
2µl dNTP-Mix (2.5mM each)
5µl 10x Mutazyme reaction buffer
1µl Mutazyme
Final volume to 50µl with H ₂ O

2.2.13 Site Directed Mutagenesis

The *Quicksite Mutagenesis Kits* (Stratagene) was used for the creation of specific point mutations in various expression constructs. The required oligo-nucleotides containing the desired point mutation were constructed and the wild type DNA was used as template. The protocol is detailed in the instruction manual provided by the manufacturer.

2.2.14 *Yeast Two-Hybrid Screens and Related Methods, (Fields and Song, 1989)*

2.2.14.1 *Overview*

The standard yeast two-hybrid system identifies an interaction between two proteins by taking advantage of the properties of yeast (the L40 *Saccharomyces cerevisiae* yeast strain was used for this study). The basic principle of the yeast two-hybrid system is that two chimeras, one containing a DNA-binding domain and one that contains a transcription activation domain, are co-transfected into an appropriate host strain, if the fusion partners interact, the DNA-binding domain and transcription activation domain are brought into close proximity and can activate transcription of reporter genes (here *LacZ*). The protein for which interaction partners are being sought (“*Bait*”) is expressed in the vector pLexN, which expresses the protein as a fusion product of the protein of interest, the DNA-binding domain of the transcription factor *LexA* and a nuclear location signal. The *LexA* protein binds to the *lexA*-operator, a DNA sequence under the control of the transcription product. The expression vector pVP16, is used for the expression of possible interaction partners (“*Prey*” constructs). The protein is expressed as a fusion product of the possible interaction partner, a cDNA library for example, and the transcriptional activator VP16 from Herpes Simplex. When there is an interaction between the “*Bait* protein” and the “*Prey* protein”, this complex is then transported into the nucleus of the yeast and this translocation process is imparted by the “*Bait*” fusion protein. Identification of interacting proteins comes through the analysis of the yeast, which contains a *LacZ* gene, which is under the control of the *lexA* operator.

In this study, the yeast two-hybrid system was not used in the conventional manner for identifying novel binding partners, but as a tool for identifying structural changes in the Munc13 proteins, which would eventually result in a functional difference in their interaction with the active zone protein, RIM1 α . To identify amino acid residues that rendered the ubMunc13-2 amino terminus non-RIM1 α binding while leaving other interactions unaffected, the random mutagenesis approach, which resulted in a bait library of mutated ubMunc13-2 amino terminal constructs (see 2.2.12) was used in cooperation with the reverse yeast two-hybrid system. Due to experimental difficulties experienced in the cloning of the Munc13-1 amino terminus, the ubMunc13-2 amino

terminal construct LexA-ubMunc13-1(1-181), which is highly homologous to the amino-terminal region of Munc13-1 and contains the minimal α RIM binding region (Betz et al., 2001) was used as a model protein in the initial yeast two-hybrid screen. As prey, the amino terminal, Rab3 binding, zinc finger region of RIM1 α (1-344) was cloned, VP16-RIM1 α .

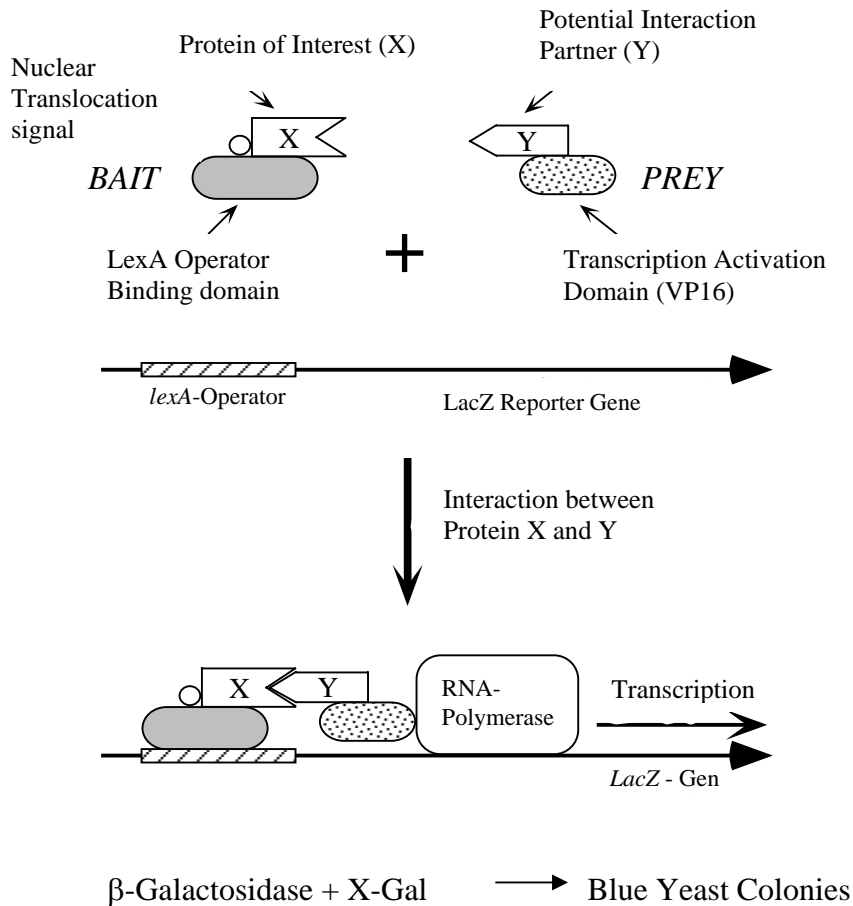


Figure 8: Schematic Diagram of the Molecular Mechanism on the Yeast Two-Hybrid System.

2.2.14.2 Media and Solutions for the Yeast Two-Hybrid System

Buffers and Solutions:

100mM Lithium Acetate (LiAc) / 0.5xTE

100mM Lithium Acetate (LiAc) / 40% PEG / 1xTE

DMSO

TE

Salmon Sperm Carrier DNA:

DNA (Sigma – D1626 Type III Sodium from Salmon Testes), was dissolved in TE, 10mg/ml, and incubated overnight at 4°C to give a homogenous viscous solution. The solution was then sonicated twice for 30 seconds with a large probe at 3/4 power. The resulting DNA has an average size of 7kb judged from an ethidium bromide gel and ranged in size from 15-2kb. The DNA solution was extracted once with TE saturated phenol, once with phenol : chloroform (50:50) and once with chloroform. The DNA was then precipitated by adding 1/10 volume of 3M sodium acetate (pH 6.0) and 2.5 volumes of ice-cold ethanol (99%). The precipitate was collected by centrifugation at 12000 x g_{max} and washed with 70% ethanol, partially dried under vacuum and redissolved in TE at 10mg/ml. This solution was then stored in aliquots at -20°C.

Media:

YPAD (per Litre)

YPED-Agar (per Litre)

Selection Media (per Litre):

1.2g yeast nitrogen base without amino acids, 5g ammonium sulphate, 10g succinic acid, 6g NaOH, 0.1g of each of the following amino acids: adenine, arginine, cysteine, leucine, lysine, threonine, tryptophane, uracile.

0.05g of each of the following amino acids: aspartic acid, histidine, isoleucine, methionine, phenylalanine, proline, serine, tyrosine, and valine.

Autoclave for 15 min and after cooling add 100ml 20% glucose, threonine and aspartic acid (which cannot be autoclaved)

-UTL Media (per Litre):

As above with the following amino acids omitted: uracile, tryptophane and leucine

-L+UT Media (per Litre):

As above with the following amino acid omitted: leucine

Selection Plates:

As above for the selection media with 20g agar added before autoclaving.

2.2.14.3 Procedure for the Yeast Two-Hybrid System

2.2.14.3.1 Transformation of DNA into Yeast

In this experiment, the yeast is transformed using a heat shock procedure with DMSO and salmon sperm carrier DNA.

10ml of YPAD was inoculated with a single colony of L40 and grown overnight at 30°C. This solution was then diluted to an OD₆₀₀ of 0.4 in 50ml YPAD and allowed to grow for an additional two hours. The cells were pelleted by centrifugation for 5 minutes at 1278 x g_{max}, and resuspended in 40ml TE. The cells were spun again, and the suspended in 2ml 100mM LiAc / 0.5x TE and incubated at RT for 10 minutes. The following were then dispensed to tubes: 1µg of each plasmid DNA, 100µg denatured, sheared salmon sperm DNA, 100µl of the yeast suspension and 700µl 100mM LiAc / 40% PEG / 1x TE. This was then incubated at 30°C for 30 minutes. 88µl DMSO was added, the solution mixed, and heat shocked at 42°C for 7 minutes. The cells were pelleted and washed with 1ml TE, resuspended in 50-100µl TE and plated on the appropriate selection plate.

2.2.14.3.2 β-Galactosidase Test

β-galactosidase activity in the yeast clones positively correlates with the intensity of interaction of the test plasmids. The qualitative filter test was used for quick analysis of the clones. The double transformed yeast was grown for 2-4 days at 30°C on – UTL plates. A dry nitrocellulose filter was placed carefully onto the yeast colonies and this was then places colony side up, on a pre-cooled aluminium boat floating in liquid nitrogen. After 30 seconds, the boat and filter were immersed for 5 seconds. The filter was placed, colony side up, at room temperature until thawed. 5ml of Z-buffer and 50µl 50mg/ml X-gal were placed in the cover of a petri dish and one Whattman filter circle was placed in the mixture, followed by the nitrocellulose filter paper, colonies facing up. The plate was then incubated at 30°C, and strong interactions yielded detectable colour in less than 30 minutes.

Buffers and Solutions:

Z-Buffer (per Litre):

60mM Na₂HPO₄, 40mM NaH₂PO₄, 10Mm KCl, 1mM MgSO₄ pH 7.0, 2.7ml β-Mercaptoethanol

X-Gal Stock Solution:

50mg/ml 5-Bromo-4-Chloro-3-Indolyl-β-D-Galactiside in Dimethylformamide

2.2.14.3.3 Preparation of Plasmid-DNA from Yeast

The enzyme, Quantazyme ylgTM, was utilised to quickly obtain the plasmid-DNA from the yeast cells by digesting the β-1,3-linked glycans in the yeast cell wall, causing lysis due the cells to becoming increasingly less stable to osmotic pressure. Quantazyme ylgTM is a recombinant β-1,3-glucanase that has yeast lytic activity. The enzyme was purified from *E. coli* and was free of protease activity, and free of detectable nucleic acids and endo- and exo-nucleases.

30μl of a 7U/ml lyticase solution was aliquoted into the wells of a 96 well plate. The white colonies detected in the filter test were picked from the –UTL master plate and placed into single wells to be digested. The plates containing the yeast were incubated at 30°C for 4 hours then frozen and thawed twice for full lysis of the cells. 1μl of the digest was then transformed into XL1-Blue via electroporation and the DNA prepared and digested as outlined in previous methods. If the clones contained an insert of the correct size, ubMunc13-2(1-181) as determined by agarose gel electrophoresis then the clone was sent for sequencing.

2.2.15 Biochemical Experiments

2.2.15.1 Sodium-Dodecyl-Sulphate-Polyacrylamide-Gel Electrophoresis (SDS-PAGE) (Laemmli, 1970)

Electrophoresis is used to separate complex mixtures of proteins, to investigate subunit compositions, to purify proteins and to verify homogeneity of protein samples. In SDS polyacrylamide gel electrophoresis, proteins are separated based on molecular size as they migrate in response to an electrical field through pores in the gel matrix towards the anode; pore size decreases with higher acrylamide concentrations. After the samples are solubilized by boiling in the presence of SDS, an aliquot of the protein is added to the lane and the individual proteins are separated electrophoretically.

Buffers and Solutions:

Stacking Gel Buffer:

0.5M Tris/HCl pH 6.8, 0.4% SDS

Separating Gel Buffer:

1.5M Tris/HCl pH 8.8, 0.4% SDS

AMBA:

30% Acrylamide/N,N'-Methylene-bis-Acrylamide Solution

10% APS:

10% Ammonium Persulphate in dH₂O

Running Buffer (per Litre):

3g Tris Base, 14.4g Glycine, 2g SDS, pH 8.8

Water Saturated 1-Butanol

BIO-Rad Prestained SDS-PAGE Standards, High Range Marker:

213 kDa, 119 kDa, 83 kDa, 47 kDa

BIO-Rad Prestained SDS-PAGE Standards, Broad Range Marker:

250 kDa, 150 kDa, 100 kDa, 75 kDa, 50 kDa, 37 kDa, 25 kDa, 15 kDa, 10 kDa

BIO-Rad Prestained SDS-PAGE Standards, Low Range Marker:

111 kDa, 77 kDa, 48 kDa, 34 kDa, 29 kDa, 21 kDa

12 % and 7.5% SDS-PAGE Gel Composition

	Separation gel 12%	Separation gel 7.5%	Stacking gel 3.75%
H ₂ O	1.75ml	2.5ml	1.25ml
AMBA	2ml	1.25ml	250µl
Buffer	1.25 ml	1.25ml	500µl
TEMED	7µl	7µl	5µl
10% APS	15µl	16µl	12µl

Preparing and running the SDS-PAGE-Gels

The glass walls, spacers (1mm) and the combs were cleaned with ethanol. After pouring the separation gel, the surface was covered with water-saturated butanol to obtain a smooth surface of the gel. After polymerisation of the gel, the butanol was removed and the remaining volume above the gel was filled with stacking gel solution and the comb was inserted. After the gel was polymerised, the samples were mixed with the SDS buffer and boiled for 5 min before loading on the gel. The gel chamber was filled with SDS running buffer and electrophoresis was performed at constant current of 15mA per gel. After the proteins reached the border of the separation gel, the current was elevated to 25mA per and ran either for the appropriate length of time or until the blue front ran out of the gel.

2.2.15.2 Coomassie-Blue Staining

After electrophoresis the stacking gel was discarded and the separation gel was stained for 15-30 min in 25% (v/v) isopropanol, 10% (v/v) acetic acid and 0.15% (w/v) Coomassie Brilliant Blue R-250 while shaking. Then the gel was destained in 30% (v/v) methanol and 10% (v/v) acetic acid for 15 min. After scanning the gel on the computer-scanner the gel was dried in the gel dryer, wrapped in cellophane foil.

2.2.15.3 Transfer of Proteins from Acrylamide Gel to Membrane, Western Blotting

Western blotting (or immunoblotting) is used to identify specific antigens recognised by polyclonal or monoclonal antibodies. The protein samples are first separated by SDS-PAGE, and the antigens are electrophoretically transferred at 250mA for two hours, or overnight at 40mA to a nitrocellulose, PVDF or nylon membrane, a process that can be monitored by reversible Ponceau S staining. The transferred proteins are bound to the surface of the membrane, providing access for reaction with immunodetection reagents.

Buffers and Solutions:

Blot Buffer:

3g Tris Base, 14.4g Glycine, 800ml dH₂O, 200ml Methanol

Ponceau S:

0.1% (w/v) Ponceau S, 5% Acetic Acid

Material:

Nitrocellulose paper, the size of the gel

4 sheets *Whatman #1 paper*, the size of the gel

2.2.15.4 Immunostaining of Blots with HRP-labelled Secondary Antibody and Visualisation with Enhanced Chemilluminescence (ECL)

For immunoblotting, a primary antibody is used which recognises a specific epitope on the protein of interest. Unspecific binding is inhibited additionally by the use of blocking solution containing either protein or detergent blocking agents. To detect the antigen-antibody binding reaction, a Horseradish peroxidase (HRP)-labelled secondary antibody is used, which binds to the first unlabelled antibody (indirect staining method). The active components of the ECL system are luminol and H₂O₂. The peroxidase reduces the hydrogen peroxide, and the resulting oxygen oxidises

the luminol, which releases light. The chemilluminescence is then strengthened through appropriate “enhancers” and this is then visible on Kodak XAR-5 film.

Buffers and Solutions:

Blocking Buffer (200ml):

5% Milk Powder (10g), 5% goat serum (10ml), 20ml 10x TBS, 0.1% Tween 20

Washing Buffer (100ml):

10ml 10x TBS, 0.1% Tween 20

1x TBS

Exposure of Nitrocellulose Membrane

Number of Washes	Buffer	Time (min)
1	Blocking Buffer A	30
1	Blocking Buffer and 1° Ab	60
5	Blocking Buffer A	5
1	Blocking Buffer and 2° Ab	60
3	Blocking Buffer	5
2	Washing Buffer B	5
1	Buffer C (1X TBS)	1

After the above incubations were done, the membrane was placed on a clean glass plate. The two components of the ECL-system were then mixed and this was pipetted onto the nitrocellulose and incubated for one minute after which the excess liquid was soaked away. A clean transparency was then placed on top of the membrane and exposed to Amersham Hyperfilm film for differing lengths of time, e.g. 1 sec, 5 sec, 10 sec, 20 sec, 30 sec, 1 min, 5 min, 10 min and a long exposure to establish the exact position of the marker.

2.2.15.5 Immunostaining of Blots with Infra-Red Labelled Secondary Antibody and Visualisation with the Odyssey System

The Odyssey™ Imaging System can accurately quantify proteins in Western blot analyses using advanced infrared imaging. Odyssey is uniquely equipped with two infrared channels for direct fluorescence detection on membranes using infrared-labelled antibodies, Alexa Fluor 680-labelled secondary antibodies (Molecular Probes) and LI-COR IRDye 800 infrared dye-labelled secondary antibodies (Rockland Immunochemicals). With two detection channels, two separate target samples can be simultaneously probed on the same gel. With direct detection, all infrared-labelled antibodies fluoresce when excited by the laser giving a wide linear range. Infrared detection produces a wider linear range than other fluorescent imaging systems because low background fluorescence results in higher sensitivity.

The procedure with the ECL detection system and the Odyssey detection system are essentially the same, the only significant difference being that all incubations from the addition of the secondary antibody onwards are done in the dark.

2.2.15.6 Expression of GST-Fusion Proteins (*Guan & Dixon, 1991*)

This procedure make use of proteins fused to the Glutathione-S-Transferase (GST fusion proteins) to affinity purify other proteins, a technique also known as GST pulldown purification. The GST fusion protein is first purified on glutathione-agarose beads and this bead-bound fusion protein is then used as “bait” to test for binding to a known or suspect proteins. This technique can be used to complement the yeast two-hybrid system to assess protein-protein interaction.

Procedure:

The pGex-KG vector is used for the expression of GST-fusion proteins in BL21DE3 bacterial cells. An over night culture of 100ml LB/Ampicillin (100µg/ml Ampicillin) medium is made from a single colony and the following day the culture was diluted

1:100 in LB-Ampicillin and shaken for an additional hour at 37°C. The bacterial culture was then cooled by shaking for half an hour at room temperature, then 0.1mM of IPTG was added and this was incubated a further four hours at room temperature to induce protein expression. The cells were then sedimented by centrifugation (4500 x g_{max} , 20min, 4°C) and the pellet resuspended in 30ml PBS, to which 0.1mg/ml freshly prepared Lysozyme and 0.1mM PMSF, 0.1mM Aprotinin and 0.1mM Leupeptin were added. The cells were then lysed by sonification using the Macro-tip from the *Labsonic U Sonifiers* (Braun) (3 x 20 seconds). 1% Triton X-100 was added to the suspension to solubilize the protein and this was shaken for 15 minutes on ice. The cells were pelleted by centrifugation (27500 x g_{max} , 30 minutes, 4°C) and the clear supernatant which contained the GST-fusion proteins was adsorbed overnight at 4°C onto the glutathione agarose (Sigma, Deisenhofen, Federal Republic of Germany). The agarose beads with the bound proteins were washed the following day five times with PBS/0.1% Triton X-100, 2mM PMSF then resuspended in an equal volume of PBS/0.1% Triton X-100, 2mM PMSF to bed-volume. The concentration of the proteins was determined by comparison with defined concentrations of marker proteins (e.g. BSA) using SDS-PAGE. The proteins, while still attached to the glutathione agarose beads, can be kept for a few days on ice, at 4°C. The proteins can also be eluted from the beads. The agarose-bead-bound protein were initially washed twice with 100mM Tris/HCl pH 8.0, 0.1% Triton X-100, 0.2mM PMSF, then incubated, while rotating with 100mM Tris/HCl pH 8.0, 0.1% Triton X-100, 0.2mM PMSF and 9mg/ml reduced Glutathione at room temperature for 45 minutes. The eluted proteins were concentrated to a volume of 1mL by centrifugation using a Centricon, and then dialysed at 4°C three times, four hours each, against the desired buffer. The dialysis tubes were pre-incubated and swollen in distilled water, then the concentrated proteins secured within the tube with the appropriate dialysis clamps and under gently stirring, dialysed against at least 500 times the volume of the desired buffer. After dialysis, the proteins were flash-frozen in liquid Nitrogen and stored at -80°C.

2.2.15.7 Production of Crude Synaptosomal Extract from Rat Brain

All steps after the complete removal of the rat brains are done on ice in the 4°C room and all centrifugation steps are done at 4°C. Twenty cortices from the rat brains were placed in 160ml ice-cold 320mM sucrose solution and homogenised at 900OpM (ten up-down strokes) with a Glass Teflon Homogeniser. The homogenate was centrifuged for 10 minutes at 900 x g_{max} , the pellet was discarded and the supernatant was again centrifuged for one hour at 4000 x g_{max} . The resulting pellet was resuspended in 50ml 320mM Sucrose using the homogeniser (2 up-down strokes, 900OpM). The crude Synaptosome solution was then aliquoted, flash frozen in liquid Nitrogen and stored at -80°C and one aliquot was utilised for the determination of the protein concentration.

2.2.15.8 Subcellular Fractionation (*Huttner et al., 1983*)

The different fractions are designated as follows: *H*, Homogenate; *P*₁, Nuclear Pellet; *S*₁ Supernatant after Synaptosome Sedimentation, *P*₂, Crude Synaptosomal Pellet; *P*₃, Light Membrane Pellet; *S*₃, Cytosolic Fraction; *LP*₁, Lysed Synaptosomal Membranes; *LS*₁, Supernatant after *LP*₁ sedimentation. All steps after the complete removal of the rat brains are done on ice in the 4°C room and all centrifugation steps are done at 4°C. Fifteen cortices from the mouse brains were placed in 40ml ice-cold 320mM sucrose solution and homogenised at 900OpM (twelve up-down strokes) with a Glass Teflon Homogeniser. The homogenate was centrifuged for 10 minutes at 800 x g_{max} , and the pellet, *P*₁ was resuspended in 40ml of 320mM sucrose, an aliquot was kept for concentration determination and the rest flash frozen in liquid nitrogen. The supernatant was centrifuged at 9200 x g_{max} for 15 minutes, producing *S*₁ and *P*₂. An aliquot of supernatant *S*₁ was kept for concentration determination and the rest centrifuged at 165000 x g_{max} for two hours, giving rise to the supernatant, *S*₃ and pellet, *P*₃. An aliquot of pellet *P*₂ was kept for concentration determination while the rest was washed through resuspension in 10ml sucrose and centrifugation at 9200 x g_{max} for 15 minutes. The crude synaptosomal pellet, *P*₂, was then resuspended in 7ml 320mM sucrose and subjected to osmotic lysis through the addition of 9 volumes of water and protease inhibitors (PMSF, Leupeptin and Aprotinin; 0.1mM end

concentration). The homogeniser (3 up-down strokes, 1500rpm) was used for resuspension. The suspension was centrifuged at $25000 \times g_{\max}$ for 20 minutes giving rise to the supernatant, LS₁ and pellet, LP₁.

2.2.15.9 Determination of Protein Concentration

The determination of protein concentration was carried out using the product manual provided for *Protein Assay* from the Bio-Rad Company and it is based on the Bradford Method (Bradford, 1976).

2.2.15.10 Cosedimentation Experiments to Investigate Protein-Protein Interactions

Solubilizing Buffer: 0.1M NaCl, 25mM HEPES/KOH pH 7.4, 2mM EGTA pH 8.0, 1% sodium cholate, 0.2mM PMSF, 1 μ g/ml Aprotinin, 0.5 μ g/ml Leupeptin

Wash Buffer: 0.1M NaCl, 25mM HEPES/KOH pH 7.4, 2mM EGTA pH 8.0, 0.25% sodium cholate

Crude synaptosomes from rat brain were solubilized at a protein concentration of 2mg/ml in the solubilizing buffer while stirring on ice for 30 minutes and all insoluble material was removed by centrifugation (10 min, $250000 \times g_{\max}$, 4°C) and the supernatant was used for further experimentation. 10mg of total protein in an appropriate volume, was incubated with 20 μ g glutathione agarose bead-bound GST-fusion protein, and incubated while rotating overnight, at 4°C. An aliquot of the supernatant was also taken and added to Laemmli buffer to be used later as the "Load" (positive control). The following day, the bead-bound proteins were washed five times with the wash buffer (the beads were pelleted for 1 minute at $1000 \times g_{\max}$, the supernatant removed and the wash buffer added, and again centrifuged). The washed bead-bound proteins were then boiled for 5 minutes in SDS-PAGE sample buffer and analysed by SDS-PAGE and immunoblotting.

2.2.16 Cell Culture and Immunocytochemistry

2.2.16.1 Treatment of Coverslips for Culturing HEK293 and Primary Neuron Cultures to be used for Microscopy

To attain better cell adhesion, the surfaces of the coverslips were coated with Poly-D-Lysine in sterile atmosphere. The coverslips were incubated with Poly-D-lysine for at least one hour (usually overnight) at 37°C. The coverslips were then washed twice with sterile water, once with HBSS and then incubated with DMEM complete (DMEM, 5% FCS, 1% Penicillin/Streptomycin, 1% GlutaMAX™ I).

2.2.16.2 HEK293 Cell Culture

To re-culture deep frozen cells, the cells were removed from the liquid nitrogen tank transported on dry ice and thawed by gentle shaking in a 37°C water-bath. All cell culture work was done under the sterile hood. The thawed cells were then transferred to a 10cm petri dish and the culture grown in a steam saturated, 37°C, 5% CO₂ incubator. The culture medium was: DMDM containing 10% Foetal Calf Serum, 2mM L-Glutamine, 100IU/ml Penicillin, and 100mg/ml Streptomycin. When the cells grew to a confluent layer in the dish, they were split after first washing with D-PBS, then adding 0.25% Trypsin. When the cells detached from the petri-dish they were diluted 1:5 or 1:10 with medium and transferred to another cell culture container. For transfection experiments where the cells were further analysed through microscopy, the cells were plated out on circular coverslips (Ø 12mm). For these experiments the cells were split at a 1:5 ratio after the Trypsin treatment, to ensure that the cells were approximately 60-70% confluent for transfection on the following day.

2.2.16.3 Primary Mouse and Rat Neuron Culture

Material:

Large ice bucket, large Petri dish with embryos

24-well plates

Falcon tubes, 15 and 50 ml

1.5 and 2ml E-cups (autoclaved)

rack for e-cups for tails, bodies, and rest of the brain

3 cm diameter Petri dishes (Nunc)

glass coverslips (autoclaved) (12 mm diameter for 24-well plates)

Dissection tools (scissors, forceps, spatula, dissection scissors)

Beakers with alcohol

Buffers and Solutions:

Poly-D-lysine 5mg, Sigma P-7280 MW30.000-70.000 (DM65), lyophilised
Prepare 0.05mg/ml in PBS (0.005%): Mix in the bottle with 40ml
PBS, transfer, fill up to 100 ml, sterile filter

HBSS 1x

DMEM high glucose 1x

Sterile distilled H₂O 1l

Neurobasal 1x

B-27 50x

D-PBS 1x

Trypsin-EDTA 10x, lyophilised, reconstitute in 10 ml water

Penicillin/

Streptomycin 100ml 10.000U/ml

DNase 1 Roche, 100 mg cell culture grade

L-Glutamine 200mM, 100x

GlutaMAXTM I supplement, 200mM

Foetal calf serum (FCS) heat inactivated, 500 ml

Solution 1 2mg Cysteine, 10ml DMEM, 1mM CaCl₂ (stock 100mM), 0.5mM
EDTA (stock 50mM), (count 0.5 ml/brain)

Papain Solution: mix 20-25 units Papain/ml of Solution and bubble with carbogen gas (95% oxygen, 5% carbon dioxide) for 10-20 minutes (until clear solution). Sterilize the Papain solution through a 0.2µm filter.

Stop solution: 25mg Albumin, 25mg Trypsin inhibitor, 9ml Dubelcco's MEM (DMEM), 1ml foetal calf serum (FCS). Keep solution in water bath at 37°C until use

Ready media

DMEM Complete: 50ml DMEM, 10% FCS, 2mM GlutaMAX™ I, Pen/Strep 1:100

Neurobasal Complete: 100ml Neurobasal, 2mM GlutaMAX™ I, 2ml 1x B-27 supplement, 10000IU Penicillin and 10mg Streptomycin

Procedure

Brain preparation

The UV lamp was turned on 30 min before starting the experiment, under the hood and on the bench.

Mutant Mice Neuron Cultures

The individual brains were collected from the newborn mice pups in HBSS 4°C. The hippocampi were dissected out and transferred immediately to 0.5ml room temperature Papain solution and incubated at 37°C for 55 minutes under gentle agitation (shaking at 400 in modern Eppendorf shaker). The Papain solution was carefully removed (by putting hippocampi at wall of tube), 0.5ml prewarmed Stop solution was added and the hippocampi were kept at 37°C for 15 minutes under gentle agitation (shaking at 400 in modern eppendorf shaker). All the supernatant was carefully removed and 0.1ml of prewarmed Neurobasal medium was added. The hippocampi were gently triturated 10 times with a yellow tip and after leaving the tubes to stand for 1 or 2 minutes, the supernatant was transferred to 1ml of prewarmed Neurobasal medium. Again, 0.1ml of prewarmed Neurobasal medium was added to the remaining hippocampi and gently triturated 10 times with a yellow

tip. After leaving the tubes to stand again for 1 or 2 minutes, the supernatant was transferred to the same 1ml of prewarmed Neurobasal medium. The cells were counted and approximately 20000-60000 cells were plated out per well in 24 well plate (with 0.5ml prewarmed Neurobasal medium per well). The medium was not changed.

Rat neuron cultures

The brains from the embryos (E18.5) were dissected out and collected in a dish with HBSS and the hippocampi were removed and pooled together in a 1ml Falcon tube. The hippocampi were washed 3 times with HBSS then 200 μ l Trypsin-EDTA (1% final) was added to 1800 μ l HBSS, and left for 20 min in the 37C water bath. After incubation, the hippocampi were wash 5 times with HBSS and transferred to a 2ml eppi-cup, where 1600 μ l HBSS was added with 400 μ l DNase (0.01% final). The hippocampi were triturated slowly with a 2ml syringe with orange canula (3 times), then with a grey canula (20 times). The triturated cells were then filtered through a cell strainer into a 50ml Falcon tube, and made up to a volume of 20ml with complete DMEM. 10 μ l of the neuron solution was used to determine the cell concentration using the Naubauer Counting Chamber (4x4 grid x 10000 cells/ml). The volume was adjusted with complete DMEM and the cells were plated out at a density of 60.000 to 80.000 cells pro well (500 μ l per well). The media was exchanged the following day to serum containing Neurobasal.

2.2.16.4 Transfection of Primary Rat Neuron Culture and HEK293 Cells by Calcium Phosphate Precipitation

Buffers and Solutions:

HBS-Buffer: 10mM HEPES/NaOH pH 7.15, 137mM NaCl, 5mM KCl, 1mM MgCl₂, 0.7mM Na₂HPO₄, dissolve in autoclaved distilled H₂O, adjust pH to 7.15 and filter the solution through a 0.22 μ m Filter.

2M CaCl₂ Solution: Dissolve CaCl₂ in distilled H₂O and autoclave.

Plasmid DNA: DNA purified using the Qiagen Purification Columns and dissolved in sterile distilled H₂O.

HEK 293 Cell Culture:

20 µg Plasmid-DNA was dissolved in a final volume of 50ml with autoclaved distilled H₂O. 500 µl HBS Buffer was added to the DNA, mixed, then 32 µl 2M CaCl₂ was added to the solution. This mixture was mixed by vortexing immediately, then left to stand for 10 to 20 minutes at room temperature. To each 2cm well, between 70 and 100ml if the Calcium Phosphate solution was added, and after 6 to 16 hours, the cells were washed once with D-PBS and then fresh medium was added. The analysis of the transfected cells could be carried out from 16 hours post-transfection.

Primary Rat Neuron Culture:

The Neurobasal medium in which the cells are growing is removed and placed into another 34 well plate, and it is replaced with 500 µl of Optimem. The transformation medium is prepared for three wells, as follows: 3 µg DNA, 5.6 µl 2M CaCl₂ and 36.4 µl H₂O, this is mixed briefly, then 45 µl HBS is added with constant shaking to the eppendorf tube. The final 90 µl mixture was incubated at room temperature for 20 to 30 minutes, then carefully added to the Optimem medium in which contains the neurons. The plate is then incubated for one hour at 37°C, after which the neuron bearing coverslips are washed three times with serum free Neurobasal and finally the original serum containing Neurobasal medium is replaced.

2.2.16.5 Phorbol Ester Binding-Translocation Assays

HEK293 cells were transfected as stated above with EGFP expression vectors two days before the experiment. The media was changed before the experiment, and 4β-TPA (Sigma) was added from an acetone stock solution directly to the cell culture (100nM final concentration). Cells were incubated for 60 min at 37°C, washed twice with phosphate-buffered saline, and fixed with 4% paraformaldehyde in phosphate-buffered saline. Cover slips were mounted onto slides with Mowiol (Calbiochem) and observed with a Zeiss confocal laser-scanning microscope.

2.2.17 Immunohistochemistry

Buffers and Solutions:

Blocking Buffer	1x PBS containing 2% Normal Goat serum, 0,25% Triton X-100
Sodium Chloride/ Sodium Nitrite Solution	9g/L NaCl and 1g/L Na Nitrite in H ₂ O
Isopentane	-40°C
4% Paraformaldehyde	
Tribromoethanol	

Animals were deeply anaesthetised with tribromoethanol and each mouse was perfused transcardially with 200 ml of Sodium Chloride (9 g/L) containing Sodium Nitrite (1 g/L) for 10 min. The brains were quickly and carefully removed and frozen in isopentane at -40° C. Sagittal 12 μ m frozen cryostat slices were collected and post-fixed with either cold 4% paraformaldehyde in PBS (pH 7.4) or methanol at -20° C. The slices were blocked in PBS containing 2% normal goat serum and 0.25% Triton X-100 for 30 min at room temperature. Thereafter, sections were incubated with polyclonal antibodies to Munc13-1 (1:10000) and monoclonal antibodies to Synaptophysin (1:1000) at 4 °C for 16 h. The antibodies were diluted in PBS that contained 5% normal goat serum and 0.1% Triton X-100. After three rinses in PBS, the sections were incubated with Alexa488- or Alexa568-labeled goat anti-rabbit or anti-mouse IgG secondary antibodies (Molecular Probes) at room temperature.

3. Results

3.1 Identification of α RIM-Binding Deficient Munc13-1 and ubMunc13-2 Mutants in Reverse Yeast Two-Hybrid Assays

An amino-terminally truncated Munc13-1 variant that lacks its entire L region including the α RIM binding domain (Munc13-1(520-1736)EGFP) exhibits reduced priming activity in neurons (Betz et al., 2001). This observation indicates that α RIM binding regulates active zone trafficking or priming activity of Munc13-1 and most likely also of ubMunc13-2. However, the elimination of the entire L region of Munc13-1 (Betz et al., 2001) may also have functional consequences that are not related to the α RIM-Munc13-1 interaction.

With this in mind, the first aim of this work was the development of more suitable tools for the functional analysis of the Munc13- α RIM interactions. I used a reverse yeast two-hybrid approach for the identification of missense mutations in Munc13-1 and ubMunc13-2 that disrupt their interaction with α RIM while leaving other interactions unaffected (see Materials and Methods). The amino-terminus of ubMunc13-2 (LexA-ubMunc13-2(1-181)), which is highly homologous to the amino-terminal region of Munc13-1 and contains the minimal α RIM binding region (Betz et al., 2001; Figures 9), was used as a model protein in this screen in combination with VP16-RIM1 α (1-344).

```

1  M S L L C V G V K K A K F D G A Q E K F N T Y V T L K V Q N V K S T T I A V R G
1  M S L L C V R V K R A K F Q G S P D K F N T Y V T L K V Q N V K S T T V A V R G

41  S Q P S W E Q D F M F E I N R L D L G L T V E V W N K G L I W D T M V G T V W I
41  D Q P S W E Q D F M F E I S R L D L G L S V E V W N K G L I W D T M V G T V W I

81  P L R T I R Q S N E E G P G E W L T L D S Q A I M A D S E I C G T K D P T F H R
81  A L K T I R Q S D E E G P G E W S T L E A E T L M K N D E I C G T K N P T P H K

121 I L L D A H F E L P L D I P E E E A R Y W A K K L E Q L N A M R D Q D E Y S F Q
121 I L L G T R F E L P F D I P E E E A R Y W T Y K L E Q I N A L A D D N E Y S S Q

161 D Q - Q D K P L P V P S S Q C C N W N Y F Munc13-1
161 E E S Q R K L L P T A A A Q C R H W T Y L ubMunc13-2

```

Figure 9. Alignment of the Amino Termini of Munc13-1 and ubMunc13-2. Amino acid residues 1 to 180 of Munc13-1 and residues 1 to 181 of ubMunc13-2 are shown. Residues that are identical in the two sequences are shown on a black background.

Of the twenty-six RIM1 α -binding deficient constructs isolated, the majority (eighteen) carried nonsense mutations that caused premature truncation of the minimum α RIM-binding region. Eight representative constructs are shown since some truncations were obtained more than once, i.e. 3 copies of LexA-ubMunc13-2(1-110), two copies of LexA-ubMunc13-2(1-69) and five truncations were obtained which were shorter than ten amino acids (Figure 10 A). This finding confirmed earlier studies, which showed that constructs such as pLexN-ubMunc13-2(1-71), pLexN-ubMunc13-2(66-181) are not sufficient for RIM1 α interaction and that amino acid residues 1-181 do indeed represent the minimum α RIM binding site of ubMunc13-2 whose further truncation abolished binding (Betz et al., 2001). In addition to these nonsense mutants, I identified eight α RIM-binding deficient pLexN-ubMunc13-2(1-181)^{mut} constructs that carried one or several missense mutations (Figure 10 B). This experiment was initially performed and documented in the Master's study (Andrews, 2001) and these results are used as the basis for all further work in this study.

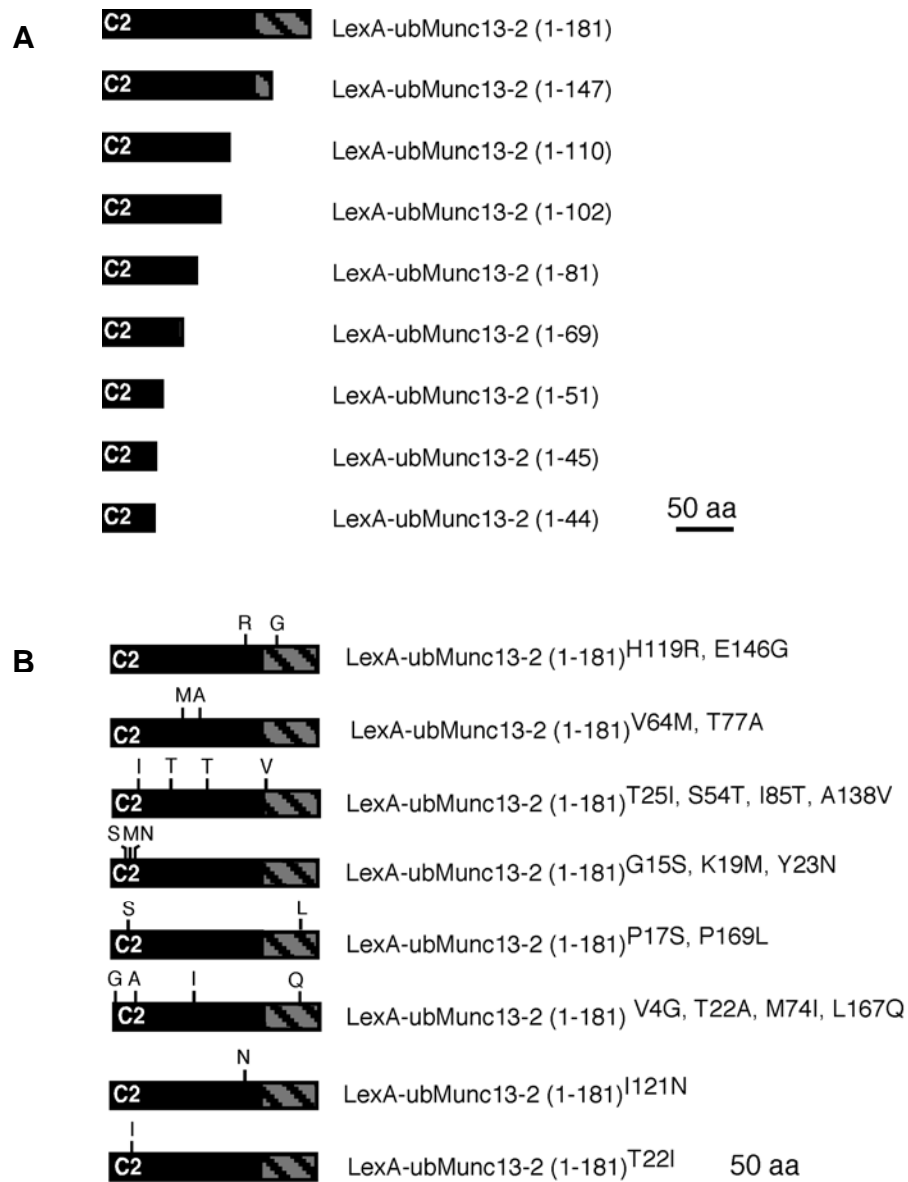


Figure 10. Identification and Characterisation of RIM1 α -Binding Deficient ubMunc13-2 Mutants. The first 181 amino acid residues of the amino terminus of ubMunc13-2 comprise the minimum-binding region for the RIM1 α interaction. **(A)** Many identified and sequenced RIM1 α -binding deficient constructs encoded proteins, which were shorter than this minimum-binding region required for RIM1 α interaction. **(B)** Multiple and single point mutation containing constructs which maintained the minimum-binding region and were non-RIM1 α interacting. Numbers in brackets indicate the ubMunc13-2 sequence covered by the indicated clones.

In cases of constructs carrying multiple missense mutations, individual mutations were introduced into pLexN-ubMunc13-2(1-181) and analysed

separately for their effects on RIM1 α binding in yeast two-hybrid screens. Using this approach, I identified a total of six missense mutations (pLexN-ubMunc13-2(1-181)^{T22I}, pLexN-ubMunc13-2(1-181)^{T22A}, pLexN-ubMunc13-2(1-181)^{Y23N}, pLexN-ubMunc13-2(1-181)^{H119R}, pLexN-ubMunc13-2(1-181)^{I121N}, pLexN-ubMunc13-2(1-181)^{P169L}) that abolished binding of LexN-ubMunc13-2(1-181)^{mut} to VP16-RIM1 α (1-344; Figure 11).

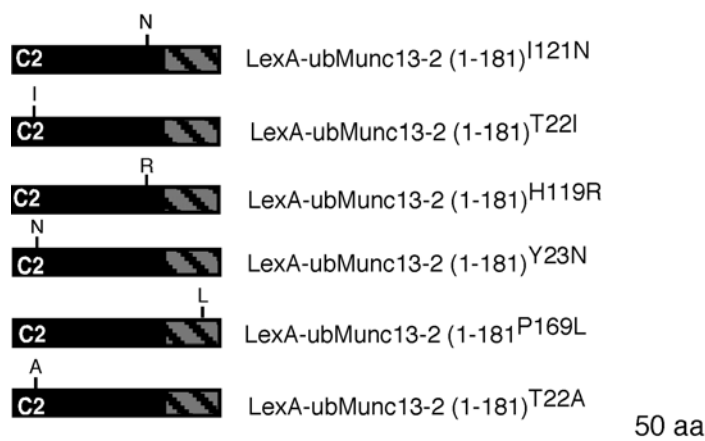


Figure 11. RIM1 α -Binding Deficient Single Point Mutants for ubMunc13-2. Single point mutation containing constructs obtained from the initial screen and single point mutations generated with site directed mutagenesis for pLexN-ubMunc13-2(1-181) and shown to be non-RIM1 α interacting in the yeast two-hybrid system.

As all affected residues are conserved in the α RIM binding regions of ubMunc13-2 and Munc13-1, the second α RIM-binding Munc13 isoform, five homologous mutations were introduced individually into a previously characterised (Betz et al., 2001) α RIM-binding bait construct of Munc13-1 (pLexN-Munc13-1(1-150)^{T22I}, pLexN-Munc13-1(1-150)^{Y23N}, pLexN-Munc13-1(1-150)^{V64M}, pLexN-Munc13-1(1-150)^{H119R}, pLexN-Munc13-1(1-150)^{I121N}).

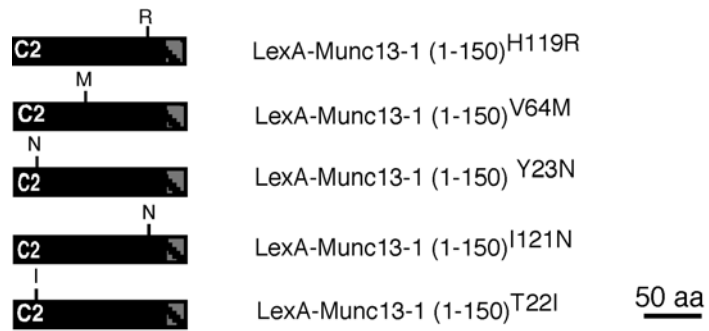


Figure 12. RIM1 α -Binding Deficient, Single Point Mutants for Munc13-1. Single point mutation containing constructs generated with site directed mutagenesis for pLexN-Munc13-1(1-150) and shown to be non-RIM1 α interacting in the yeast two-hybrid system.

As was the case with the corresponding ubMunc13-2 constructs, all these LexN-Munc13-1(1-150)^{mut} constructs failed to bind VP16-RIM1 α (1-344) in the reverse yeast two-hybrid assays (Figure 12).

3.2 Confirmation of α RIM-Binding Deficient Mutants

3.2.1 Analysis of α RIM-Binding Deficient Mutants of Munc13-1 and ubMunc13-2 in *in vitro* Binding Assays

To further examine the α RIM-binding deficient mutants of ubMunc13-2 and Munc13-1, which I had identified in reverse yeast two-hybrid screens I performed biochemical cosedimentation experiments. Glutathione-S-Transferase (GST) fusion proteins of wild type and mutant amino termini of ubMunc13-2 (GST-ubMunc13-2(3-320), GST-ubMunc13-2(3-320)^{T22I}, GST-ubMunc13-2(3-320)^{I121N}, GST-ubMunc13-2(3-320)^{P169L}) and Munc13-1 (GST-Munc13-1(3-317), GST-Munc13-1(3-317)^{T22I}, GST-Munc13-1(3-317)^{H119R}, GST-Munc13-1(3-317)^{I121N}, GST-Munc13-1(3-317)^{P168L}) were expressed in bacteria, immobilised on glutathione agarose beads and first tested for binding of native RIM1 α using rat brain synaptosome extracts.

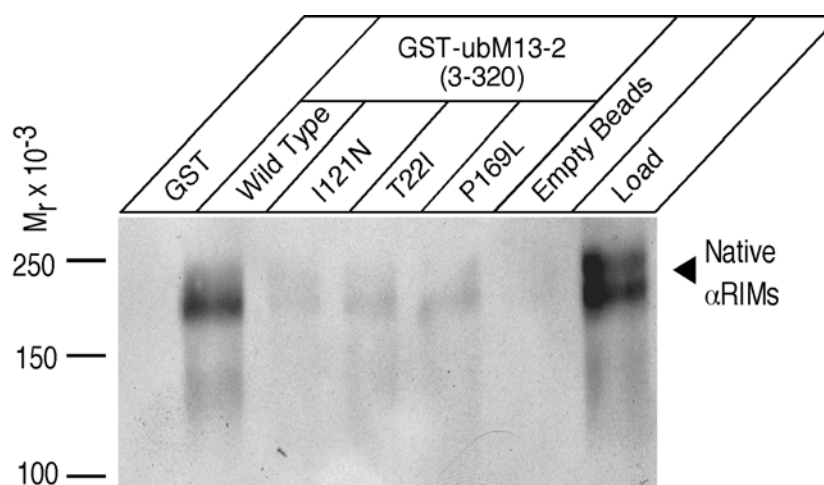


Figure 13. Cosedimentation Assay Binding of GST-ubMunc13-2 Wild Type and Mutant Constructs to Endogenous α RIM. Identical amounts of GST fusion proteins containing either the wild type ubMunc13-2 amino terminus or various single point mutants, as well as GST alone were immobilised to glutathione agarose beads and used in cosedimentation assays with rat brain synaptosome extract. Proteins that bound to the immobilised GST fusion proteins were analysed by SDS-PAGE and immunoblotting with antibodies specific to α RIM1/2. Endogenous α RIM bound to GST-ubMunc13-2 wild type but not to the point mutants and not to GST alone.

All tested mutant GST-ubMunc13-2(3-320) constructs showed either no interaction with RIM1 α or the binding was significantly reduced (Figure 13). However, in the case of GST-Munc13-1(3-317) constructs only GST-Munc13-1(3-317)^{I121N} showed significantly reduced binding to RIM1 α in cosedimentation assays (Figure 14). Because the I121N point mutation was the only modification that robustly interfered with RIM1 α binding of the Munc13-1 and ubMunc13-2 amino-termini (Figure 13, 14), this mutation was concentrated on and used for all subsequent experiments analysing α RIM-Munc13 interactions.

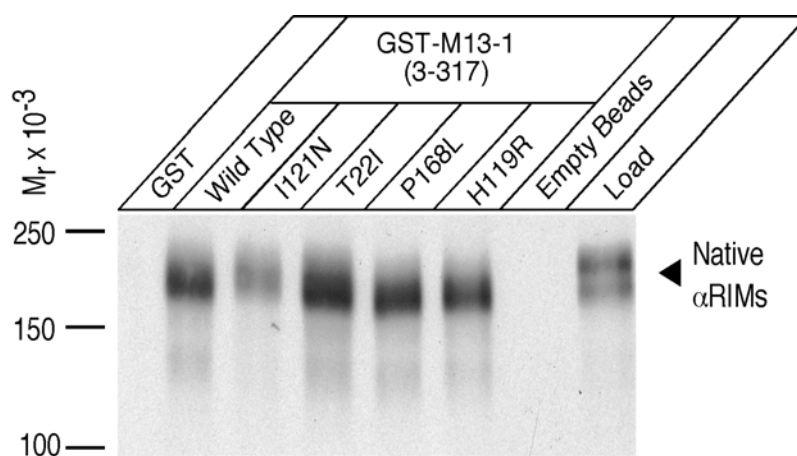


Figure 14. Cosedimentation Assay Binding of GST Munc13-1 Wild Type and Mutant Constructs to Endogenous α RIM. Identical amounts of GST fusion proteins containing either the Munc13-1 amino terminus wild type or various single point mutants, as well as GST alone were immobilised to glutathione agarose beads and used in cosedimentation assays with rat brain synaptosome extract. Proteins that bound to the immobilised GST fusion proteins were analysed by SDS-PAGE and immunoblotting with antibodies specific to α RIM1/2. Native α RIM showed no binding to GST alone, but bound to the Munc13-1 wild type fusion proteins as well as all single point mutated constructs with the exception of Isoleucine 121 to Asparagine (I121N), which showed significantly reduced binding.

For direct comparison between the isoforms, GST-Munc13-1(3-317) and GST-ubMunc13-2(3-320) were again analysed for precipitation of endogenous RIM1 α from rat brain synaptosomal extracts. The Munc13 amino terminal wild type constructs were each directly compared with the only point mutation found to show alteration in RIM1 α interaction for both Munc13-1 and

ubMunc13-2, I121N. It was again seen that both GST-Munc13-1(3-317) and GST-ubMunc13-2(3-320) wild type proteins bound to endogenous RIM1 α while GST-Munc13-1(3-317)^{I121N} and GST-ubMunc13-2(3-320)^{I121N} showed either significantly reduced RIM1 α -binding or complete loss of α RIM-binding, respectively (Figure 15).

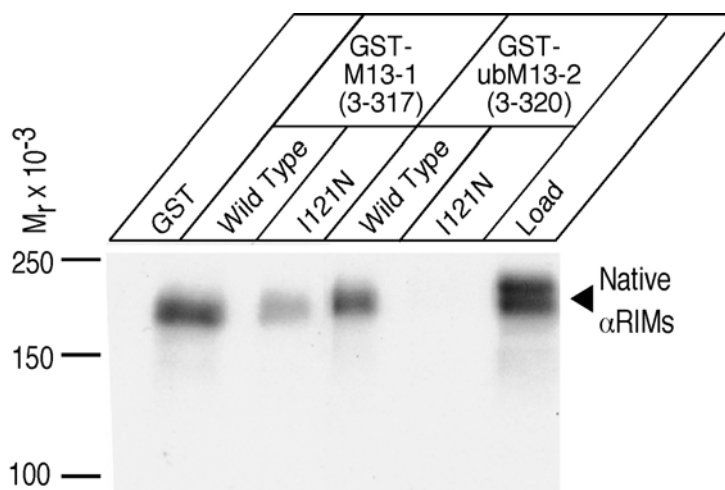


Figure 15. Cosedimentation Assay Binding of GST-Munc13-1 and ubMunc13-2 Wild Type and I121N Constructs to Endogenous α RIM. Identical amounts of GST fusion proteins containing either the Munc13-1 and ubMunc13-2 amino terminus wild type or I121N point mutation, as well as GST alone were immobilised to glutathione agarose beads and used in cosedimentation assays with rat brain synaptosome extract. Proteins that bound to the immobilised GST fusion proteins were analysed by SDS-PAGE and immunoblotting with antibodies specific to α RIM1/2. Native α RIM bound to both the Munc13-1 and ubMunc13-2 wild type fusion proteins but either at significantly decreased levels or not at all to the point mutants (I121N) and not to GST alone.

In a set of *in vitro* cosedimentation experiments, wild type and I121N mutant constructs, i.e. GST-Munc13-1(3-317), GST-Munc13-1(3-317)^{I121N}, GST-ubMunc13-2(3-320) and GST-ubMunc13-2(3-320)^{I121N} were tested for binding to the bacterially expressed, recombinant His-tagged amino-terminus of RIM1 α , His-RIM1 α (131-214). In these experiments, the respective wild type Munc13 constructs bound robustly to His-RIM1 α (131-214) while the I121N mutants showed no interaction (Figure 16). Taken together, these data indicate that the I121N mutation abolishes α RIM binding of Munc13-1 and

ubMunc13-2 and thus can be used as a model to study the α RIM-Munc13 interaction in further detail.

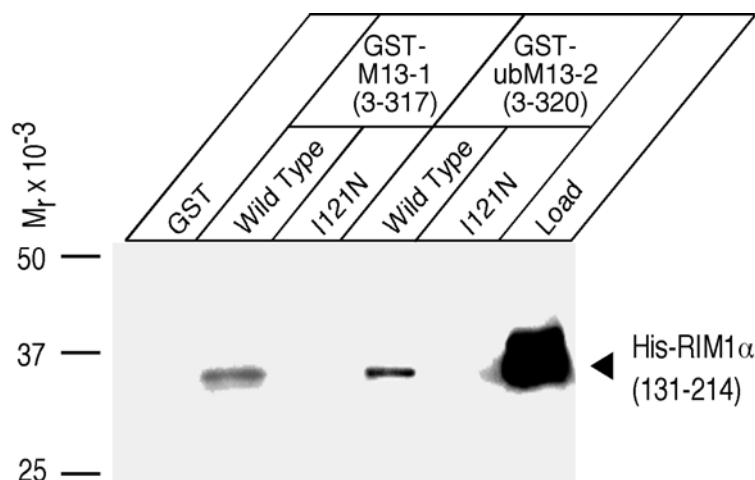


Figure 16. Cosedimentation Assay with Purely Recombinant Munc13 and α RIM Proteins. Identical amounts of GST fusion proteins containing either the wild type Munc13-1 and ubMunc13-2 amino terminus or I121N point mutations, as well as GST alone were immobilised to glutathione agarose beads and used in cosedimentation assays with His-RIM1 α (131-214). Proteins that bound to the immobilised GST fusion proteins were analysed by SDS-PAGE and immunoblotting with anti-His antibodies. RIM1 α bound to both the Munc13-1 and ubMunc13-2 wild type fusion proteins but not to the point mutants (I121N) and not to GST alone.

In all further experiments where the RIM1 α -binding deficient point mutation, Isoleucine 121 to Asparagine (I121N) was compared to wild type Munc13, Munc13-1 was concentrated on for the following reasons. (i) Munc13-1 is by far the most abundant Munc13 isoform in the brain, with expression levels that exceed those of ubMunc13-2 by at least one order of magnitude (Rosenmund et al., 2002). (ii) In wild type hippocampal glutamatergic neurons, 90% of all synapses are exclusively dependent on Munc13-1 (Augustin et al., 1999b). (iii) Studies in deletion mutant mice show that Munc13-1 is essential for survival (Augustin et al., 1999b), while ubMunc13-2 is not (Varoqueaux et al., 2002). (iv) Munc13-1 is the Munc13 isoform for which the best detection tools are available (Brose et al., 1995; Betz et al., 1997, 1998; Augustin et al., 1999a).

3.2.2 Immunocytochemical Analysis

3.2.2.1 Analysis of α RIM-Binding Deficient Mutants of Munc13-1 and ubMunc13-2 in Living Cells

To analyse the effect of the I121N mutation on α RIM binding in the context of living cells, eukaryotic expression vectors encoding full-length recombinant versions of wild type and mutant Munc13-1 with a carboxy-terminally attached enhanced green fluorescent protein (EGFP) tag were generated in pEGFP-N1 (Munc13-1-EGFP and Munc13-1^{I121N}-EGFP). These EGFP-tagged Munc13-1 variants and full-length RIM1 α were then overexpressed in HEK293 cells either alone or in combination.

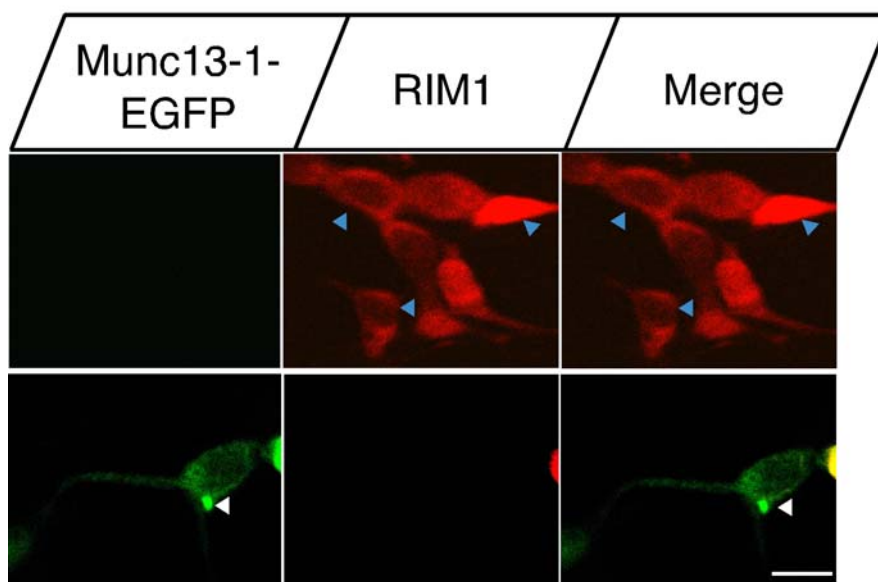


Figure 17. Subcellular Localisation of Munc13-1/Munc13-1^{I121N} and RIM1 α in HEK293 Cells. HEK293 cells were co-transfected with the expression vector pEGFP-N1, encoding full-length Munc13-1/Munc13-1^{I121N} with GFP attached to the carboxy terminal and a pCMV5 expression vector encoding full-length RIM1 α . 48 hours after transfection the cells were methanol fixed and the subcellular localization of expressed proteins was analysed with a confocal laser-scanning microscope. Munc13-1 was visualised by direct fluorescence and RIM1 α by staining with monoclonal anti- α RIM antibodies. HEK293 cell expressing Munc13-1 alone is indicated with white arrowhead and cells expressing only RIM1 α , with blue arrowheads. Munc13-1 forms large aggregates and shows cytoplasmic localisation, while RIM1 α displays cytoplasmic as well as nuclear staining. Scale bar 10 μ M.

When expressed singly in HEK293 cells, Munc13-1-EGFP and Munc13-1^{I121N}-EGFP formed large aggregates in addition to a diffuse cytoplasmic pool of protein (Figure 17). In contrast, overexpressed RIM1 α was found in the nucleus as well as diffusely distributed in the cytoplasm when singly expressed in the fibroblasts (Figure 17). When Munc13-1-EGFP and RIM1 α were coexpressed, Munc13-1 again formed large aggregates and RIM1 α was invariably coenriched with Munc13-1 in these aggregates (Figure 18).

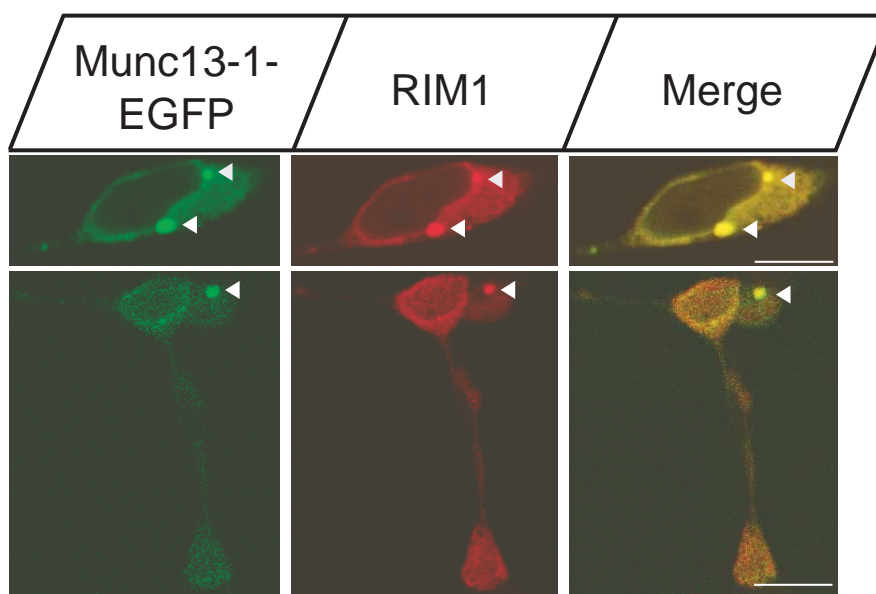


Figure 18. Aggregation of Munc13-1 Wild Type and Recruitment of RIM1 α into the Aggregates in HEK293 Cells. HEK293 cells were co-transfected with the expression vector pEGFP-N1, encoding full-length Munc13-1 wild type with GFP attached to the carboxy terminal and a pCMV5 expression vector encoding full-length RIM1 α . 48 hours after transfection the cells were methanol fixed and the subcellular localization of expressed proteins were analysed with a confocal laser-scanning microscope. Munc13-1 was visualised by direct fluorescence and RIM1 α by staining with monoclonal anti- α RIM antibodies. Both Munc13-1 and RIM1 α show cytoplasmic localisation and colocalization of Munc13-1 and RIM1 α in aggregates are indicated with white arrowheads. Scale bar 10 μ M.

On the other hand, when Munc13-1^{I121N}-EGFP and RIM1 α were coexpressed in HEK293 cells, RIM1 α was never recruited into Munc13-1^{I121N}-EGFP aggregates. Rather, the cellular RIM1 α distribution remained diffuse and

partially nuclear, as was the case when it was expressed in the absence of Munc13-1-EGFP (Figure 19). Taken together, these data indicate that Munc13-1 binding recruits RIM1 α into Munc13-1 aggregates and that the I121N mutation disrupts binding and coaggregation of RIM1 α .

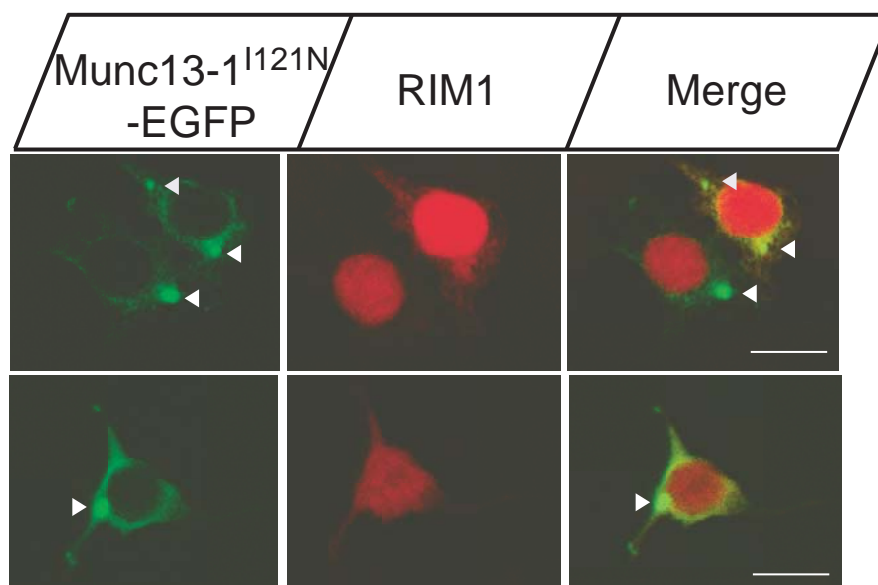


Figure 19. Aggregation of Munc13-1^{I121N} without Recruitment of RIM1 α into the Aggregates in HEK 293 Cells. HEK293 cells were co-transfected with the expression vector pEGFP-N1, encoding full-length Munc13-1^{I121N} with GFP attached to the carboxy terminal and a pCMV5 expression vector encoding full-length RIM1 α . 48 hours after transfection the cells were methanol fixed and the subcellular localization of expressed proteins were analysed with a confocal laser-scanning microscope. Munc13-1 was visualised by direct fluorescence and RIM1 α by staining with monoclonal anti- α RIM antibodies. Munc13-1^{I121N} aggregates are indicated with white arrowheads and RIM1 α is never co-enriched in the aggregates. Scale bar 10 μ M.

3.2.2.2 Phorbol Ester Induced Translocation of Munc13-1

C1-domains were originally discovered as regulatory regions in PKC (Newton 1995, Newton 1997) where they serve as high-affinity diacylglycerol/phorbol ester receptors that act in synergy with C2-domains to recruit the enzyme to the plasma membrane and lock it in an activated state. Structure and function of C1-domains in Unc13 protein family members are very similar to those in PKC (Betz et al., 1998; Ashery et al., 1999). The C1-domains of *C. elegans*

Unc13 and the three mammalian Munc13 isoforms, Munc13-1, Munc13-2 and Munc13-3, bind diacylglycerol and phorbol esters with affinities that are comparable to those observed in PKC. Upon binding, all of the isoforms translocate to the plasma membrane (Betz et al., 1998, Brose and Rosenmund, 2002). I took advantage of this phorbol ester dependent translocation of Munc13-1 and tested if the binding to Munc13-1 causes the cotranslocation of RIM1 α in coexpressing cells. Indeed, I found that Munc13-1-EGFP and RIM1 α cotranslocated to the plasma membrane of coexpressing HEK293 cells upon treatment with 100nM 4 β -12-O-tetradecanolyphorbol-13-acetate (4 β -TPA) (Figure 20).

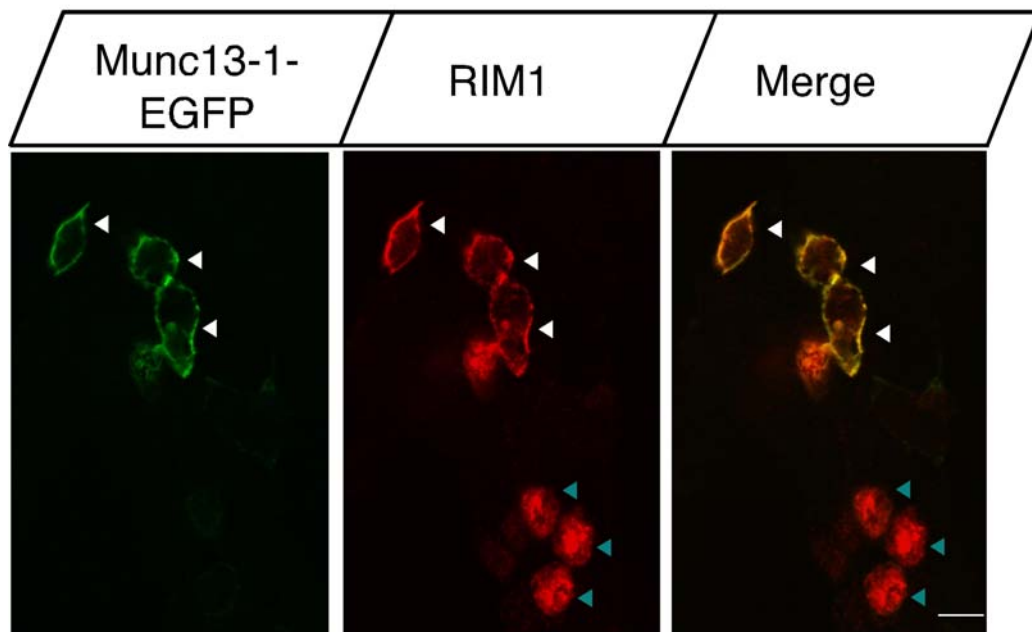


Figure 20. Phorbol Ester-Induced Translocation of Munc13-1 Wild Type to the Plasma Membrane. HEK293 cells were co-transfected with pEGFP-N1 Munc13-1 full-length and a pCMV5 expression vector encoding full-length RIM1 α . 48 hours after transfection the cells were incubated for one hour in the presence of 100 nM 4 β -TPA, methanol fixed and the subcellular localization of expressed proteins were analysed with a confocal laser-scanning microscope. Upon 4 β -TPA treatment, cells co-transfected with both Munc13-1 and RIM1 α , indicated with white arrowheads, showed translocation of both proteins to the plasma membrane, whereas cell expressing RIM1 α alone, indicated with blue arrowheads, showed no such translocation of RIM1 α to the plasma membrane. Scale bar 10 μ M.

In contrast to coexpressed Munc13-1-EGFP and RIM1 α , when RIM1 α was expressed alone (blue arrowheads; Figure 20, 21) or in combination with Munc13-1^{I121N}-EGFP (Figure 21) RIM1 α did not translocate to the plasma membrane in response to phorbol ester treatment.

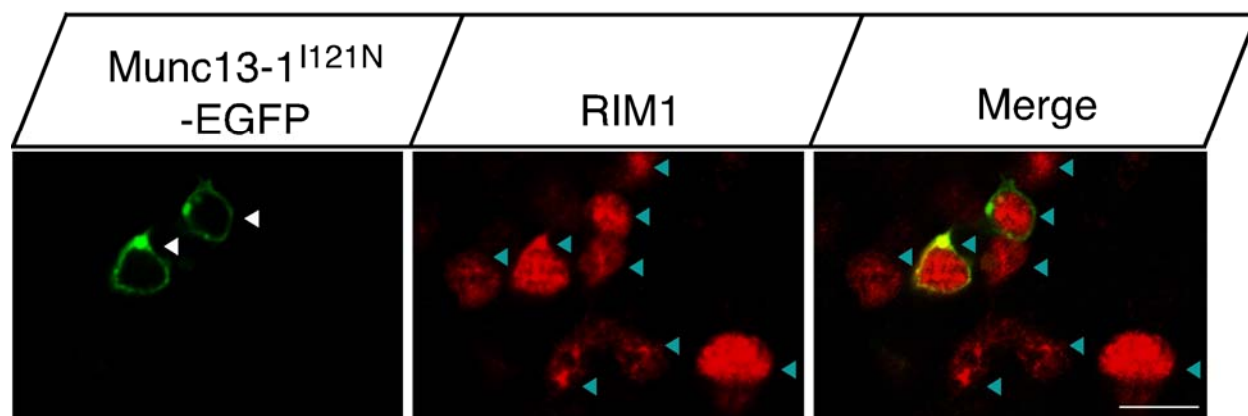


Figure 21. Phorbol Ester-Induced Translocation of Munc13-1^{I121N} to the Plasma Membrane. HEK293 cells were co-transfected with the expression vector, pEGFP-N1, encoding full-length, RIM1 α binding deficient, Munc13-1^{I121N} with GFP attached to the carboxy terminal and full-length RIM1 α in pCMV5. 48 hours after transfection the cells were incubated for one hour in the presence of 100 nM 4 β -TPA, methanol fixed and the subcellular localization of expressed proteins were analysed with a confocal laser-scanning microscope. Note that in cells co-transfected with and coexpressing both Munc13-1^{I121N} and RIM1 α , only the Munc13-1- α RIM-binding deficient construct showed the expected migration to the plasma membrane (white arrowheads). However, the RIM1 α protein in the double expressing cells, as well as cells, which were singly expressing α RIM1, showed no translocation to the plasma membrane (blue arrow heads). Scale bar 10 μ M.

Taken together, our coexpression studies in HEK293 cells show that Munc13-1 binds α RIM in a cellular environment and that the I121N is sufficient to abolish the α RIM-Munc13-1 interaction, without altering the phorbol ester sensitivity and translocation properties of the Munc13-1 protein.

3.2.3 Analysis of Intracellular Trafficking of Munc13-1 and Munc13-1^{I121N} in Primary Cultures of Hippocampal Neurons

Previous studies performed in our laboratory indicated that α RIM binding of Munc13-1 may play a role in synaptic targeting of Munc13-1 to presynaptic active zones (Betz et al., 2001). To study the role of α RIM binding in targeting of Munc13-1, I overexpressed Munc13-1-EGFP and Munc13-1^{I121N}-EGFP in hippocampal primary cultures and studied their subcellular localisation. Neurons were transfected on day 4 *in vitro* (DIV 4) and the subcellular localisation of the fusion proteins was analysed in mature neurons at DIV 15. Methanol extraction was used as a method of fixation, which resulted in the washing out of soluble proteins. Synaptic markers such as Bassoon, Piccolo, are excellently preserved and detected in immunofluorescence studies on methanol fixed neurons (tom Dieck et al., 1998). In addition, other markers used in this study such as Synapsin, Vesicular Glutamate Transporter 1 and 2 (VGLUT1/2) and the axonal marker, Neurofilament, were readily detectable upon methanol fixation (Figure 22 - 24).

To ascertain that soluble EGFP fusion proteins were indeed quantitatively washed out rather than quenched upon methanol fixation, immunodetection of EGFP with anti-GFP antibodies was performed, which considerably increased the sensitivity of detection. The use of anti-GFP antibodies resulted in the detection of five times more transfected cells per coverslip compared to detection by EGFP autofluorescence. This was observed for all recombinant proteins including EGFP alone, but was particularly useful for detection of sufficient numbers of cells expressing the very large constructs analyzed here (Figure 22). Axons of DIV 15 neurons in these cultures were visualised with antibodies against Neurofilament and were several hundred micrometers to millimetres long, whereas dendrites span no more than 10 soma diameters. A presynaptic pattern of immunofluorescence could therefore be easily detected.

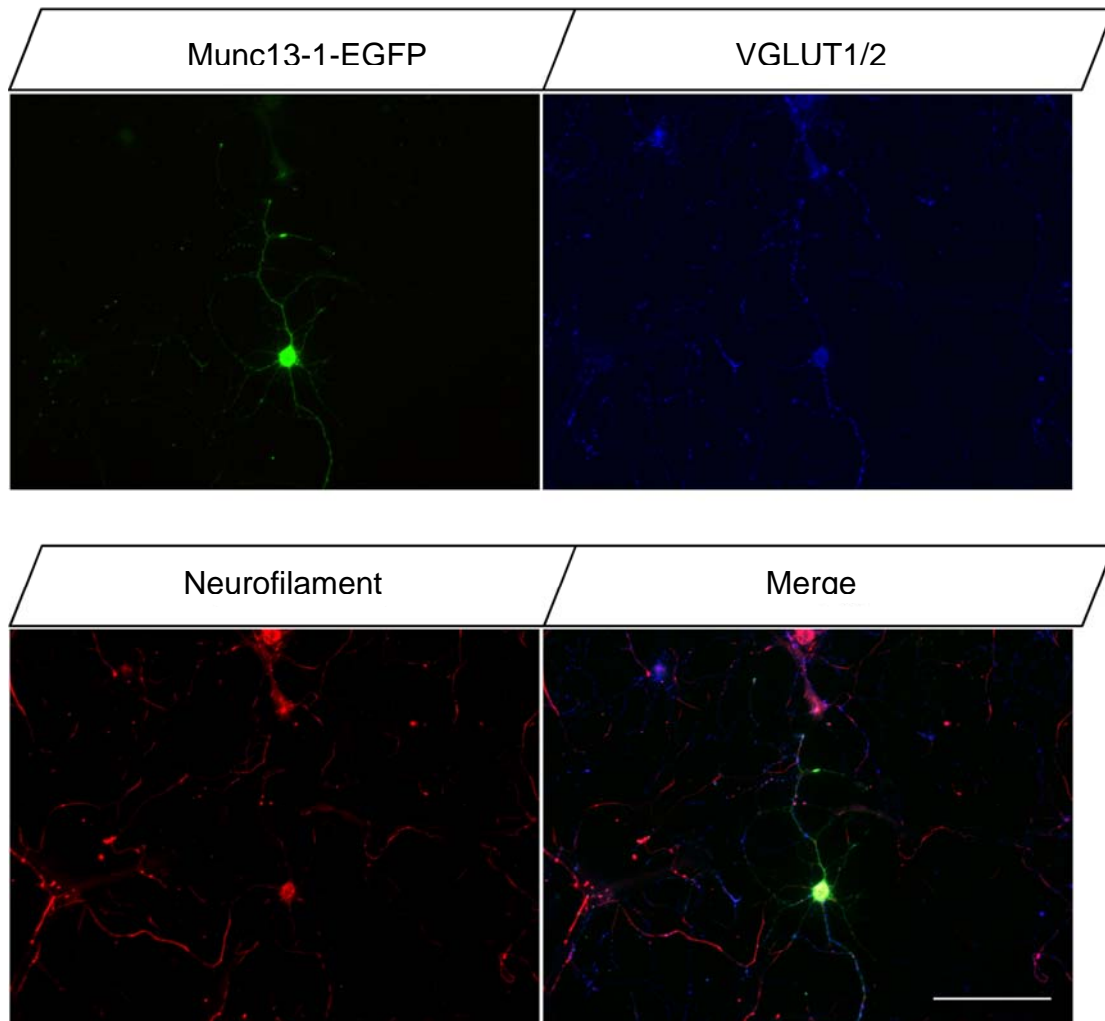


Figure 22. Expression of Full-Length Wild Type Munc13-1 in Transfected Hippocampal Neurons. Neurons were fixed using methanol, which resulted in wash out of soluble proteins. Green colour represents GFP stained Munc13-1-EGFP; blue and red colours represent immunofluorescence of VGLUT1/2 and Neurofilament respectively. The soma and dendrites of neurons overexpressing Munc13-1 are flooded with protein. Scale bar 100 μ M.

Neurons expressing Munc13-1-EGFP were always characterised by diffuse fluorescence in the dendrites and nucleus, due to large overexpression and flooding of the soma and dendrites (Figure 22), while axons of transfected neurons contained puncta of fluorescence (Figure 23, 24).

Similar puncta were not detected inside dendrites, but were abundant in neurofilament positive axons winding around neurites and cell. The axonal puncta colocalised with VGLUT1/2, which are presynaptic markers of glutamatergic synapses (Figure 23).

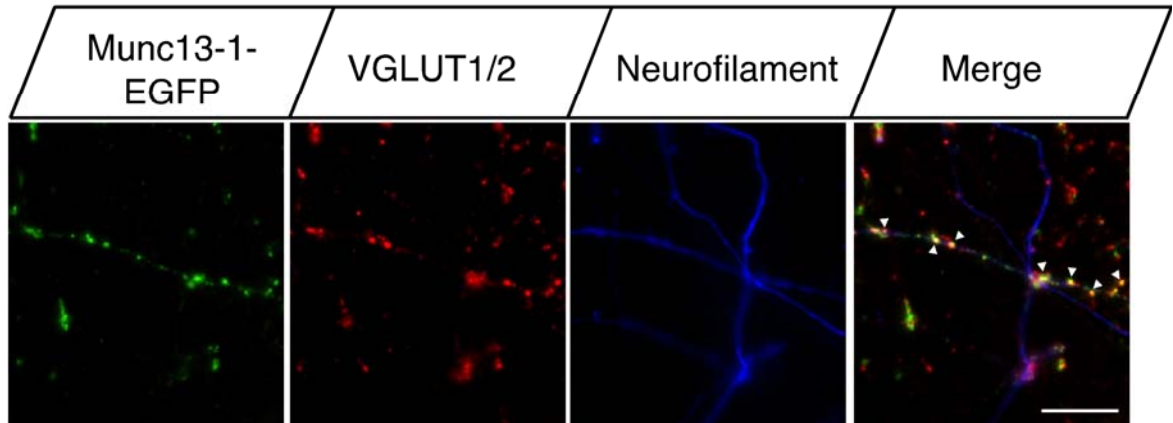


Figure 23. Synaptic Targeting of Munc13-1-EGFP in Hippocampal Neurons. Neurons were fixed using methanol, which resulted in wash out of soluble proteins. Green colour represents GFP stained Munc13-1-EGFP; red and blue colours represent immunofluorescence of the presynaptic markers VGLUT1/2 and the axonal marker Neurofilament, respectively. Puncta colocalise with VGLUT1/2 in axons identified by the presence of Neurofilament. Arrowheads indicate examples of colocalisation. Scale bar 10 μ M.

To further verify correct subcellular targeting of the full-length fusion protein, colocalisation with other presynaptic markers, such as Bassoon and Synapsin was tested, and the puncta were found to colocalise with all presynaptic markers tested in the methanol fixed cultures (Figure 24). Together these observations indicate that the full-length wild type Munc13-1 fusion protein was correctly targeted to presynaptic specialisations.

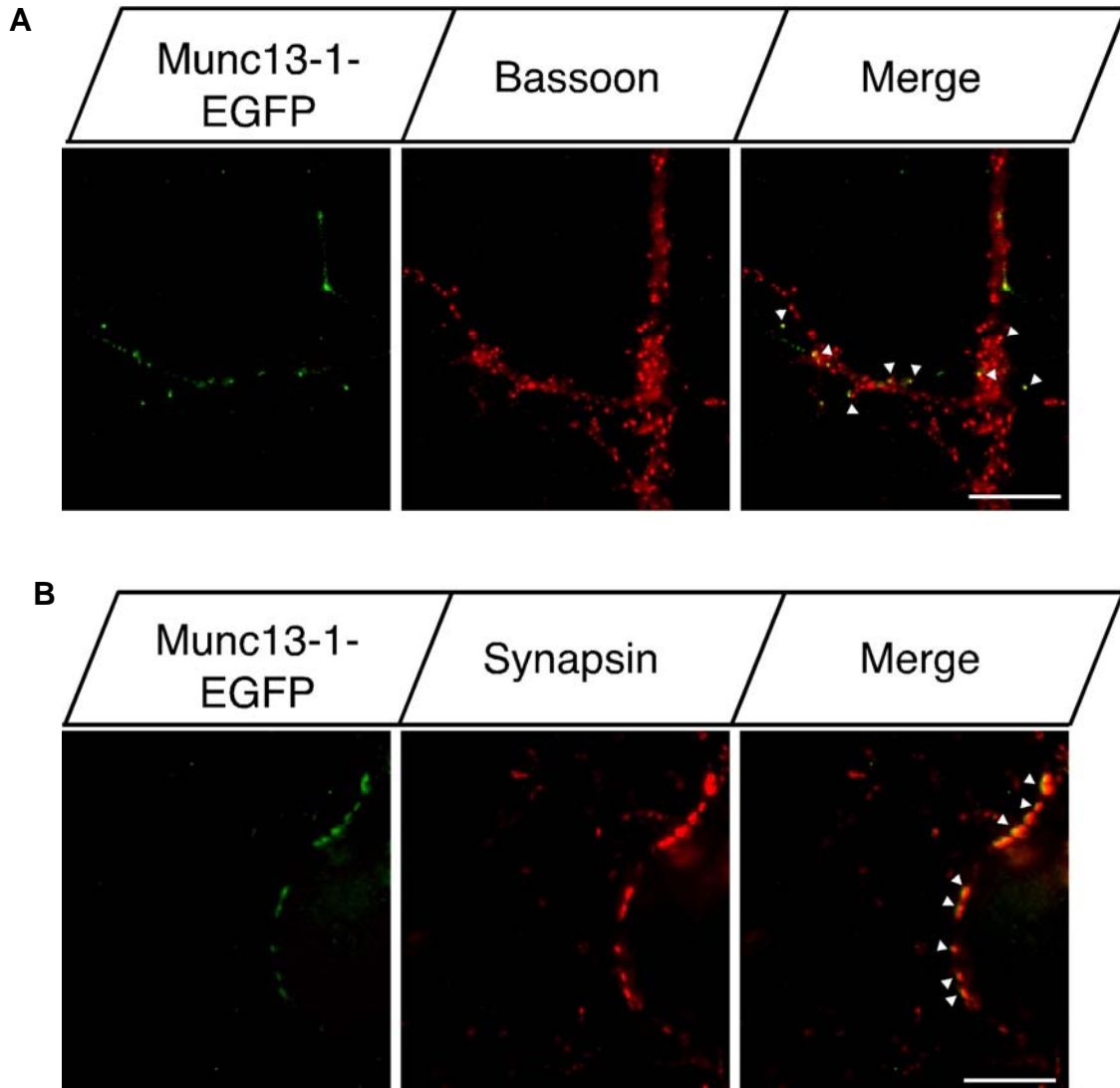


Figure 24. Localisation of Munc13-1-EGFP with Bassoon and Synapsin in Primary Hippocampal Neurons. Neurons were fixed using methanol, which resulted in wash out of soluble proteins. Green colour represents GFP stained Munc13-1-EGFP. Red colour represents immunofluorescence of presynaptic markers. **(A)** Puncta in axon of a Munc13-1 transfected neuron immunostained for GFP and colocalised with Bassoon and **(B)** Synapsin, indicating that they represent intact fusion protein sorted into axons. Scale bar 10 μ M.

3.2.4 Potential Role of RIM1 α in Synaptic Localisation of Munc13

To determine if RIM1 α binding plays a role in the localisation of Munc13 proteins, the RIM1 α -binding deficient Munc13-1 full-length fusion protein,

Munc13-1^{I121N}-EGFP was analysed using the transfection and analysis paradigms outlined above for the wild type fusion protein. The subcellular distribution of Munc13-1^{I121N}-EGFP was compared to the characteristics of the wild type protein, Munc13-1-EGFP (Figure 23, 25).

As with the wild type protein, there was overexpression of the RIM1 α -binding deficient protein, which resulted in diffuse staining in the soma and dendrites of the transfected hippocampal neurons. However, in contrast to the wild type protein, which showed punctate staining, the axonal distribution of Munc13-1^{I121N}-EGFP was also quite diffuse and showed a number of puncta, which did not colocalise with synaptic markers (Figure 25). However, though a rare occurrence, the RIM1 α -binding deficient protein did occasionally end up in punctate staining which showed colocalisation with presynaptic markers such as VGLUT1/2 (Figure 25).

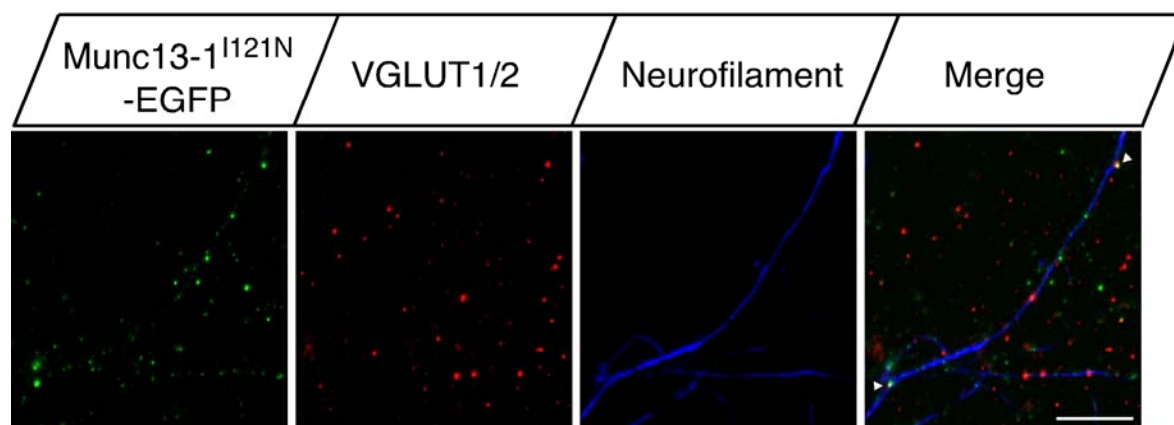


Figure 25. Diffuse Distribution and Rare Synaptic Targeting of Munc13-1^{I121N}-EGFP in Primary Hippocampal Neurons. Neurons were fixed using methanol, which resulted in wash out of soluble proteins. Green colour represents GFP stained Munc13-1^{I121N}-EGFP; red and blue colours represent immunofluorescence of the presynaptic markers VGLUT1/2 and the axonal marker Neurofilament, respectively. Munc13-1^{I121N}-EGFP, which carries the point mutation that disrupts RIM1 α binding, displays diffuse and ectopic expression throughout the neuron. Additionally, few Munc13-1^{I121N}-EGFP puncta colocalised with VGLUT1/2 in axons identified by the presence of Neurofilament. Arrowheads indicate examples of colocalisation. Scale bar 10 μ M.

Quantification of the Munc13-1^{I121N}-EGFP protein which showed VGLUT1/2 positive puncta along a neurofilament positively stained axon, revealed a 10-fold decrease in the number of synapses containing Munc13-1^{I121N}-EGFP protein, as compared to the Munc13-1-EGFP protein (Figure 26).

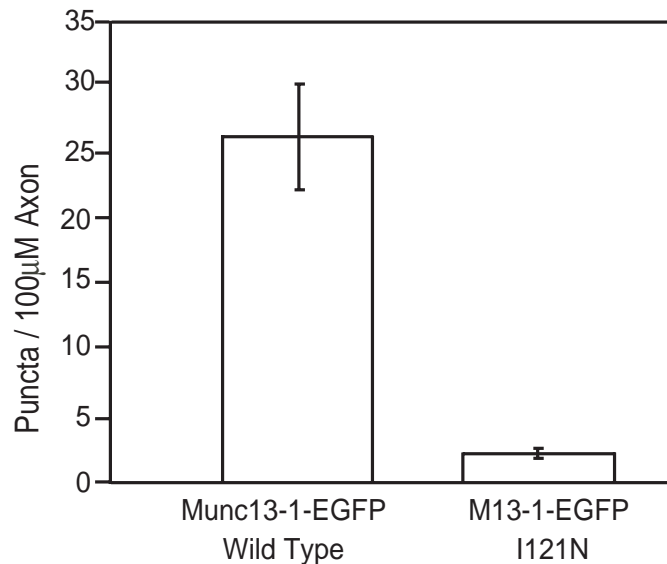


Figure 26. Quantitative Analysis of Synaptic Puncta for Munc13-1-EGFP and Munc13-1^{I121N}-EGFP. Quantification of VGLUT1/2 positive puncta along neurofilament positive stained axons, revealed a 10-fold decrease in the number of synapses containing Munc13-1^{I121N}-EGFP as compared to Munc13-1-EGFP. Error bars represent standard error of the mean. Number of neurons (N) = 25, number of experiments (n) = 7.

These results suggest that RIM1 α plays an important role either in the targeting to or retaining of Munc13-1 at the presynaptic active zone.

3.3 Analysis of the Subcellular Distribution of Munc13-1 and ubMunc13-2 in RIM1 α Knock Out Mice

3.3.1 Whole Brain Protein Level Analysis

To further analyse the role of α RIMs in the targeting/retention of Munc13 at the synapse, I analysed RIM1 α knock out mice (Schoch et al., 2002). Previously published studies on these mouse mutants showed that Munc13-1 expression levels are strongly reduced in the absence of RIM1 α (Schoch et al., 2002). I quantified the levels of Munc13-1 as well as both splice variants of Munc13-2, i.e. ubMunc13-2, which binds RIM1 α (Betz et al., 2001; Dulubova et al., 2005), and bMunc13-2, which is not a RIM1 α -interacting protein. Wild type and RIM1 α deficient littermates were used for ratiometric quantification of Munc13-1, ubMunc13-2 and bMunc13-2 with respect to the loading control N-methyl D-aspartate receptor 1 (NMDAR1). As previously published, Munc13-1 showed approximately a 60% reduction in the RIM1 α knock out animals (Figure 27, 29).

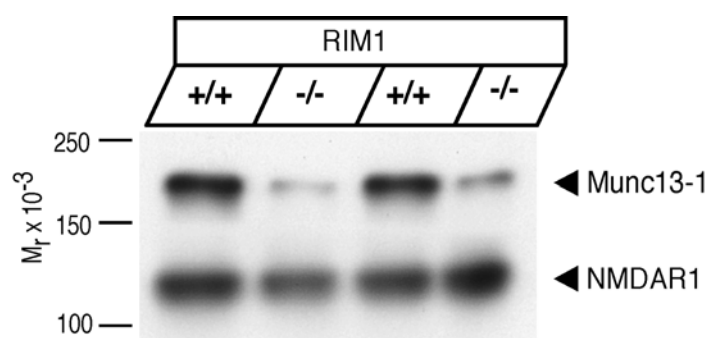


Figure 27. Analysis of Whole Brain Protein Levels of Munc13-1 in Wild Type and RIM1 α Knock Out Animals. Representative immunoblot of the level of Munc13-1 in brains from wild type and homozygous RIM1 α knockout mice. The levels of NMDAR1 were probed on the same blot as loading control. Munc13-1 shows significantly reduced protein levels in the RIM1 α knock out animals.

In contrast to previous findings where no changes were observed for Munc13-2 (Schoch et al., 2002), similar results to that of Munc13-1 were obtained for the RIM1 α -interacting protein, ubMunc13-2. This finding was not observed for bMunc13-2, which has a completely unrelated amino terminus to Munc13-1 and ubMunc13-2 and shows no RIM1 α interaction. Protein levels of ubMunc13-2 showed an approximate 60% reduction in the absence of its interaction partner RIM1 α (Figure 28A, 29), whereas bMunc13-2 showed no changes in protein level in the RIM1 α knock out animals (Figure 28B).

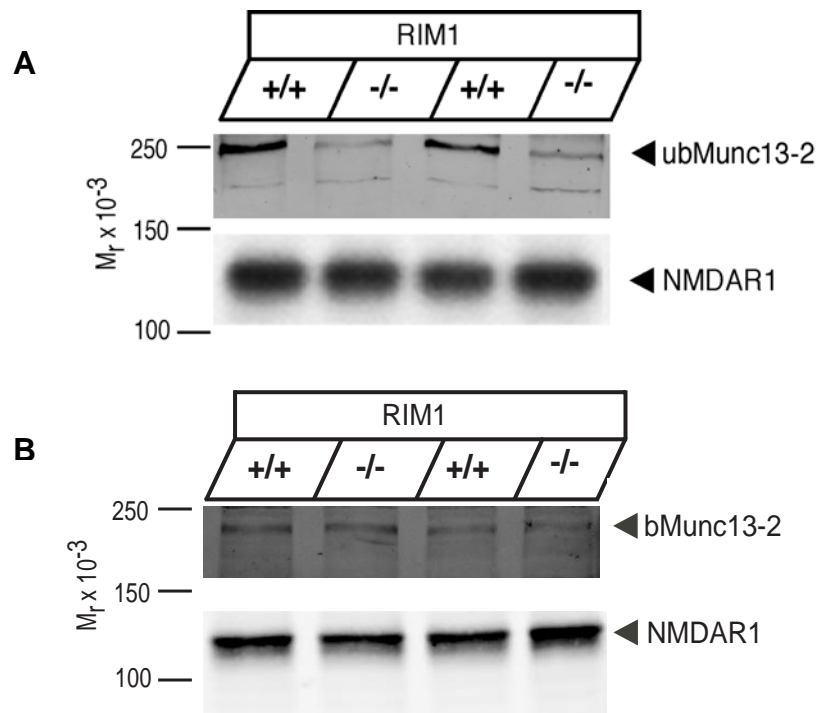


Figure 28. Analysis of Whole Brain Protein Levels of the Different Splice Variants of Munc13-2 in Wild Type and RIM1 α Knock Out Animals. Representative immunoblots of the level of (A) ubMunc13-2 and (B) bMunc13-2 in brains from wild type and homozygous RIM1 α knockout mice. The levels of NMDAR1 were probed on the same blots as loading controls. ubMunc13-2 shows significantly reduced protein levels in the RIM1 α knock out animals. No change was observed for bMunc13-2.

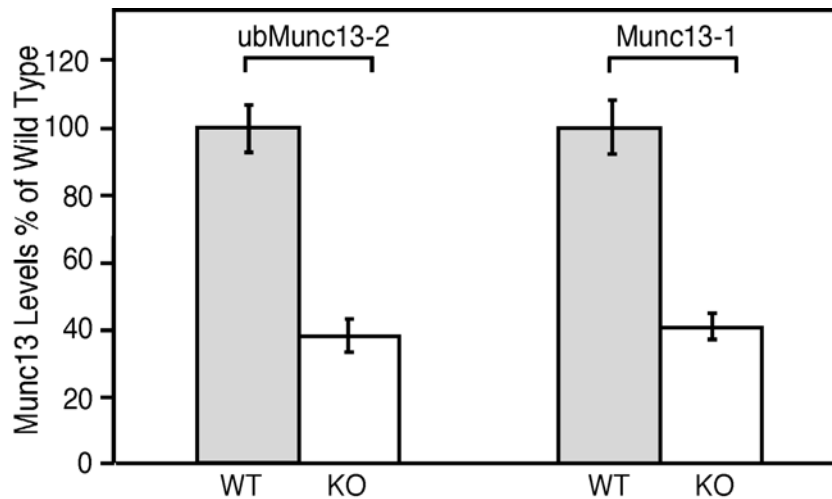


Figure 29. Quantification of Munc13-1 and ubMunc13-2 Levels in Whole Brains from Wild Type and RIM1 α Knock Out Animals. The levels of ubMunc13-2 and Munc13-1 in wild type and RIM1 α deficient littermates were quantified by immunoblotting with Alexa Infra Red labelled secondary antibodies and the OdysseyTM detection system. All signals were normalised using the levels of NMDAR1, which were probed on the same blot as loading control. Both Munc13-1 and ubMunc13-2 showed a 60% decrease in protein levels in knock out as compared to wild type RIM1 α animals. Error bars represent standard error of the mean.

3.3.2 Subcellular Distribution of Munc13-1 and ubMunc13-2

In the previous experiments, protein levels of Munc13-1 and ubMunc13-2 in wild type and RIM1 α knock out littermate whole brains were analysed. I next tried to determine whether the Munc13-1 and ubMunc13-2 fractions that remain in the absence of RIM1 α are distributed abnormally. For that purpose, I performed subcellular fractionation experiments on cerebral cortex homogenates from wild type and RIM1 α -deficient littermates and examined the distribution of Munc13-1 and ubMunc13-2 in the various subcellular fractions obtained. In agreement with previously published data (Augustin et al., 1999), I found Munc13-1 to be enriched in synaptosomal (P2) and synaptic membrane fractions (LP1), but also present in soluble fractions (S1, S3, LS1; Figure 30 A). A similar subcellular distribution was observed for ubMunc13-2 (Figure 31 A).

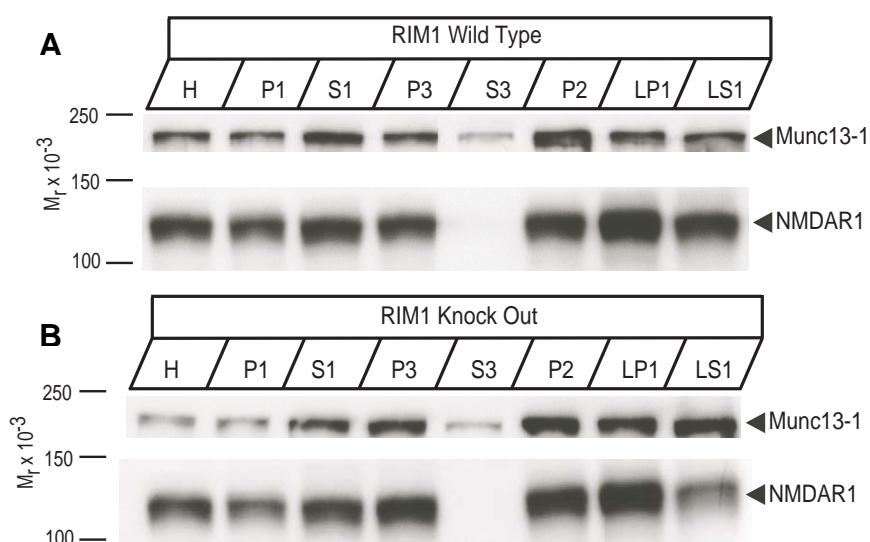


Figure 30. Subcellular Fractionation of Munc13-1 in Wild Type and RIM1 α Knock Out Mice. Immunoblots of subcellular fractions of brain homogenate from mice cortices were analysed with antibodies against Munc13-1 and NMDAR1. NMDAR1 levels and distribution remained unchanged. However, while the distribution of Munc13-1 stayed the same in wild type and knock out animals, the Munc13-1 protein levels were decreased in knock outs. Subcellular fractions were designated as follows: *H*, homogenate; *P1*, nuclear pellet; *P2*, crude synaptosomal pellet; *P3*, light membrane pellet; *S3*, cytosolic fraction; *LP1*, lysed synaptosomal membranes; *S1*, supernatant after synaptosome sedimentation; *LS1*, supernatant after LP1 sedimentation.

Analysis of the distribution of Munc13-1 and ubMunc13-2 in these cortical subcellular fractions in RIM1 α knock out animals showed that the subcellular distribution of Munc13-1 was not altered, although the overall protein levels were reduced (Figure 30B). Likewise, the subcellular distribution of ubMunc13-2 was similar in wild type and RIM1 α knock out brains, despite an overall reduction of expression levels. A notable exception was fraction S1, which arises after removal of crude synaptosomes from total homogenates (Figure 31B). The levels of ubMunc13-2 in this fraction appeared to be increased in the case of RIM1 α deficient brains as compared to wild type controls, indicating that ubMunc13-2 is less efficiently anchored within the presynaptic protein network in the absence of RIM1 α .

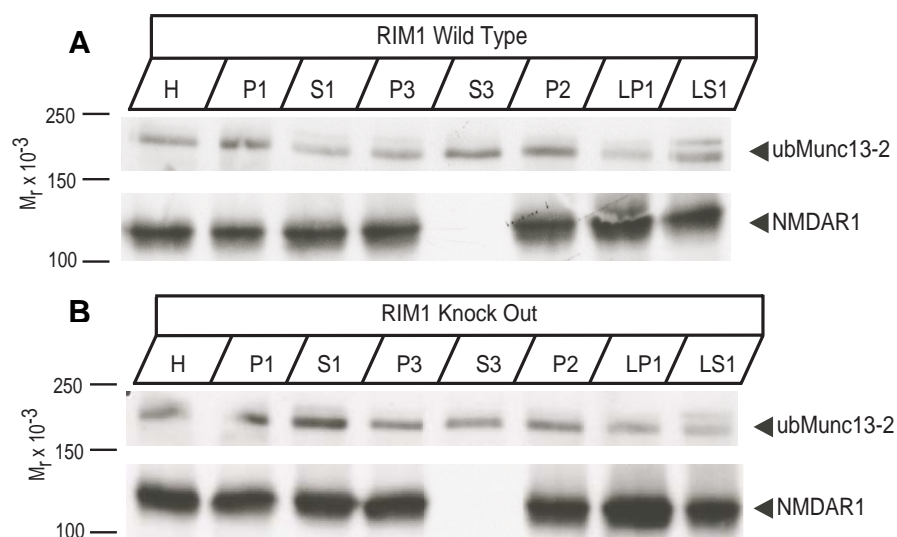


Figure 31. Subcellular Fractionation of ubMunc13-2 in Wild Type and RIM1 α Knock Out Littermates. Immunoblots of subcellular fractions of brain homogenate from mice cortices were analysed with antibodies against ubMunc13-2 and NMDAR1. NMDAR1 levels and distribution remained unchanged between wild type and RIM1 α knock out animals whereas the ubMunc13-2 protein levels were decreased and its distribution changed slightly between wild type and knock out animals, with a larger amount of ubMunc13-2 in the S1 soluble fraction in the RIM1 α knock out mice. Subcellular fractions were designated as follows: *H*, homogenate; *P1*, nuclear pellet; *P2*, crude synaptosomal pellet; *P3*, light membrane pellet; *S3*, cytosolic fraction; *LP1*, lysed synaptosomal membranes; *S1*, supernatant after synaptosome sedimentation; *LS1*, supernatant after LP1 sedimentation.

3.3.3 Analysis of Membrane-Bound and Soluble Protein Levels of Munc13-1 and ubMunc13-2

To analyse the subcellular distribution of the Munc13 proteins in wild type and RIM1 α knock outs in more detail, soluble proteins were carefully separated from membrane-bound proteins with the ultra-thorax homogenisation and high-speed centrifugation. The levels of membrane-bound and soluble Munc13 proteins were determined by quantitative Western blotting using NMDAR1 and GDP Disassociation Inhibitor (GDI) levels as loading controls, and the ratio between insoluble and soluble protein levels were calculated. Levels of Munc13-1 in the membrane bound fraction were reduced in RIM1 α knock out animals (Figure 32, 34).

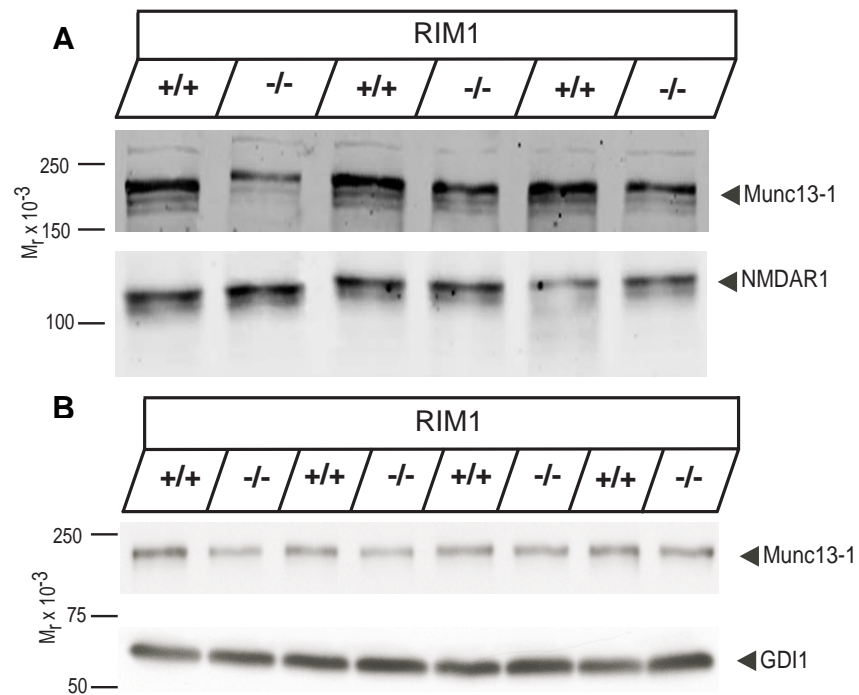


Figure 32. Soluble and Insoluble Fractions of Munc13-1 in Wild Type and RIM1 α Knock Out Animals. (A) Membrane-bound Munc13-1 protein levels were significantly reduced in RIM1 α knock out mice. The levels of NMDAR1 were probed on the same blots as loading controls. (B) Soluble protein levels were only slightly reduced in the RIM1 α knock out animals. The levels of GDP Disassociation Inhibitor (GDI) were probed on the same blots as loading controls.

In the case of ubMunc13-2, the protein levels in the membrane-bound fraction were also reduced (Figure 33, 34). I found that in the absence of RIM1 α , the relative amounts of soluble Munc13-1 and ubMunc13-2 are significantly increased as compared to the wild type situation (Figure 32-34).

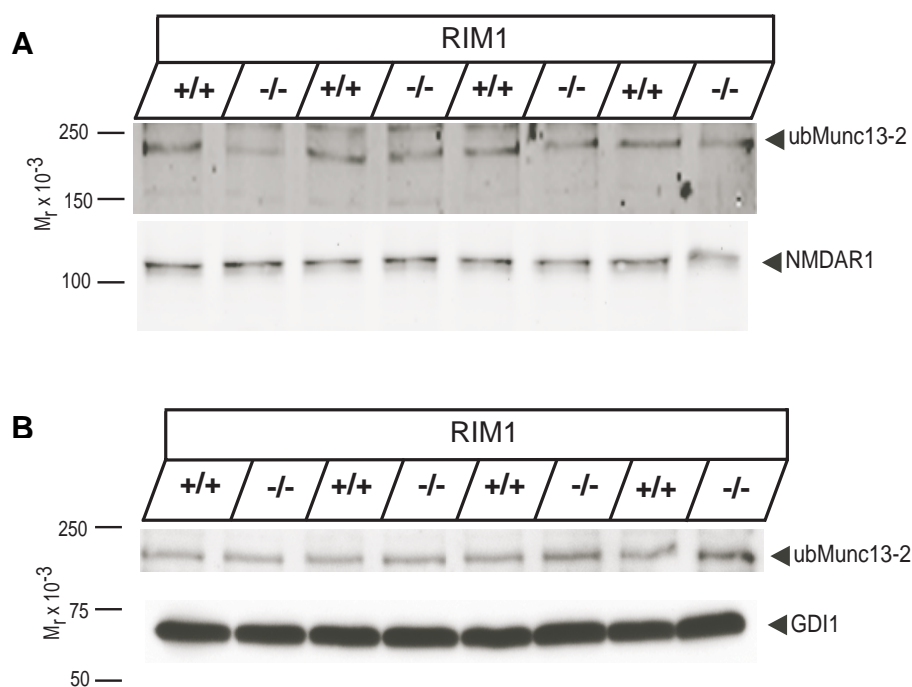


Figure 33. Soluble and Insoluble Fractions of ubMunc13-2 in Wild Type and RIM1 α Knock Out Animals. (A) Membrane-bound ubMunc13-2 protein levels were significantly reduced in RIM1 α knock out mice. The levels of NMDAR1 were probed on the same blots as loading controls. **(B)** Soluble protein levels showed a significant increase in the RIM1 α knock out animals. The levels of GDP Disassociation Inhibitor (GDI) were probed on the same blots as loading controls.

Taken together, my analyses of Munc13 protein levels in subcellular fractions from wild type and RIM1 α deficient brains show that both RIM1 α -binding partners, i.e. Munc13-1 and ubMunc13-2, are less efficiently anchored to synaptic membranes and, presumably as a consequence, exhibit a higher turnover rate and lower total expression levels in the absence of RIM1 α . These findings further support the notion that binding of Munc13-1 and ubMunc13-2 to α RIMs is critical for their proper recruitment to and anchoring at active zones.

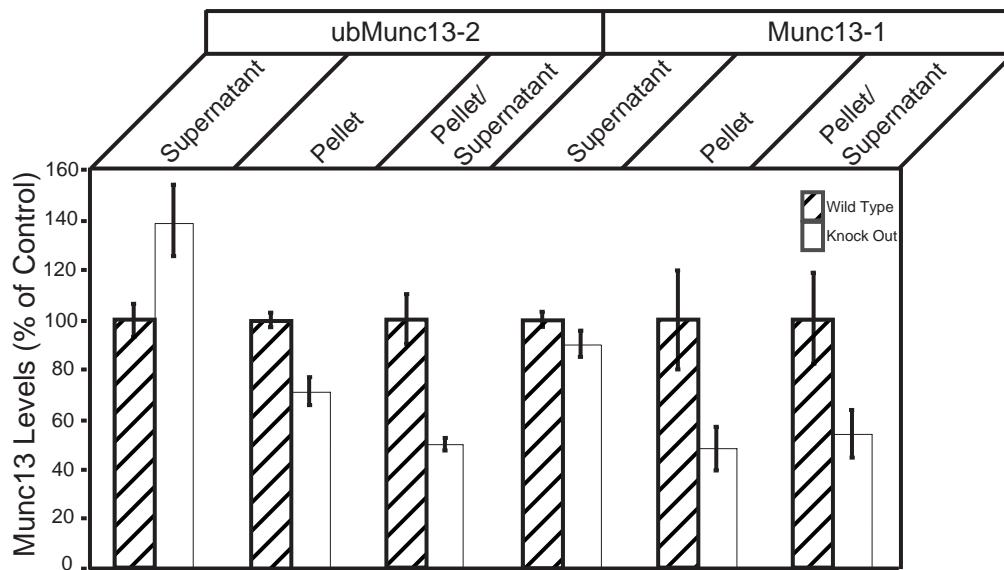


Figure 34.

Quantification of Soluble and Insoluble Fractions of Munc13-1 and ubMunc13-2. The levels of ubMunc13-2 and Munc13-1 in wild type and RIM1 α deficient littermates were quantified by immunoblotting with Alexa Infra Red labelled secondary antibodies and the OdysseyTM detection system. All signals were normalised using the levels of NMDAR1 (membrane bound fractions) and GDI (soluble fractions), which were probed on the same blots as loading control. Both Munc13-1 and ubMunc13-2 showed a 60% decrease in protein levels in knock out as compared to wild type RIM1 α animals. Membrane-bound Munc13-1 protein levels showed a 50% reduction in RIM1 α knock out mice while only a 10% reduction of soluble Munc13-1 was observed. Analysis of membrane-bound ubMunc13-2 protein levels indicated a 30% reduction in RIM1 α knock out animals while soluble ubMunc13-2 showed an approximate 40% increase. Error bars represent standard error of the mean.

3.3.4 Distribution of Munc13-1 in Hippocampus of Wild Type and RIM1 α Knock Out Littermates

Two main forms of long-term potentiation (LTP) have been distinguished in the mammalian brain (Nicoll et al. 1995). One requires activation of postsynaptic NMDA receptors, whereas the other, called mossy fibre LTP (mfLTP), has a principal presynaptic component. Mossy fibre LTP is expressed in hippocampal mossy fibre synapses (Nicoll et al., 1995; Henze et al., 2000) cerebellar parallel fibre synapses (Salin et al., 1996; Linden and Ahn, 1999) and corticothalamic synapses (Castro-Alamancos et al., 1999) where it apparently operates by a mechanism that requires activation of protein kinase A. RIM1 α is a protein kinase A substrate (Wang et al., 1997; Wang et al., 2000) and it has been shown that mossy fibre LTP in the hippocampus and the cerebellum is abolished in mice lacking RIM1 α (Castillo et al., 2002). Although mfLTP was measured and found to be normal in Munc13-1 heterozygous animals, where Munc13-1 levels are reduced by 50%, but show otherwise normal distribution (Castillo et al., 2002), I investigated the distribution of Munc13-1 in hippocampal slices of wild type and RIM1 α knock out animals to determine if, like in the Munc13-1 heterozygote knock out animals, Munc13-1 protein expression is simply reduced but distributed normally, or if its distribution is also disturbed.

So far, all of my experimental data indicated that α RIMs are likely to be involved in the presynaptic targeting and/or anchoring of Munc13-1 and ubMunc13-2. To further analyse such a role of α RIMs in the intact brain, I studied the distribution of Munc13-1 in wild type and RIM1 α deficient hippocampi by immunofluorescence staining. In my investigation of Munc13-1 in wild type and RIM1 α knock out littermates, immunohistochemical analysis of mossy fibre terminals in hippocampal slices from RIM1 α animals showed a striking difference not only between the Munc13-1 levels in wild type as compared to knock out animals, but also in the Munc13-1 distribution. In the wild type hippocampus, Munc13-1 was found to be strongly enriched in the granule cell mossy fibre terminals, which terminate within the *stratum lucidum*

of the CA3 region, and much less abundant in the surrounding neuropil and pyramidal cell body layers (Figure 35).

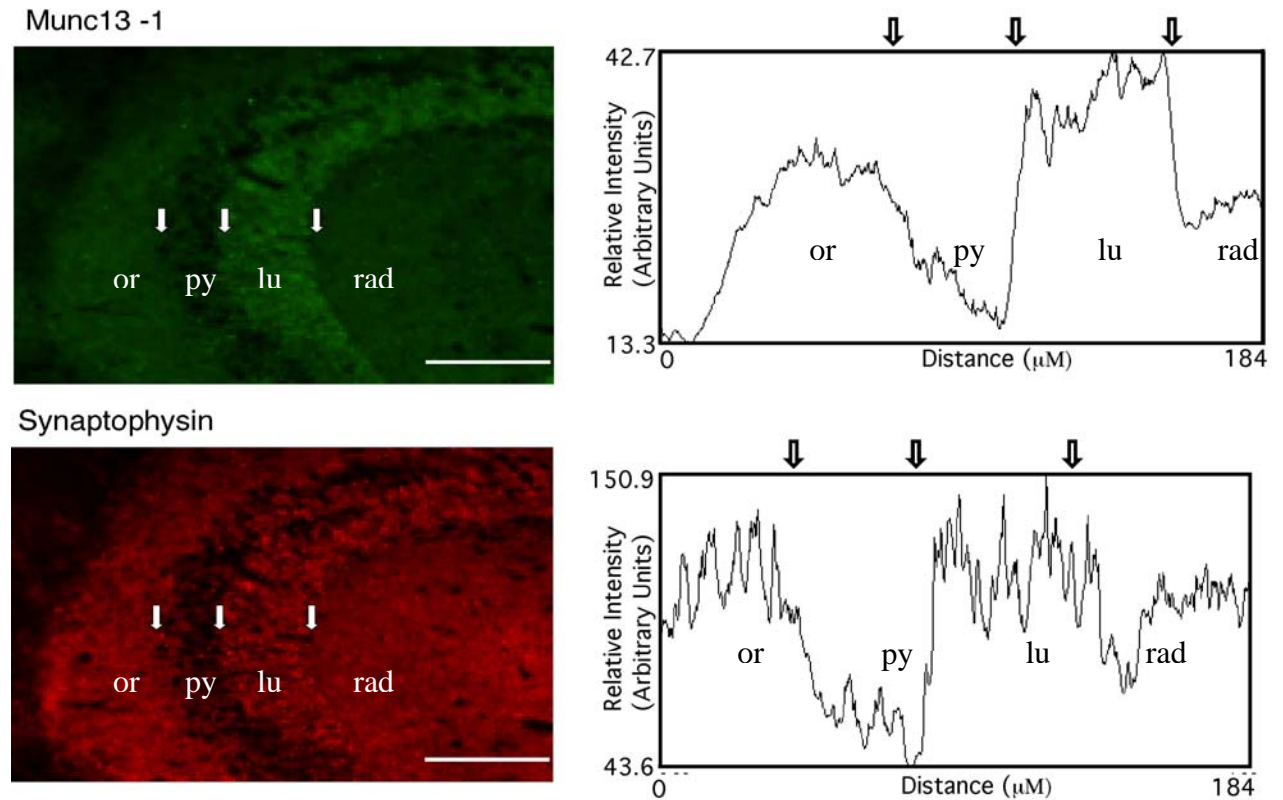


Figure 35. Immunofluorescence Localisation of Munc13-1 in Hippocampal Slices from RIM1 α Wild Type Animals. Immunofluorescence double staining for Munc13-1 (green) and Synaptophysin (red). The first arrow indicates the beginning of the pyramidal cell layer, the second arrow, the beginning of the *stratum lucidum*, and the third arrow, the beginning of the *stratum radiatum* of the hippocampus slice. Intensity plots indicate relative fluorescence intensity across the slice. On slices, the *stratum lucidum* is clearly defined with both Munc13-1 and Synaptophysin fluorescence. The intensity plots show a clear jump in fluorescence for the *stratum lucidum* area for both Munc13-1 and Synaptophysin. The different hippocampal layers are designated as follows: or, *stratum oriens*; py, pyramidal cell layer; lu, *stratum lucidum*; rad, *stratum radiatum*. Scale bar 100 μ M.

In contrast, hippocampal sections from RIM1 α deficient brains showed not only the expected reduction in Munc13-1 protein levels, but there was also no evidence of a relative accumulation of Munc13-1 in mossy fibre terminals of

the *stratum lucidum* (Figure 36), although the presynaptic marker Synaptophysin was distributed normally.

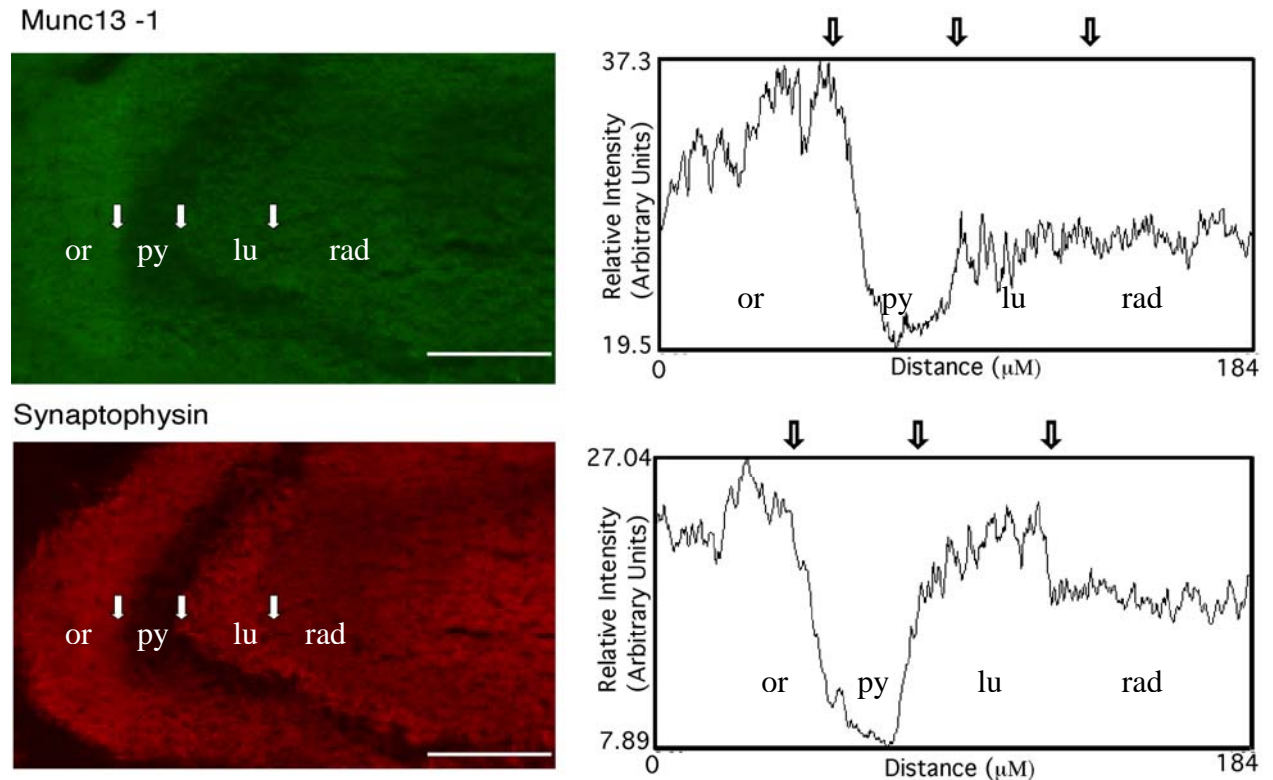


Figure 36. Immunofluorescence Localisation of Munc13-1 in Hippocampal Slices from RIM1 α Knock Out Animals. Immunofluorescence double staining for Munc13-1 (green) and Synaptophysin (red). The first arrow indicates the beginning of the pyramidal cell layer, the second arrow, the beginning of the *stratum lucidum*, and the third arrow, the beginning of the *stratum radiatum* of a hippocampus slice. Intensity plots indicate relative fluorescence intensity across the slice. The *stratum lucidum* is clearly defined with Synaptophysin fluorescence, but not with Munc13-1 fluorescence staining. The respective intensity plots show a clear jump in fluorescence for the *stratum lucidum* area for Synaptophysin but not for Munc13-1. The different hippocampal layers are designated as follows: or, *stratum oriens*; py, pyramidal cell layer; lu, *stratum lucidum*; rad, *stratum radiatum*. Scale bar 100 μ M.

This misdistribution of Munc13-1 in RIM1 α deficient hippocampi was most apparent upon analysis of the Munc13-1 immunofluorescence intensity across the neuropil and cell body layers of the CA3 region. In wild type sections,

Munc13-1 immunofluorescence intensity increased sharply at the interface between the pyramidal cell body layer and *stratum lucidum* and decreased sharply at the interface between *stratum lucidum* and the adjacent neuropil layer (Figure 35). In RIM1 α deficient hippocampal sections, on the other hand, Munc13-1 immunofluorescence intensity increased only moderately at the interface between the cell body layer and *stratum lucidum* and remained constant at the interface between *stratum lucidum* and the adjacent neuropil layer (Figure 36). These findings provide *in vivo* evidence for a role of α RIMs in presynaptic targeting and/or anchoring of Munc13-1 at active zones.

3.4 Generation of Munc13-1 Conditional Knock Out Vector

Compensatory mechanisms, functional redundancies, and lethal phenotypes often hinder complete analysis of gene functions in germ-line null mutations in the mouse (Metzger and Chambon, 2001). All of the above stated drawbacks are relevant in the case of Munc13-1: (i) In certain brain regions the other Munc13 isoforms, for example, Munc13-2 in the hippocampus and Munc13-3 in the cerebellum, carry out the priming function in the synaptic vesicle cycle; (ii) Complete functional redundancy is observed in some synapses, where Munc13-2 can substitute for Munc13-1 in all GABAergic synapses and a small subpopulation of glutamatergic synapses (Varoqueaux et al., 2001); (iii) Mice lacking Munc13-1 die immediately after birth, demonstrating that this protein is an essential component of a functional nervous system (Augustin et al., 1999). For the design of a conditional targeting vector for the Munc13-1 gene, I took advantage of the facts that Cre recombinase can invert or excise a DNA fragment depending on the orientation of the flanking loxP sites and that wild type mutant loxP sites (loxP511) can be recognized by Cre recombinase but do not recombine with each other.

A previously published mouse genomic Munc13-1 clone (pM13-27.1; Augustin et al., 1999b) was used to construct the targeting vector for conditional Munc13-1 knock outs. Exons 5 and 6, whose loss leads to the elimination of Munc13-1 expression (Augustin et al., 1999b) was targeted for deletion. The vector contains one pair of wild type loxP sites (red arrowheads in Figure 37) and one pair of mutant loxP511 sites (blue arrowheads in Figure 37) as well as two FRT sites flanking a Neomycin resistance cassette for positive selection. The targeting vector contained one loxP site in the intron upstream of exon 5 and one, in the opposite orientation, upstream of the FRT-Neo-FRT cassette. One loxP511 site was inserted into the intron downstream of exon 6, and a second one, in opposite orientation, downstream of the FRT-Neo-FRT cassette. In addition, a lacZ-IRES cassette was inserted between the nested loxP and loxP511 sites in antisense orientation. Two copies of the Herpes Simplex Virus thymidine kinase gene were attached 5' to the short arm of the

vector for negative selection (Figure 37). ES stem cell clones that incorporate this vector in the desired fashion can be analysed by Southern blotting of BglII digested genomic DNA using 5' flanking PstI fragment as a probe (wild type band of 4.6 kb, knock out band of 2.7 kb).

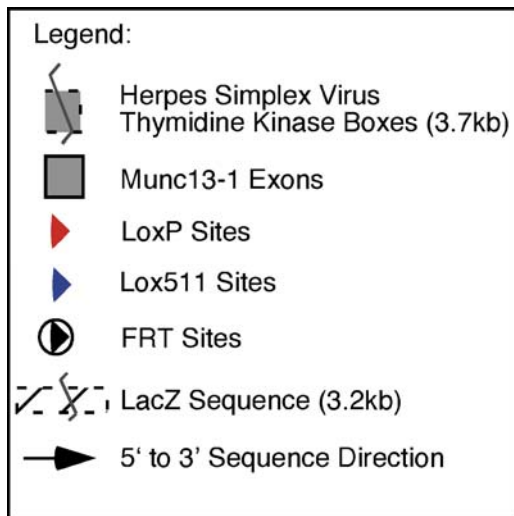
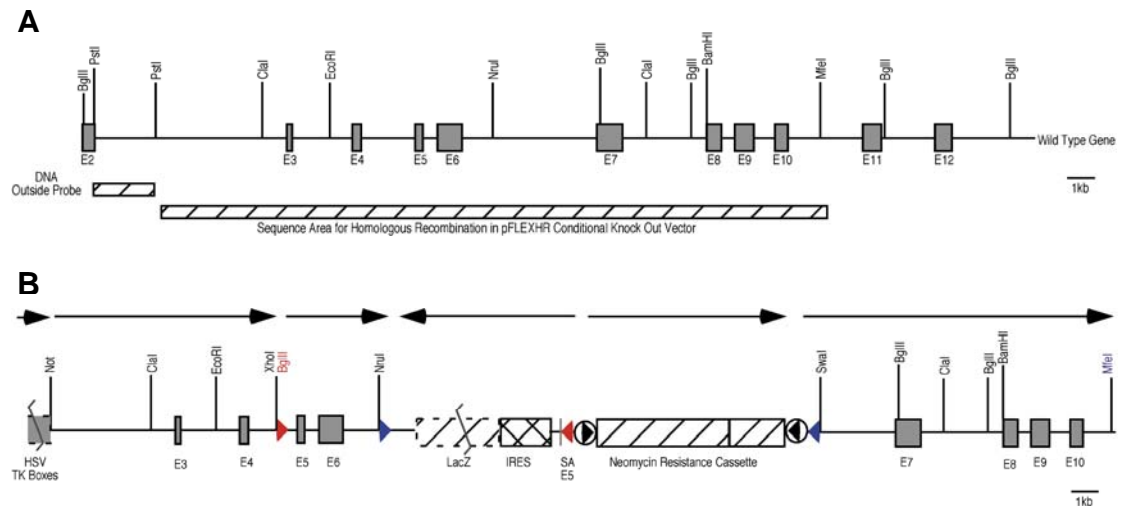


Figure 37. Generation of the Munc13-1 Conditional Knock Out Vector. (A) Map of the Munc13-1 wild type gene covered by the genomic clone pM13-27.1. The hatched bars indicate the region of the wild type Munc13-1 gene to be recombined and the outside DNA PstI probe. (B) The targeting vector pFlexHR with the Munc13-1 genomic fragments inserted. The vector can be linearised with MfeI/MunI highlighted in blue, and an extra BglII site (highlighted in red) was inserted to facilitate Southern blot screening.

Once introduced into the Munc13-1 gene, this vector arrangement, which has been used successfully for the conditional knock out of several genes, will allow elimination of exons 5 and 6 of the Munc13-1 gene and concomitant expression of lacZ from the Munc13-1 promoter. Flp-mediated recombination will allow removal of the Neomycin resistance gene. Cre-mediated recombination will then invert one of the two DNA fragments flanked by loxP or loxP511 sites and put the IRES-lacZ cassette in sense orientation, allowing

for lacZ expression from the Munc13-1 promoter. A second Cre-mediated recombination will excise the DNA fragment containing exons 5 and 6, leading to the inactivation of the Munc13-1 gene.

Depending on the Cre expressing mouse line used, this gene targeting strategy will allow the knock out of Munc13-1 in certain brain regions and/or at different times during development. At the same time, lacZ expression can be used for the analysis of Munc13-1 expression domains.

4. Discussion

Munc13s and α RIMs are multidomain active zone proteins, which act in the priming reaction that prepares synaptic vesicles for neurotransmitter release. Both proteins are additionally involved in short- and long-term synaptic plasticity. However, it is unclear how α RIMs and Munc13s perform these multiple functions, and an immense gap separates the extensive genetic and physiological data available on α RIMs and Munc13s from a molecular understanding of their roles. This gap is in part due to a lack of structural information about how α RIMs and Munc13s interact with each other and with other synaptic proteins. The data in this work now provide a functional analysis of the α RIM-Munc13 interaction by examining the consequences of structural changes in the Munc13 protein that abolish α RIM binding. Additionally, RIM1 α knock out and wild type animals were analysed to determine the effect of RIM1 α loss on Munc13-1 and ubMunc13-2 protein levels, distribution and synaptic localisation.

4.1 Differential Evolution of RIM Binding and Priming Modules in Munc13 Proteins

The mammalian Unc-13 homologs, Munc13-1, bMunc13-2, ubMunc13-2 and Munc13-3, the corresponding *C. elegans* amino-terminal alternative splice variants, Unc-13-MR and Unc-13-LR, as well as the *Drosophila melanogaster* protein Dr-Unc-13 are very similar in their carboxy-terminal regions, including their regulatory C1 and C2 domains (Brose et al., 1995; Augustin et al., 1999a; Eustance Kohn et al., 2000). The Unc-13-LR splice variant contains an amino terminus that is highly homologous to that of Munc13-1 and ubMunc13-2, while the other variant, Unc-13-MR and the amino terminal regions of all other isoforms are otherwise completely unrelated (Brose et al., 2000; Betz et al., 2001). The differentially evolved Munc13 modules have distinct functional roles in Munc13-1. The conserved carboxy-terminal R region is necessary and sufficient for secretory vesicle priming in chromaffin cells and neurons (Ashery et al., 2000; Betz et al., 2001). The amino-terminal

α RIM binding L region of Munc13-1/ubMunc13-2 conveys a synapse-specific function that is not directly involved in the priming reaction but has been demonstrated to influence it indirectly (Betz et al., 2001; Dulubova et al., 2005). Disruption of the RIM1 α -Munc13-1 interaction in wild type neurons results in a deficiency in synaptic vesicle priming that is reminiscent of the Munc13-1 knock out phenotype (Betz et al., 2001). This finding indicates that RIM binding to Munc13-1 has an important regulatory function in the presynapse, for example by anchoring Munc13-1 in the active zone and thereby positioning it for optimal function or by modulating the priming and secretion apparatus. Indeed, the α RIM binding-deficient Munc13-1 is functionally compromised in neurons, as it is not able to completely rescue the Munc13-1 knock out phenotype upon overexpression (Betz et al., 2001). Moreover, in the calyx of Held synapse, introduction of a short α RIM fragment spanning the zinc finger domain, which is responsible for Munc13-1 binding, severely decreases the readily releasable pool of vesicles, while a mutated form of this zinc finger region, which is unable to bind Munc13-1, does not (Dulubova et al., 2005).

Studies carried out in *C. elegans* support the view that the amino-terminal α RIM binding L region of Munc13-1 conveys a synapse-specific function. Here one of the major differences between the Unc-13 isoforms, Unc-13-MR and Unc-13-LR, was observed with regard to their subcellular localisation (Eustance Kohn et al., 2000). The Unc-13-LR form, which is entirely homologous to Munc13-1/ubMunc13-2 and contains both a putative RIM binding domain in its L region as well as the highly conserved R region that harbours the priming activity, is mainly localised to the presynapse. In contrast, the Unc-13-MR splice variant that has a completely unrelated amino terminus exhibits a more diffuse distribution along axons. However, the Unc-13-MR protein is also present in synapses and can be further recruited to synapses upon elevation of DAG levels, indicating the existence of multiple synaptic targeting sequences and mechanisms in Unc-13 proteins (Eustance Kohn et al., 2000). An additional parallel exists between data from *C. elegans* and mammals with respect to the rescue ability of different Unc-13/Munc13-1

constructs in the Unc-13/Munc13-1 null mutant background. As mentioned above, full-length Munc13-1 completely rescues the Munc13-1 knock out phenotype, while an α RIM binding deficient Munc13-1 construct lacking the L region is partly dysfunctional. Unlike priming deficient constructs, which show no rescue regardless of expression levels, the α RIM binding-deficient Munc13-1 construct was able to partially rescue the Munc13-1 deletion mutant phenotype upon very strong overexpression (Betz et al., 2001). Similarly, transgenic rescue of *C. elegans unc-13* null alleles using a cosmid that is only able to replace the RIM binding-deficient Unc-13-MR is incomplete, as determined on the basis of behavioural parameters, while rescue with a cosmid that also replaces the RIM binding Unc-13-LR form is much more effective (Eustance Kohn et al., 2000).

Together, these observations clearly document a functional role of α RIM-Munc13 interactions. However, the tools used in the corresponding studies did not allow one to distinguish effects related to the α RIM-Munc13 interaction from effects caused by the perturbation of other processes. Moreover, none of those studies could clearly define whether α RIM binding to Munc13s regulated protein trafficking or function, or even both. The present study resolved this problem by using point mutations of Munc13s that do not bind α RIMs and studying their synaptic targeting characteristics.

4.2 Identification of Structural Changes in the Munc13-1 and ubMunc13-2 Amino Termini which Abolish α RIM Binding

The creation of a complex LexA-ubMunc13-2 mutant library was critical to the success in finding point mutations that disrupt the interaction between ubMunc13-2 and RIM1 α . The yeast two-hybrid system proved to be a simple yet powerful tool for identifying structural alterations that lead to functional changes. Although the majority of changes identified (18 out of 26) were either insertions or deletions that led to a frame shift in the ubMunc13-2 reading frame and caused premature stops, eight constructs were obtained which contained single or multiple point mutations in the gene (Figure 10).

The constructs with multiple point mutations were used as a basis for the production of single point mutation containing constructs. This enabled the pinpointing of specific mutations, which resulted in the abolishment of binding between ubMunc13-2 and RIM1 α (Figure 11). Interestingly, all identified point mutations that abolished the α RIM-ubMunc13-2 interaction concerned residues that are conserved between ubmunc13-2 and Munc13-1. Indeed, when these mutations were inserted at the homologous positions in the Munc13-1 amino terminus, RIM1 α binding by this Munc13 isoform was also abolished in the yeast two-hybrid system (Figure 12). These findings document the power and reliability of the yeast two-hybrid approach used here.

4.3 Identified Munc13-1 and ubMunc13-2 Mutants do not Bind to RIM1 α in *in vitro* Binding Assays and in Living Cells

The α RIM binding deficient mutant Munc13 fusion proteins showed expression levels in bacterial and eukaryotic cells that were similar to the respective wild type proteins. This indicates that the point mutations did not cause any severe misfolding or alteration in the overall structure of the Munc13 proteins, and it excluded the possibility that the proteins were trapped in inclusion bodies. The α RIM binding deficient ubMunc13-2 mutants, identified in the yeast two-hybrid system, all showed no interaction in the *in vitro* binding assays with native α RIM (Figure 13). However, in the case of Munc13-1 only one mutation, Munc13-1^{I121N} demonstrated a significantly lower level of binding (Figure 14). One explanation for these data may be that Munc13-1 either forms a homodimer or binds to another, yet unknown or uncharacterised Munc13-1 interacting molecule in the rat brain synaptosomal extract and this interaction is not interrupted by the mutation that abolishes the Munc13- α RIM interaction. Both wild type and α RIM binding deficient Munc13-1 mutants may then indirectly bind to α RIM through this interaction, leading to a false positive binding phenotype in this assay. To circumvent this problem, purely recombinant proteins were used for the cosedimentation assays. This approach allows the analysis of the RIM1 α -Munc13 interaction

only and prevents any interference from other interacting molecules. In the cosedimentation assay with purely recombinant proteins, both Munc13-1^{I121N} and ubMunc13-2^{I121N}, showed no RIM1 α binding, while the wild type proteins bound strongly (Figure 16). The cosedimentation assay, with both native α RIM from synaptosomal extracts and bacterially expressed recombinant RIM1 α gave conclusive evidence that the single point mutation, Isoleucine 121 Asparagine, identified in the yeast two-hybrid screen, abolishes binding of Munc13-1 and ubMunc13-2 to α RIM.

EGFP-tagged, full-length wild type Munc13-1 and RIM1 α binding deficient mutant Munc13-1^{I121N} both form large aggregates in HEK293 cells, when expressed singly and also when co-expressed with RIM1 α . RIM1 α was recruited into the Munc13-1-EGFP aggregates but not into the aggregates formed by Munc13-1^{I121N}-EGFP (Figure 18, 19), providing further evidence for the effectiveness of the identified mutation in disrupting the α RIM-Munc13 interaction. This confirmed point mutation provides a powerful tool to study the importance of the α RIM-Munc13 interaction for Munc13 function.

The C1-domains of the three known Munc13 isoforms are extremely homologous and contain all critical residues necessary for phorbol ester binding (Kazanietz et al., 1994). Activation of Munc13s by β -phorbol esters or diacylglycerol induces membrane association and enhances neurotransmitter release (Betz et al., 1998; Ashery et al. 2000). Munc13 proteins may be responsible for a number of phorbol ester effects on synaptic transmission and membrane traffic that cannot be attributed to protein kinase C (Scholfield and Smith, 1989; Fabbri et al., 1994; Redman et al., 1997). For example, Munc13s and not protein kinase C are the only receptors involved in the acute regulation of presynaptic transmitter release by β -phorbol esters or diacylglycerol in hippocampal neurons (Rhee et al., 2002). In my experiments, both full-length wild type Munc13-1, Munc13-1-EGFP, and the non-RIM1 α binding mutant, Munc13-1^{I121N}-EGFP, showed translocation to the plasma membrane upon treatment with β -phorbol esters. RIM1 α , however, exhibited cotranslocation only when co-expressed with wild type Munc13-1 (Figure 20,

21). Coexpression studies in HEK293 cells show that Munc13-1 binds α RIM in a cellular environment and that the I121N mutation is sufficient to abolish the α RIM-Munc13-1 interaction without altering the phorbol ester sensitivity and translocation properties of the Munc13-1 protein. The latter finding further supports the notion that the I121N mutation does not perturb the entire structure of Munc13-1.

4.4 Potential Role of α RIMs in the Targeting/Anchoring of Munc13-1 and ubMunc13-2

Neurotransmitter release at the presynaptic terminal is characterised by high temporal resolution and spatial restriction to the active zone. Another characteristic of transmitter release is its efficiency, even at very high action potential frequencies. These characteristics indicate that sequential steps in the synaptic vesicle cycle are occurring in a highly coordinated manner. In order to guarantee such spatial and temporal coordination, the main active zone processes of vesicle tethering, priming, and fusion are likely to be coupled through direct protein-protein interaction at the molecular level. The priming step of synaptic vesicle exocytosis is thought to require the formation of the SNARE complex. The amino terminal region of Syntaxin 1 contains a three-helix domain that folds back onto the SNARE motif forming a closed conformation. This 'closed' Syntaxin is unable to bind other SNARE proteins and therefore is incompatible with formation of the SNARE complex (Dulubova et al., 1999). The amino terminus of Syntaxin 1 also binds to Unc-13/Munc13-1 (Betz et al., 1997). Munc13-1, is thought to promote vesicle priming by modifying this 'closed' Syntaxin 1 conformation, thereby regulating the availability of Syntaxin 1 for core complex formation (Augustin et al., 1999b; Ashery et al., 2000; Brose et al., 2000; Richmond et al., 2001; Rizo & Südhof, 2002). The Munc13- α RIM interaction is essential for a step in the synaptic vesicle cycle that precedes vesicle fusion (Betz et al., 2001; Dulubova et al, 2005). Similar to total loss of Munc13-1, disruption of this interaction in wild type hippocampal neurons leads to a drastically reduced

primed and readily releasable vesicle pool, which in turn causes a strong reduction in evoked release (Betz et al., 2001; Dulubova et al., 2005).

In a previous study, striking functional differences were observed between full-length Munc13-1(1-1736), amino-terminally truncated α RIM binding deficient Munc13-1(520-1736), and a priming-deficient Munc13-1(1-451) (Betz et al., 2001). In that study, differences were observed with respect to the functioning of the full-length, the priming deficient and RIM1 α binding deficient constructs, but no conclusions could be drawn about the targeting of the constructs or the potential role of α RIM binding in that targeting. In my analysis of targeting of wild type Munc13-1 and RIM1 α binding deficient Munc13-1^{I121N} in primary hippocampal neurons, the RIM1 α binding deficient protein exhibited a 10-fold reduction in localisation at the active zone when compared to the wild type protein and, more often than not, displayed mislocalised, ectopic localisation within the axon (Figure 23-26). One explanation for this phenotype may be that the Munc13-1^{I121N}-EGFP protein is aggregating due to misfolding and thus not being targeted to the synapses. However, this is unlikely, as the protein is targeted to the presynapse, albeit at reduced efficiency. Another explanation could be that Munc13-1 and ubMunc13-2 are anchored to active zones by two different presynaptic anchoring proteins, one of which is RIM1 α . When both targeting/anchoring proteins are present, Munc13 localises at synapses with highest efficiency. However, when α RIMs are absent, then only one binding partner remains which can target the Munc13s to the active zone, which is why I still observe limited synaptic localisation even in the absence of α RIM binding.

Considered along with other electrophysiological experiments (Betz et al., 2001), my results indicate that RIM1 α plays an important role in the targeting to or retention of Munc13-1/ubMunc13-2 at active zones. It is therefore likely that Munc13-1 contains at least two different presynaptic targeting sequences, the more important of which is the α RIM binding site. Munc13-3, which contains no α RIM binding sequence but is otherwise highly homologous to Munc13-1, exhibits a presynaptic localisation in the cerebellum that is

indistinguishable from that of Munc13-1 (Augustin et al., 1999a). Other scaffolding molecules, such as Piccolo, Bassoon and ERCs, exist at the active zone and may act as targeting or tethering proteins for the other Munc13 isoforms. While this demonstrates that α RIM binding to Munc13s may not be essential for Munc13 presynaptic targeting, it also shows clearly that the interaction plays an important role, at least in part, in the localisation of Munc13-1.

4.5 Munc13-1 and ubMunc13-2 Show Altered Protein Concentration Levels and Distribution in RIM1 α Knock Out Animals

A detailed analysis of the active zone proteins Munc13-1 and ubMunc13-2 in RIM1 α knock outs was carried out to determine what effect the deletion of RIM1 α has on both protein concentration levels and subcellular localisation of these proteins. In a previously published report (Schoch et al., 2002), it was demonstrated that only Munc13-1 showed a change in expression in the absence of RIM1 α (60% decrease), likely due to destabilization in the absence of RIM1 α . In the same study, it was also reported that Munc13-2, which is expressed widely, showed no change in its expression level in RIM1 α knock outs (Schoch et al., 2002). In my study, I replicated the Munc13-1 results by showing a 60% reduction in protein concentration in RIM1 α knock outs. However, in contrast to previous findings, I was also able to show that the levels of ubMunc13-2 are reduced by 60% in the absence of RIM1 α . Only bMunc13-2, which has an amino-terminus that is unrelated to that of Munc13-1 and ubMunc13-2, and which exhibits no α RIM interaction, showed no change in protein expression in the RIM1 α knock out animals (Figure 27-29). The likely explanation for the difference between my data and those published on the Munc13-2 protein levels in RIM1 α knock outs, is that bMunc13-2 specific antibodies were used by Schoch et al. (2002) and hence no change in levels between wild type and RIM1 α deficient animals were observed.

In agreement with previously published data (Augustin et al., 1999), a synaptic enrichment of Munc13-1 and ubMunc13-2 was observed in subcellular fractionation experiments. Moreover, the subcellular fractionation of Munc13-1 and ubMunc13-2 was similar in samples from wild type and RIM1 α knock outs with the notable exception of ubMunc13-2 levels in fraction S1, which arises after removal of crude synaptosomes from total homogenates (Figure 30, 31). The levels of ubMunc13-2 in this fraction were increased in the case of RIM1 α deficient brains as compared to wild type controls, indicating that ubMunc13-2 is less efficiently anchored within the presynaptic protein network in the absence of RIM1 α . Upon more detailed analysis of the soluble and membrane bound fractions of Munc13-1 and ubMunc13-2 in wild type and RIM1 α deficient brains, I found that in the absence of RIM1 α , the relative amounts of soluble Munc13-1 and ubMunc13-2 are significantly increased as compared to the wild type situation (Figure 32-34). These data indicate that both Munc13 isoforms shift from membrane bound to soluble fractions. The fact that ubMunc13-2 but not Munc13-1 is actually enriched in soluble fraction S1 may be due to a longer half-life of ubMunc13-2 in the cytosol.

In summary, my analyses of Munc13 protein levels in subcellular fractions from wild type and RIM1 α deficient brains show that both RIM1 α -binding partners, i.e. Munc13-1 and ubMunc13-2, are less efficiently anchored to synaptic membranes and, presumably as a consequence, exhibit a higher turnover rate and lower total expression levels in the absence of RIM1 α . These findings support the notion that binding of Munc13-1 and ubMunc13-2 to α RIMs is critical for their proper recruitment to and anchoring at active zones.

4.6 Munc13-1 and ubMunc13-2 are the Main “Output” Molecules of RIM1 α Function

All of my data indicate that α RIMs are involved in the presynaptic targeting

and/or anchoring of Munc13-1 and ubMunc13-2. This hypothesis was further supported by the finding that the distribution of Munc13-1 differed dramatically in wild type and RIM1 α deficient hippocampi. In wild type hippocampus, Munc13-1 was found to be strongly enriched within the *stratum lucidum* of the CA3 region, but much less abundant in the surrounding neuropil and cell body layer. In contrast, hippocampal sections from RIM1 α deficient brains showed no evidence of a relative accumulation of Munc13-1 in mossy fiber terminals of the *stratum lucidum*, although, the presynaptic marker Synaptophysin was distributed normally and enriched in the *stratum lucidum* (Figure 35, 36). This misdistribution of Munc13-1 in RIM1 α deficient hippocampi was confirmed upon quantitative analysis of the Munc13-1 immunofluorescence intensity across the neuropil and cell body layers of the CA3 region. These findings provide for the first time, *in vivo* evidence for a role of α RIMs in presynaptic targeting and/or anchoring of Munc13-1 at active zones.

It was previously postulated that the decrease in Munc13-1 concentration observed in the RIM1 α knock out mice could not be responsible for the mfLTP deficient phenotype seen in hippocampal mossy fibre synapses of RIM1 α mutants (Castillo et al., 2002). The basis for this line of reasoning was that the Munc13-1 heterozygote mice, in which Munc13-1 levels are reduced to 50% (as opposed to a 60% loss of Munc13-1 protein level in the RIM1 α knock out animals), showed no alteration in mfLTP. Based on my experiments however, this argument is no longer valid, since upon examination of the RIM1 α knock out mice, I observed not only the 60% reduction in overall Munc13-1 concentration, but also a similar 60% reduction in ubMunc13-2, which may have effects on synaptic plasticity. Moreover, there is also a redistribution of both proteins upon loss of RIM1 α , most striking being the observation that this redistribution of the Munc13-1 isoform was very prominent in the *stratum lucidum* of the hippocampi of RIM1 α mutant mice, where mfLTP occurs. A number of experiments can be carried out to determine if Munc13-1 and ubMunc13-2 are indeed responsible for the mfLTP phenotype observed in the absence of RIM1 α . Mossy Fibre LTP can be measured in mice, which are Munc13-1 heterozygote knock out crossed with Munc13-2 heterozygote knock

out. Here both Munc13-1 and ubMunc13-2 levels are reduced by 50%, which closer reflects the Munc13 levels (60% loss), though not the disturbed distribution, observed in the RIM1 α knock out mice. The Munc13-1 heterozygote knock out can additionally be crossed with Munc13-2 knock out animals, where the complete Munc13-1/ubMunc13-2 loss is at or below a postulated threshold of 60% for observing possible changes in mfLTP. The planned Munc13-1 conditional knock out mice can also be utilised for mfLTP analysis, where one can selectively remove Munc13-1 from the hippocampus via crossing with transgenic mice that express cre-recombinase under the control of the promoter for the α subunit of calcium-calmodulin-dependent protein kinase II (CaMKII α) (Dragatsis and Zeitlin, 2000). The mice lacking Munc13-1 in the hippocampus can be further crossed with the Munc13-2 knock out before mfLTP measurements.

α RIM binding to the Munc13-1 amino terminus may directly regulate the priming activity of Munc13-1. Munc13-1 is essential for synaptic vesicle priming (Augustin et al., 1999b), and vesicle priming is likely to be the rate-limiting step in many secretory processes, including catecholamine release from chromaffin cells (Ashery et al., 2000). Thus, modulation of the activity of the Munc13-1 pool in the active zone by protein interactors such as RIM1 α or by second messengers such as diacylglycerol (Betz et al., 1998) is a likely mechanism that dynamically regulates the pool of readily releasable vesicles and synaptic efficacy. In wild type animals, Munc13s may experience increased targeting to synapses by phosphorylated RIM1 α . In view of the present data, it is tempting to speculate that the functions of RIM1 α , for example in mossy fibre LTP, are mediated via Munc13-1 as the main "output" molecule with core complex formation and vesicle priming as the target processes. Indeed, RIM1 α binding to Munc13-1 may serve as a switch to activate the priming apparatus once an appropriate Rab3-bearing vesicle has arrived.

5. Outlook

The next stage of the project would involve further experiments with full-length, wild type and α RIM binding deficient mutants, Munc13-1-EGFP, Munc13-1^{121N}-EGFP, ubMunc13-2-EGFP and ubMunc13-2^{121N}-EGFP. These constructs have been cloned into the Lentivirus expression system. Gene transfer based on lentiviruses is distinguished by the virus' ability to transduce non-dividing cells (Naldini et al., 1996; Naldini, 1998). Lentiviruses allow efficient delivery, integration and long-term expression of transgenes and the expression levels of proteins expressed with the lentivirus system are lower than those observed with the calcium phosphate overexpression approach. The Munc13 lentiviral constructs will be used for studies in Munc13-1/2 double knock out neuron cultures, to assess the functionality of the α RIM binding deficient mutant forms of Munc13 and to analyse the targeting of Munc13-1 and ubMunc13-2 in more detail.

Additional planned experiments with the Munc13 lentiviral constructs include Fluorescence Recovery After Photobleaching (FRAP) studies, which are currently in progress. In FRAP experiments, a region with fluorescent molecules is irradiated or photo-bleached with laser light, which results in the fluorescent molecules inside that region to become non-fluorescent. The recovery of fluorescence then reflects the subsequent redistribution of fluorescent and bleached molecules throughout the volume. This effect provides information on the proteins' mobility. FRAP allows quantification of a number of 'dynamic parameters' such as diffusion coefficient, immobile fraction and binding or residence time of proteins. The amount of fluorescence that recovers relative to the amount of fluorescence that was there before the photobleaching is the percent recovery. The speed with which the fluorescent molecules migrate back into the photobleached area is a measure of the "diffusional mobility" which is usually called lateral mobility. With these experiments, one can directly compare the above listed parameters for the α RIM binding deficient mutants and wild type proteins. The predicted outcome

of these experiments is that the α RIM binding deficient Munc13 constructs will exhibit faster FRAP than the wild type proteins. This is predicted since the fluorescence of the α RIM binding deficient proteins will recover by a diffusional process only, while the wild type proteins must be targeted and anchored in the active zone protein network through their α RIM binding.

Further experiments could also include rescue experiments in the Munc13-1 deletion mutant background using electrophysiological methodology. Semliki-Forest virus constructs of Munc13-1-EGFP and ubMunc13-2-EGFP, wild type and α RIM binding deficient mutants have already been produced to facilitate these experiments. With these studies, I actually expect to replicate the electrophysiological findings published by Betz et al. (2001) and Dulubova et al. (2005). There, it was demonstrated that disruption of the RIM1 α -Munc13-1 interaction in wild type neurons results in a reduction in the size of the readily releasable pool of synaptic vesicles and a deficiency in synaptic vesicle priming.

The final stage of the α RIM-Munc13 project would be the cloning of the 5' end of the Munc13-1 and ubMunc13-2 genes and development of targeting vectors to create knock in mice with the point mutation, I121N, which abolishes RIM1 α binding. Expression of only the RIM1 α binding deficient Munc13-1 and ubMunc13-2 forms from the endogenous genomic loci would provide me with a tool for studying the effect of this mutation in a non-overexpression environment. Parameters such as mfLTP could then be re-examined, taking a better look at the role of Munc13-1 and ubMunc13-2 in this form of synaptic plasticity.

The conditional knock out vector for Munc13-1 has been completed and the stem cell experiments, which would lead to homologous recombination and finally production of conditional knock out mice, are currently being planned.

6. References

Aalto, M., Ronne, H. and S. Keranen (1993). "Yeast syntaxins Sso1p and Sso2p belong to a family of related membrane proteins that function in vesicular transport." *EMBO J.* **12**(11):4095-104.

Abbott, L. and S. Nelson (2000). "Synaptic plasticity: taming the beast." *Nature Neuroscience* **3 Suppl**: 1178-83.

Akert, K. (1971). "Fine structure of neurons and synapses in the central nervous system." *Nord Med.* **21**;86(42):1219.

Andersson, S., Davis, D., Dahlback, H., Jornvall, H. and D. W. Russell (1989). "Cloning, structure, and expression of the mitochondrial cytochrome P-450 sterol 26-hydroxylase, a bile acid biosynthetic enzyme." *Journal of Biological Chemistry* **264**(14): 8222-9.

Andrews, Y (2001). "Interaction Between the Active Zone Components Munc13-1 and RIM1: Definition of Binding Sites Using a Random Mutagenesis Approach". *Master's Thesis*. Max Planck Research School, Georg August Universität Göttingen.

Aravamudan, B., Fergestad, T., Davis, W., Rodesch, C. and K. Broadie (1999). "Drosophila UNC-13 is essential for synaptic transmission." *Nature Neuroscience* **2**(11): 965-71.

Ashery, U., Varoqueaux, F., Voets, T., Betz, A., Thakur, P., Koch, H., Neher, E., Brose, N. and J. Rettig (2000). "Munc13-1 acts as a priming factor for large dense-core vesicles in bovine chromaffin cells." *EMBO Journal* **19**(14): 3586-96.

Augustin, I., Betz, A., Herrmann, C., Jo, T. and N. Brose (1999a). "Differential expression of two novel Munc13 proteins in rat brain." *Biochemical Journal*

337(Pt 3): 363-71.

Augustin, I., Rosenmund, C., Südhof, T. and N. Brose (1999b). "Munc13-1 is essential for fusion competence of glutamatergic synaptic vesicles." *Nature* **400**(6743): 457-61.

Augustin, I., Korte, S., Rickmann, M., Kretzschmar, H., Südhof, T., Herms, J. and N. Brose (2001). "The cerebellum-specific Munc13 isoform Munc13-3 regulates cerebellar synaptic transmission and motor learning in mice." *J Neurosci.* **21**(1):10-7.

Bennett, M., Calakos, N. and R. Scheller (1992). "Syntaxin: a synaptic protein implicated in docking of synaptic vesicles at presynaptic active zones." *Science.* **257**(5067):255-9.

Betz, A., Okamoto, M., Benseler, F. and N. Brose (1997). "Direct interaction of the rat unc-13 homologue Munc13-1 with the N terminus of syntaxin." *Journal of Biological Chemistry* **272**(4): 2520-6.

Betz, A., Ashery, U., Rickmann, M., Augustin, I., Neher, E., Südhof, T., Rettig, J. and N. Brose (1998). "Munc13-1 is a presynaptic phorbol ester receptor that enhances neurotransmitter release." *Neuron* **21**(1): 123-36.

Betz, A., Thakur, P., Junge, H., Ashery, U., Rhee, J. S., Scheuss, V., Rosenmund, C., Rettig, J. and N. Brose (2001). "Functional interaction of the active zone proteins Munc13-1 and RIM1 in synaptic vesicle priming." *Neuron* **30**(1): 183-96.

Brenner, S. (1974). "The genetics of *Caenorhabditis elegans*." *Genetics* **77**(1): 71-94.

Brose, N., Hofmann, K., Hata, Y., and T. Südhof (1995). "Mammalian homologs of *C. elegans unc-13* gene define novel family of C2-domain proteins." *J Biol Chem*, **270**: 25273–25280.

Brose, N., Rosenmund, C. and J. Rettig (2000). "Regulation of transmitter release by Unc-13 and its homologues." *Current Opinion in Neurobiology* **10**(3): 303-11.

Brose, N. and C. Rosenmund (2002). "Move over protein kinase C, you've got company: alternative cellular effectors of diacylglycerol and phorbol esters." *Journal of Cell Science* **115**(Pt 23): 4399-411.

Brünger, A. (2000). "Structural insights into the molecular mechanism of Ca²⁺-dependent exocytosis." *Curr Opin Neurobiol*, **10**:293-302.

Calakos, N., Schoch, S., Sudhof, T. and R. Malenka (2004). "Multiple roles for the active zone protein RIM1alpha in late stages of neurotransmitter release." *Neuron* **42**(6):889-96.

Carr, C., Grote, E., Munson, M., Hughson, F. and P. Novick (1999). "Sec1p binds to SNARE complexes and concentrates at sites of secretion." *J Cell Biol.* **146**(2):333-44.

Cases-Langhoff, C., Voss, B., Garner, A., Appeltauer, U., Takei, K., Kindler, S., Veh, R., De Camilli, P., Gundelfinger, E. and C. Garner (1996). "Piccolo, a novel 420 kDa protein associated with the presynaptic cytomatrix." *Eur J Cell Biol.* **69**(3):214-23.

Castillo, P., Weisskopf, M. and R. Nicoll (1994). "The role of Ca²⁺ channels in hippocampal mossy fiber synaptic transmission and long-term potentiation." *Neuron* **12**(2): 261-9.

Castillo, P., Janz, R., Sudhof, T., Tzounopoulos, T., Malenka, R. and R. Nicoll (1997). "Rab3A is essential for mossy fibre long-term potentiation in the hippocampus." *Nature* **388**(6642): 590-3.

Castillo, P., Schoch, S., Schmitz, F., Sudhof, T. and R. Malenka (2002). "RIM1alpha is required for presynaptic long-term potentiation." *Nature*

415(6869): 327-30.

Coppola, T., Magnin-Luthi, S., Perret-Menoud, V., Gattesco, S., Schiavo, G. and R. Regazzi (2001). "Direct interaction of the Rab3 effector RIM with Ca²⁺ channels, SNAP-25, and synaptotagmin." *Journal of Biological Chemistry* **276**(35): 32756-62.

Dobrunz, L. and C. Stevens (1997). "Heterogeneity of release probability, facilitation, and depletion at central synapses." *Neuron* **18**(6):995-1008.

Dragatsis, I. and S. Zeitlin S (2000). "CaMKIIalpha-Cre transgene expression and recombination patterns in the mouse brain." *Genesis* **26**(2):133-5.

Dresbach, T., Qualmann, B., Kessels, M., Garner, C. and E. D. Gundelfinger (2001). "The presynaptic cytomatrix of brain synapses." *Cellular and Molecular Life Sciences* **58**(1): 94-116.

Dulubova, I., Sugita, S., Hill, S., Hosaka, M., Fernandez, I., Sudhof, T. and J. Rizo (1999). "A conformational switch in syntaxin during exocytosis: role of munc18." *EMBO Journal* **18**(16): 4372-82.

Dulubova, I., Lou, X., Lu, J., Huryeva, I., Alam, A., Schneggenburger, R., Sudhof, T. and J. Rizo (2005). "Munc13/RIM/Rab3 tripartite complex: from priming to plasticity?" *EMBO J.* **24**(16): 2839-50.

Fabbri, M., Bannykh, S. and W. Balch (1994). "Export of protein from the endoplasmic reticulum is regulated by a diacylglycerol/phorbol ester binding protein." *J. Biol. Chem.* **269**: 26848–26857.

Fields, S. and O. Song (1989). "A novel genetic system to detect protein-protein interactions." *Nature* **340**(6230): 245-6.

Fischer von Mollard, G., Mignery, G., Baumert, M., Perin, M., Hanson, T., Burger, P., Jahn, R. and T. Sudhof (1990). "rab3 is a small GTP-binding

protein exclusively localized to synaptic vesicles." *Proc. Natl. Acad. Sci. USA* **87**, 1988–1992.

Garner, C., Kindler, S. and E. D. Gundelfinger (2000). "Molecular determinants of presynaptic active zones." *Curr. Opin. Cell Biol.* **10**, 321–327

Geppert, M., Bolshakov, V., Siegelbaum, S., Takei, K., De Camilli, P., Hammer, R. and T. Südhof (1994). "The role of Rab3A in neurotransmitter release." *Nature* **9**;369(6480):493-7.

Geppert, M., Goda, Y., Stevens, C. and T. Südhof (1997). "The small GTP-binding protein Rab3A regulates a late step in synaptic vesicle fusion." *Nature* **387**(6635): 810-4.

Guan, K. L. and J. E. Dixon (1991). "Eukaryotic proteins expressed in *Escherichia coli*: an improved thrombin cleavage and purification procedure of fusion proteins with glutathione S-transferase." *Analytical Biochemistry* **192**(2): 262-7.

Harlow, M., Ress, D., Stoschek, A., Marshall, R. and U. McMahan (2001). "The architecture of active zone material at the frog's neuromuscular junction." *Nature*. **409**(6819):479-84

Holmes, D. S. and M. Quigley (1981). "A rapid boiling method for the preparation of bacterial plasmids." *Analytical Biochemistry* **114**(1): 193-7.

Hosono, R. and Y. Kamiya (1991). "Additional genes which result in an elevation of acetylcholine levels by mutations in *Caenorhabditis elegans*." *Neuroscience Letters* **128**(2): 243-4.

Jahn, R., Lang, T. and T. Südhof (2003). "Membrane fusion." *Cell*. **112**(4): 519-33.

.

Junge, H., Rhee, J., Jahn, O., Varoqueaux, F., Spiess, J., Waxham, M., Rosenmund, C. and N. Brose (2004). "Calmodulin and Munc13 form a Ca²⁺ sensor/effector complex that controls short-term synaptic plasticity." *Cell*. **118**(3):389-401.

Kaufmann, N., DeProto, J., Ranjan, R., Wan, H. and D. Van Vactor (2002). "Drosophila liprin- α and the receptor phosphatase Dlar control synapse morphogenesis." *Neuron* **34**: 27–38.

Ko, J., Na, M., Kim, S., Lee, J. and E. Kim (2003). "Interaction of the ERC family of RIM-binding proteins with the liprin-alpha family of multidomain proteins." *J Biol Chem*. **278**(43):42377-85.

Kohn, R., Duerr, J., McManus, J., Duke, A., Rakow, T., Maruyama, H., Moulder, G., Maruyama, I., Barstead, R. and J. Rand (2000). "Expression of multiple UNC-13 proteins in the Caenorhabditis elegans nervous system." *Mol Biol Cell*. **11** 3441-52.

Koushika, S., Richmond, J., Hadwiger, G., Weimer, R., Jorgensen E. and M. L. Nonet (2001). "A post-docking role for the active zone protein Rim." *Nature Neuroscience* **4**(10): 997-1005.

Laemmli, U. K. (1970). "Cleavage of structural proteins during the assembly of the head of bacteriophage T4." *Nature* **227**(259): 680-5.

Lonart G (2002). "RIM1: an edge for presynaptic plasticity." *Trends Neurosci*. **25**(7):329-32. Review.

Lonart, G., Schoch, S., Kaeser, P., Larkin, C., Sudhof, T. and D. Linden (2003). "Phosphorylation of RIM1alpha by PKA triggers presynaptic long-term potentiation at cerebellar parallel fiber synapses." *Cell* **115**(1): 49-60.

Maruyama, I. N. and S. Brenner (1991). "A phorbol ester/diacylglycerol

binding protein encoded by the *unc-13* gene of *Caenorhabditis elegans*." *Proceedings of the National Academy of Sciences of the United States of America* **88**: 5729-5733.

Metzger, D. and P. Chambon (2001). "Site- and time-specific gene targeting in the mouse." *Methods* **24**(1):71-80.

Misura, K., Scheller, R. and W. Weis (2000). "Three-dimensional structure of the neuronal-Sec1-syntaxin 1a complex." *Nature*. **404**(6776):355-62

Monier, S., Jollivet, F., Janoueix-Lerosey, I., Johannes, L. and B. Goud (2002). "Characterization of novel Rab6-interacting proteins involved in endosome-to-TGN transport." *Traffic* **3** 289–297.

Nagy, A. (2000). "Cre recombinase: the universal reagent for genome tailoring." *Genesis* **26**(2):99-109. Review.

Nakata, T., Kitamura, Y., Shimizu, K., Tanaka, S., Fujimori, M., Yokoyama, S., Ito, K. and M. Emi (1999). "Fusion of a novel gene, ELKS, to RET due to translocation t(10;12) (q11;p13) in a papillary thyroid carcinoma." *Genes Chromosomes Cancer* **25** 97–103.

Naldini, L., Blomer, U., Gallay, P., Ory, D., Mulligan, R., Gage, F., Verma, I. and D. Trono (1996). "In vivo gene delivery and stable transduction of nondividing cells by a lentiviral vector." *Science*. **272**(5259):263-7.

Naldini, L (1998). "Lentiviruses as gene transfer agents for delivery to non-dividing cells." *Curr Opin Biotechnol*. **9**(5):457-63. Review.

Neeb, A., Koch, H., Schurmann, A. and N. Brose (1999). "Direct interaction between the ARF-specific guanine nucleotide exchange factor msec7-1 and presynaptic Munc13-1." *European Journal of Cell Biology* **78**(8): 533-8.

Newton, A (1995). "Protein kinase C: structure, function, and regulation." *J Biol Chem* **270**: 28495–28498.

Newton, A (1997). "Regulation of protein kinase C." *Curr Opin Cell Biol* **9**: 161–167.

Nonet, M., Staunton, J., Kilgard, M., Fergestad, T., Hartweg, E., Horvitz, H., Jorgensen, E. and B. Meyer (1997). "*Caenorhabditis elegans* rab-3 mutant synapses exhibit impaired function and are partially depleted of vesicles." *J Neurosci.* **17**(21):8061-73.

Ohtsuka, T., Takao-Rikitsu, E., Inoue, E., Inoue, M., Takeuchi, M., Matsubara, K., Deguchi-Tawarada, M., Satoh, K., Morimoto, K., Nakanishi H. and Y. Takai (2002). "Cast: a novel protein of the cytomatrix at the active zone of synapses that forms a ternary complex with RIM1 and munc13-1." *Journal of Cell Biology* **158**(3): 577-90.

Ostermeier, C. and A. T. Brunger (1999). "Structural basis of Rab effector specificity: crystal structure of the small G protein Rab3A complexed with the effector domain of rabphilin-3A." *Cell* **96**(3): 363-74.

Oyler, G., Higgins, G., Hart, R., Battenberg, E., Billingsley, M., Bloom, F. and M. Wilson (1989). "The identification of a novel synaptosomal-associated protein, SNAP-25, differentially expressed by neuronal subpopulations." *J Cell Biol.* **109**(6 Pt 1):3039-52.

Powell, C., Schoch, S., Monteggia, L., Barrot, M., Matos, M., Feldmann, N., Sudhof T., Nestler, E (2004). "The presynaptic active zone protein RIM1alpha is critical for normal learning and memory." *Neuron* **42**(1):143-53.

Redman, R. S., Searl, T. J., Hirsh, J. K. and E. Silinsky (1997). "Opposing effects of phorbol esters on transmitter release and calcium currents at frog motor nerve endings." *J. Physiol.* **501**: 41–48.

Rettig, J., and E. Neher (2002). "Emerging roles of presynaptic proteins in

Ca₂R-triggered exocytosis." *Science*, **298**:781-785.

Rhee, J. S., Betz, A., Pyott, S., Reim, K., Varoqueaux, F., Augustin, I., Hesse, D., Südhof, T., Takahashi, M., Rosenmund, C. and N. Brose (2002). "Beta phorbol ester- and diacylglycerol-induced augmentation of transmitter release is mediated by Munc13s and not by PKCs." *Cell* **108**(1): 121-33.

Richmond, J., Davis W. and E. Jorgensen (1999). "UNC-13 is required for synaptic vesicle fusion in *C. elegans*." *Nature Neuroscience* **2**(11): 959-64.

Richmond, J., Weimer, R. and E. Jorgensen (2001). "An open form of syntaxin bypasses the requirement for UNC-13 in vesicle priming." *Nature* **412**(6844): 338-41.

Rizo, J. and T. Südhof (2002). "Snares and Munc18 in synaptic vesicle fusion." *Nat Rev Neurosci* **3**(8):641-53. Review.

Roos, J. and R. Kelly. 1999. "The endocytic machinery in nerve terminals surrounds sites of exocytosis." *Curr. Biol.* **9**:1411–14.

Rosenmund, C. and C. F. Stevens (1996). "Definition of the readily releasable pool of vesicles at hippocampal synapses." *Neuron* **16**(6): 1197-207.

Rosenmund, C., Sigler, A., Augustin, I., Reim, K., Brose, N. and J. S. Rhee (2002). "Differential control of vesicle priming and short-term plasticity by Munc13 isoforms." *Neuron* **33**(3): 411-24.

Saiki, R., Gelfand, D., Stoffel, S., Scharf, S., Higuchi, R., Horn, G., Mullis, K. and H. Erlich (1988). "Primer-directed enzymatic amplification of DNA with a thermostable DNA polymerase." *Science* **239**, 487-91.

Sakaba, T. and E. Neher (2001). "Calmodulin mediates rapid recruitment of fast-releasing synaptic vesicles at a calyx-type synapse." *Neuron*. **32**(6):1119-31.

Sakaguchi, G., Manabe, T., Kobayashi, K., Orita, S., Sasaki, T., Naito, A., Maeda, M., Igarashi, H., Katsuura, G., Nishioka, H., Mizoguchi, A., Itohara, S., Takahashi, T. and Y. Takai (1999). "Doc2alpha is an activity-dependent modulator of excitatory synaptic transmission." *European Journal of Neuroscience* **11**(12): 4262-8.

Sassa, T., Harada, S., Ogawa, H., Rand, J., Maruyama, I. and R. Hosono (1999). "Regulation of the UNC-18-Caenorhabditis elegans syntaxin complex by UNC-13." *Journal of Neuroscience* **19**(12): 4772-7.

Scannevin, R. and R. Huganir (2002). "Postsynaptic organization and regulation of excitatory synapses." *Nat Rev Neurosci.* **1**(2):133-41. Review.

Schluter, O., Khvotchev, M., Jahn, R. and T. Sudhof (2002). "Localization versus function of Rab3 proteins. Evidence for a common regulatory role in controlling fusion." *Journal of Biological Chemistry* **277**(43): 40919-29.

Schnutgen, F., Doerflinger, N., Calleja, C., Wendling, O., Chambon, P. and N. Ghyselinck (2003). "A directional strategy for monitoring Cre-mediated recombination at the cellular level in the mouse." *Nat Biotechnol.* **21**(5):562-5.

Schoch, S., Castillo, P., Jo, T., Mukherjee, K., Geppert, M., Wang, Y., Schmitz, F., Malenka, R. and T. Sudhof (2002). "RIM1alpha forms a protein scaffold for regulating neurotransmitter release at the active zone." *Nature* **415**(6869): 321-6.

Scholfield, C. and A. Smith (1989). "Phorbol diester-induced enhancement of synaptic transmission in olfactory cortex." *Br J Pharmacol.* **98**(4):1344-50.

Serra-Pages, C., Medley, Q., Tang, M., Hart, A. and M. Streuli (1998). "Liprins, a family of LAR transmembrane protein-tyrosine phosphatase-interacting proteins." *J Biol Chem.* **273**(25):15611-20.

Siegel, R., Jain, R. and A. Bradbury (2001). "Using an in vivo phagemid system to identify non-compatible loxP sequences." *FEBS Lett.* **505**(3):467-73.

Söllner, T., Bennet, M., Whiteheart, S., Scheller, R. and J. Rothman (1993). "A protein assembly-disassembly pathway in vitro that may correspond to sequential steps of synaptic vesicle docking, activation, and fusion." *Cell* **75** 409–418 .

Söllner, T., Whiteheart, S., Brunner, M., Erdjument-Bromage, H. and S., Geromanos (1993). "SNAP receptors implicated in vesicle targeting and fusion." *Nature* **362**: 318-24.

Söllner, T. H. and J. E. Rothman (1996). "Molecular machinery mediating vesicle budding, docking and fusion." *Cell Structure and Function* **21**(5): 407-12.

Song, Y., Ailenberg, M. and M. Silverman (1998). "Cloning of a novel gene in the human kidney homologous to rat Munc13s: its potential role in diabetic nephropathy." *Kidney Int*, **53**: 1689–1695.

Südhof, T. (1995). "The synaptic vesicle cycle: a cascade of protein-protein interactions." *Nature* **375**(6533): 645-53.

Südhof, T. (2000). "The synaptic vesicle cycle revisited." *Neuron* **28**(2): 317-20.

Sun, L., Bittner, M. and R. W. Holz (2001). "Rab3a binding and secretion enhancing domains in Rim1 are separate and unique. Studies in adrenal chromaffin cells." *Journal of Biological Chemistry* **276**(16): 12911-7.

Sutton, R., Fasshauer, D., Jahn, R, and A. T. Brunger (1998). "Crystal structure of a SNARE complex involved in synaptic exocytosis at 2.4 Å resolution." *Nature* **395**(6700): 347-53.

Trimble, W., Cowan, D. and R. Scheller (1988). "VAMP-1: a synaptic vesicle-associated integral membrane protein." *Proc Natl Acad Sci* **85**(12):4538-42.

tom Dieck, S., Sanmarti-Vila, L., Langnaese, K., Richter, K., Kindler, S., Soyke, A., Wex, H., Smalla, K., Kampf, U., Franzer, J., Stumm, M., Garner, C. and E. D. Gundelfinger (1998). "Bassoon, a novel zinc-finger CAG/glutamine-repeat protein selectively localized at the active zone of presynaptic nerve terminals." *Journal of Cell Biology* **142**(2): 499-509.

Toonen, R., de Vries, K., Zalm, R., Südhof, T. and M. Verhage (2005). "Munc18-1 stabilizes syntaxin 1, but is not essential for syntaxin 1 targeting and SNARE complex formation." *J Neurochem.* **93**(6):1393-400.

Varoqueaux, F., Sigler, A., Rhee, J. S., Brose, N., Enk, C., Reim K., and C. Rosenmund (2002). "Total arrest of spontaneous and evoked synaptic transmission but normal synaptogenesis in the absence of Munc13-mediated vesicle priming." *Proceedings of the National Academy of Sciences of the United States of America* **99**(13): 9037-42.

Verhage, M., Maia, A., Plomp, J., Brussaard, A., Heeroma, J., Vermeer, H., Toonen, R., Hammer, R., van den Berg, T., Missler, M., Geuze, H. and T. Südhof (2000). "Synaptic assembly of the brain in the absence of neurotransmitter secretion." *Science* **287**(5454):864-9.

Wang, Y., Okamoto, M., Schmitz, F., Hofmann, K. and T. Südhof (1997). "Rim is a putative Rab3 effector in regulating synaptic-vesicle fusion." *Nature* **388**(6642): 593-8.

Wang, Y., Sugita, S. and T. Südhof (2000). "The RIM/NIM family of neuronal C2 domain proteins. Interactions with Rab3 and a new class of Src homology 3 domain proteins." *Journal of Biological Chemistry* **275**(26):20033-44.

Wang, X., Hu, B., Zimmermann, B. and M. and W. Kilimann (2001). "Rim1 and rabphilin-3 bind Rab3-GTP by composite determinants partially related

through N-terminal alpha -helix motifs." *Journal of Biological Chemistry* **276**(35): 32480-8.

Wang, Y., Liu, X., Biederer, T. and T. Südhof (2002). "A family of RIM binding proteins regulated by alternative splicing: Implications for the genesis of synaptic active zones." *Proceedings of the National Academy of Sciences of the United States of America* **99**(22): 14464-9.

Wang, Y. and T. Südhof (2003). "Genomic definition of RIM proteins: evolutionary amplification of a family of synaptic regulatory proteins." *Genomics* **81**: 126-137.

Weber, K. and M. Osborn (1969). "The reliability of molecular weight determinations by dodecyl sulfate-polyacrylamide gel electrophoresis." *Journal of Biological Chemistry* **244**(16): 4406-12.

Weisskopf, M., Castillo, P., Zalutsky, R. and R. Nicoll (1994). "Mediation of hippocampal mossy fiber long-term potentiation by cyclic AMP." *Science* **265**(5180): 1878-82.

Xu, X., Wes, P., Chen, H., Li, H., Yu, M., Morgan, S., Liu, Y. and C. Montell (1998). "Retinal targets for calmodulin include proteins implicated in synaptic transmission." *Journal of Biological Chemistry* **273**(47): 31297-307.

Zhen, M. and Y. Jin (1999). "The liprin protein SYD-2 regulates the differentiation of presynaptic termini in *C. elegans*." *Nature* **401**(6751): 371-5.

Zucker, R. (1996). "Exocytosis: a molecular and physiological perspective." *Neuron*, **17**: 1049–1055.

7. Curriculum Vitae

Personal Information

Name: Yaisa Seretha Andrews-Zwilling

Date of birth: 03.12.1977

Place of birth: Trinidad and Tobago, WI

Telephone number: +49 179 116 8017 (Mobile)
+49 551 3899 714 (Work)

e-mail: yaisaa@hotmail.com; andrews@em.mpg.de

Address: Burg Str. 37/A,
37073 Goettingen,
Germany

Scientific Education

March 2002 - Sept 2005: Doctoral Thesis in Neurobiology
Targeting and Anchoring of Munc13-1 and ubMunc13-2 to Active Zones by RIM1 α
Max Planck Research School
Department of Molecular Neurobiology (Prof. N. Brose)
Max Planck Institute for Experimental Medicine
37075 Göttingen, Germany

Oct 2000 - March 2002: M.Sc. in Neurosciences
International M.Sc./PhD Programme in Neuroscience
Max Planck Research School
Göttingen, Germany
<http://www.gpneuro.uni-goettingen.de>

Sept 1999 – July 2000: M.Phil in Biochemistry
The University of the West Indies,
St. Augustine Campus, Trinidad

Oct 1996 - June 1999: B.Sc. Double Major in Biochemistry and Chemistry
The University of the West Indies,
St. Augustine Campus, Trinidad,
Upper Second Class Honours

Scholarships:

Dean's Award for Excellence; The University of the West Indies

Computer Skills:

-Microsoft Office Programs

-Lasergene Navigator

Other skills and Courses

-Cross-cultural Communication Workshop

International Max Planck Research School (IMPRS), May 2004

-Drug Discovery Course

IMPRS and Schering Deutschland GmbH, May-June 2004

-Scientific Communication

IMPRS, January 2002

-Synaptic Transmission

MPI Biophysical Chemistry, Göttingen, April-July 2002

-Bioethics and Research Ethics

IMPRS, Oct -Sept 2002

Languages:

-English: Native

-German: Intermediate writing and advanced speaking

Interests and hobbies:

-Scuba diving

-Reading

-Aerobics

-Yoga

References:

Prof. Nils Brose

brose@em.mpg.de

Max-Planck-Institute for Experimental Medicine

Hermann-Rein-Str. 3

37075 Göttingen, Germany

+49 551 3899 725

Prof. Antti Hervonen

antti.hervonen@uta.fi

Professor of Gerontology M.D. Ph.D.

Tampere School of Public Health

University of Tampere, Finland

+358 3 215 7025

8. Publication

Lalla, A., Alleyne, T. and Y. Andrews (2001). "Understanding the Mechanism of Action of Cytochrome c Oxidase in Normal and Diseased States: Shark Heart Enzyme, a Potential Model". *The West Indian Medical Journal* **50**(2): 111-6.

Andrews-Zwilling, Y., Reim, K., Varoqueaux, F., Kawabe, H., Südhof, T. and N. Brose (2005). "Targeting and Anchoring of Munc13-1 and ubMunc13-2 to Active Zones by RIM1 α ." Manuscript in preparation.

9. Acknowledgements

I would like to thank Prof. Nils Brose for his support and helpful criticism and for giving me the opportunity to work in his laboratory on this project, which enabled me to learn so many valuable techniques. I am also indebted to Prof. Reinhard Jahn and Prof. Friedrich-Wilhelm Schürmann for their support as my additional thesis committee members and for their assistance whenever it was needed.

I would also like to thank Prof. Michael Hörner, Dr. Steffen Burkhardt, Dr. Simone Cardoso de Oliveira, Sandra Drube, Dr. Dorotee Wegener and Nina McGuinness-Hoppe for all of their support in administrative matters and for creating a wonderful and supportive environment for the graduate students of Göttingen. I am very grateful to everyone in the Neurobiology Department for providing a great learning environment and whose help and friendship I couldn't have done without during the entire PhD and especially in the last few months. Equally, I would like to give great thanks to all of my friends and colleagues in Göttingen and my friends from Trinidad and Tobago, who have supported me in many ways from near and from afar over the past years...you are so many that to thank you all personally would take another thesis, but you know who you are and I am ever grateful to you all.

I would like to thank my family for all of their love and encouragement over the oceans and for sending me sunshine through the telephone wires and over the internet when I needed it.

Finally I would like to thank my husband, best friend and favourite giggle partner, Daniel H. G. H. Zwilling. Thank you for being all that a husband should be and more and for seeing me through the ups and downs of the PhD.